



# Remote Emission Sensing as a means of detection and enforcement of gross-polluting vehicles

Åke Sjödin, Yingying Cha  
IVL Swedish Environmental Research Institute, Sweden

Justin Plogmann, Panayotis Dimopoulos Eggenschwiler  
Empa, Swiss Federal Laboratories for Materials  
Science & Technology, Switzerland

Signe Damtoft Siersbæk  
Danish Environmental Protection Agency,  
Ministry of Environment of Denmark, Denmark

Shaojun Zhang, Hui Wang, Dongbin Wang, Ye Wu  
Tsinghua University, China

Rasmus Pettinen  
VTT Technical Research Centre of Finland Ltd,  
Finland

March / 2024

## Summary

The IEA-AMF TCP Task 61 was initiated to answer the key question how remote emission sensing (RES) can be used - for policy purposes as well as for direct or indirect enforcement - to detect high-emitting/gross-polluting road vehicles in real-world traffic.

The scope of the task included to review recent research involving development and applications of the three main technological types of remote emission sensing, namely conventional (or commercial) RES (type 1), which has been around and further developed and refined over the last 35 years, point sampling RES (type 2) and plume chasing RES (type 3), of which the latter two have (mainly) evolved only in the last 5-10 years. In addition, the task has also included recent research involving applications of onboard real driving emission measurement technique (i.e., PEMS) as well as research and development in the field of exhaust plume modelling, both representing instruments that are vital to help fully understand the possibilities and limitations of remote emission sensing to assess the real-world emission performance of road vehicles, both on individual vehicle level and fleet level.

The main results of Task 61 can be summarized as:

- RES type 1 has proven very useful to measure average emissions on fleet level, e.g., by emission standard, vehicle brand, engine family, etc., in good agreement with PEMS RDE measurements, which may serve in-service conformity and in-use compliance testing, e.g., to evaluate needs to further improve emission legislation.
- Adopted in the right manner RES type 1 can also be used for direct enforcement, the best example likely being supporting roadside inspections for roadworthiness testing.
- Single RES measurements (type 1 & 2) are of limited use to identify high-emitters; to do so at least 3-5 repeat measurements on the same individual vehicle are required.
- RES type 1 has proven a useful tool to derive relationships between emissions, e.g., by emission standard, and vehicle age/mileage as well as ambient temperature, important for road transport emission inventories. It has also proven useful to validate – on an aggregate level – underlying emission models to the emission inventories.
- Through the successful development of RES type 2 in the last 5-10 years, passing vehicles' emissions of particulate matter (particle number, particle mass and Black Carbon) can now be accurately measured from the roadside, which is a shortcoming of RES type 1 instruments. There are clear indications that RES type 2 is capable of identifying vehicles with non-functional diesel particulate filters from the roadside.
- Furthermore, measurements of gaseous pollutants (mainly NO and NO<sub>2</sub>) have also been adopted to RES type 2. A good agreement between RES type 2 and PEMS has been observed for both PN and NO<sub>x</sub> emissions.
- The main limitations of RES type 2 are generally the lower hit-rates (i.e., the share of valid measurements) compared to RES type 1, especially when traffic is dense and under certain unfavorable wind conditions. On the other hand, contrary to type 1, RES type 2 is capable of full operability also during rainy conditions.
- RES type 3 has proven very capable of identifying gross-polluting HDTs. Recent studies in both China and EU have shown that the SCR systems on substantial shares of SCR-equipped heavy-duty trucks are tampered with, or deviate from normal operation for other reasons, increasing their NO<sub>x</sub> emissions by up to one order of magnitude, or even more. For China this resulted in an underestimation of the NO<sub>x</sub> emissions in the national emission inventory in 2019 by 18%.

- Furthermore, ambient temperature was identified as a primary driver of NO<sub>x</sub> emissions for heavy-duty trucks, and the low-temperature penalty has caused a 9–29% increase in NO<sub>x</sub> emissions in winter in major regions of China.
- PEMS data analysis demonstrates that Euro 6 diesel cars, that comply with the emission limit set in the RDE regulation, may still occasionally produce significant spikes of NO<sub>x</sub> emissions, e.g., during strong accelerations. This is crucial for RES type 1 and type 2 measurements aiming at identifying high-emitters and implies that measurement sites characterized by strong accelerations should be avoided.
- The good news for RES type 1 and 2 high-emitter identification capability from the PEMS data analysis was that the Euro 6 diesel car equipped with an SCR was the one that produced the least variable momentary NO<sub>x</sub> concentrations. Further, the problem with large variations in momentary emissions of NO<sub>x</sub> was not observed for PN emissions, indicating that there is not a great variation in the performance of the DPF even for varying trip conditions.
- SEMS measurements demonstrate that also NO<sub>x</sub> emissions from diesel powered light- and heavy-duty Euro VI trucks are sensitive to driving conditions, in particular when comparing highway (low emissions) and city (high emissions) driving, due to lower temperatures of the aftertreatment system at lower engine loads and idling. Thus, it is not ideal to carry out RES measurements to identify NO<sub>x</sub> high-emitting trucks and buses in typical city driving, i.e., in heavy traffic, causing a lot of low speed and stop-and-go situations. However, just as for the corresponding diesel cars, PN emissions from Euro VI trucks were quite unaffected by driving conditions and load.
- Advanced numerical simulations for a passenger vehicle show that the exhaust gas plume is strongly diluted in the near vehicle wake, so that no significant proportion of exhaust gas can be measured 1.5-3 m downstream of the vehicle. That is for all investigated speeds (30-80 km/h) and wind conditions, with the peak concentration of exhaust gases found less than 0.5 m downstream of the vehicle, explaining the lower hit-rates for RES type 2 compared to type 1, due to the lower measuring frequency.

The conclusions of Task 61 are that there are many promising and valid applications of RES, especially when considering that the three different types have both overlapping and complementary features, and may well be applied in assembly, not only as single systems.

To target and enforce deliberately tampered vehicles RES may be the only option. This would require a shift from some of today's focus on PTI's to roadside inspections, in which case all types of RES have proven capable to drastically increase the efficiency in targeting and finding gross-polluters. This could have a considerable impact regarding reducing the emissions of NO<sub>x</sub> and particulate matter (PM) from in particular Euro 5 (PM) and Euro 6 (NO<sub>x</sub> and PM) diesel light- as well as heavy-duty vehicles.

Finally, RES technologies and associated pollutant measurement and analytical instruments are being further developed to improve performance and to meet new challenges to reduce road vehicle emissions.

## Authors

Åke Sjödin, Yingying Cha

IVL Swedish Environmental Research Institute, Sweden

Justin Plogmann, Panayotis Dimopoulos Eggenschwiler

Empa, Swiss Federal Laboratories for Materials  
Science & Technology, Switzerland

Signe Damtoft Siersbæk

Danish Environmental Protection Agency,  
Ministry of Environment of Denmark, Denmark

Shaojun Zhang, Hui Wang, Dongbin Wang, Ye Wu

Tsinghua University, China

Rasmus Pettinen

VTT Technical Research Centre of Finland Ltd, Finland

## Content

Summary .....	i
Authors .....	iii
Content .....	3
List of Figures .....	6
List of Tables .....	9
Introduction .....	10
Objectives .....	11
Methodology .....	14
RES type 1 - conventional/commercial RES .....	14
RES type 2 - point sampling RES .....	15
RES type 3 - plume chasing RES .....	17
On-board emission measurements – PEMS and SEMS .....	18
Exhaust plume modelling.....	20
Activities and data .....	21
RES type 1 measurements.....	21
Danish studies on roadside remote sensing.....	21
CONOX project - RES type 1 data pooling and comparison with PEMS data.....	22
Swedish study focusing on early Euro 6 diesel cars.....	22
RES type 1 measurements in the CARES project.....	22
Other RES type 1 measurement campaigns in Europe of relevance for Task 61 .....	23
RES type 1 databases .....	24
RES type 2 measurements.....	24
China .....	24
Europe .....	24
RES type 3 measurements.....	25
China .....	25
Europe .....	26
PEMS measurements.....	28
RDE/PEMS measurements on light-duty vehicles in Helsinki in 2019 .....	28
SEMS measurements on a diesel van and heavy-duty trucks in Copenhagen in 2020 .....	29
Exhaust plume modelling.....	30
Results.....	31
RES type 1 .....	31

Truck tampering studies in Denmark.....	31
CONOX project.....	34
Light-duty diesel vehicle on-road emission performance study in Sweden .....	36
RES type 1 measurements in the CARES project.....	38
Other RES type 1 measurement campaigns in Europe of relevance for Task 61 .....	39
RES type 2.....	47
China .....	47
Europe.....	50
RES type 3.....	56
China .....	56
Europe.....	63
PEMS/SEMS.....	66
PEMS RDE measurements of Euro 6 diesel passenger cars .....	66
SEMS measurements of light- and heavy-duty Euro VI diesel trucks .....	70
Exhaust plume modelling.....	71
Approach .....	71
Pollutant dispersion.....	71
Parameter study.....	73
Hybrid LES/RANS framework .....	74
Results summary .....	75
RES type 1 .....	75
RES type 2.....	76
RES type 3.....	77
China .....	77
Europe.....	77
PEMS and SEMS .....	78
Exhaust plume modelling.....	79
Applicability and potential impact .....	80
Statistical emissions analysis for emission legislation policy follow-up.....	80
Detection of gross-polluting vehicles for enforcement purposes .....	81
What can RES learn from exhaust plume modelling? .....	81
Derivation of emission deterioration factors .....	82
Temperature dependence of emission factors .....	83
Validation of vehicle emission models .....	83
Providing input to the design and follow-up of Low Emission Zones .....	83

Conclusions .....	85
Outlook .....	87
References .....	89

## List of Figures

Figure 1: Overview of the three different types of remote emission sensing (RES) techniques.....	9
Figure 2: Schematic principle and set up for a RES type 1 instrument.....	11
Figure 3: Schematic principle and set-up for RES type 2 instrument.....	12
Figure 4: Example of measured concentrations with an RES type 2 instrument from three successive passages of the same vehicle.....	12
Figure 5: Field study of chasing tests.....	14
Figure 6: A typical PEMS and SEMS setup.....	15
Figure 7: Sample distribution of plume chasing tests in China.....	22
Figure 8: Fleet composition of chased vehicles.....	23
Figure 9: An example of a PEMS route in the Helsinki region.....	26
Figure 10: Computational mesh for exhaust plume simulations.....	27
Figure 11: Average real driving NO <sub>x</sub> emission factors (in g/kg fuel burned) for Euro 5... and Euro 6 diesel passenger cars	32
Figure 12: Comparison of NO <sub>x</sub> emission factors (in g/kg fuel) derived from RES type 1 measurements and governmental and 3rd party PEMS testing by vehicle model.....	33
Figure 13: Average PM emissions (in g/kg fuel burned) by Euro standard for diesel passenger cars as measured by remote sensing in four European countries.....	33
Figure 14: Average NO <sub>x</sub> emissions by Euro standard and Euro 6ab emission control technology for diesel passenger cars as measured by PEMS and RES type 1 .....	34
Figure 15: Average NO <sub>x</sub> emissions for common Euro 6ab diesel engine families as measured by PEMS RDE and by RES type 1.....	35
Figure 16: PEMS NO <sub>x</sub> emissions vs NO <sub>x</sub> emissions as measured by RES type 1.....	35
Figure 17: Average NO <sub>x</sub> emissions for diesel, petrol and LPG passenger cars as measured by RES type 1 in Prague, Milan and Krakow in the CARES project.....	36
Figure 18: Average NO <sub>x</sub> emissions by engine family for Euro 6d-temp and Euro 6d diesel passenger cars according to RES type 1 measurements in the CARES project...	36
Figure 19: Overview of the evolution of NO <sub>x</sub> emissions by Euro class for passenger cars as measured by RES type 1 in Flanders 2019.....	37
Figure 20: Overview of the evolution of NO <sub>x</sub> and PM emissions by Euro class for heavy goods vehicles as measured by RES type 1 in Flanders 2019.....	37
Figure 21: Average NO <sub>x</sub> emissions (in g/kg fuel) by different vehicle categories according to RES type 1 measurements in Flanders in 2019.....	38
Figure 22: Average NO <sub>x</sub> emissions by Euro standard for petrol and diesel passenger cars according to RES type 1 measurements Berlin 2019 and Frankfurt 2020.....	38
Figure 23: NO <sub>x</sub> emissions for petrol and diesel passenger cars as a function of vehicle age and ambient air temperature, as measured by RES type 1 in Frankfurt.....	39



Figure 24: Average NOX emissions for petrol and diesel passenger cars according to RES type 1 measurements in Berlin 2019 and to PHEM modeling results.....	40
Figure 25: Mean estimated distance-specific NOx emissions from diesel and petrol passenger cars by emissions standard for Brussels and TRUE remote sensing data.....	41
Figure 26: Mean fuel-specific PM emissions for light-duty diesel vehicles from remote sensing compared to PN concentration from road inspection at idle, by Euro standard...	41
Figure 27: Comparison of repeat NOX emission measurements by means of RES type 1 and SEMS on a Euro 5 diesel car on a test track in Switzerland in 2021.....	42
Figure 28: Comparison of repeat NOX emission measurements by means of RES type 1 and SEMS on a Euro VI HDT with trailer on a test track in Switzerland in 2021...	43
Figure 29: Average fuel-specific NOx emissions from measurements at speeds in rural areas (below 80 km/h) by instrument, fuel type and emission standard.....	44
Figure 30. Average fuel-specific NOx emissions from measurements at highway speeds (above 80 km/h) by fuel type and emission standard for passenger cars.....	44
Figure 31: Time series of pollutant signals for continuous driving throughs and a selected single drive-through.....	45
Figure 32. Distribution of PN and NO emission factors for tested vehicles.....	46
Figure 33: Comparison between roadside sensor platform measurement and PEMS measurement for NO-EF and PN-EF.....	47
Figure 34: EFs for PM and PN for Euro V-SCR buses operating on different fuels as measured by RES type 2.....	48
Figure 35: Average emissions of PM, PN and BC for Swedish Euro III to Euro VI and non-Swedish heavy-duty trucks as measured by RES type 2.....	49
Figure 36: NO <sub>x</sub> /CO <sub>2</sub> ratios for three light- and heavy-duty diesel vehicles, measured by RES type 2 grouped by test session in CARES controlled test track experiments.....	49
Figure 37: PN and BC emission factors measured by RES type 2 grouped by test session in the CARES controlled test track experiments.....	50
Figure 38: Mean NO <sub>x</sub> /CO <sub>2</sub> emission ratios for three light- and heavy-duty diesel vehicles, measured by point sampling and remote sensing.....	51
Figure 39: Comparison of the PN and BC emissions of a Euro 6b diesel car measured by RES type 2 with PN emissions measured by PEMS.....	51
Figure 40: Comparison of average NO <sub>x</sub> and NO <sub>2</sub> emissions of test vehicles measured with PEMS, RES type 2 and RES type 1 in Milan in 2021.....	52
Figure 41: Average emissions of BC and PN from diesel passenger cars by Euro standard as measured by means of RES type 2 instruments in Prague/Brno in 2022....	53
Figure 42: RES type 2 measurements for the detection of particle high-emitting diesel cars in Prague/Brno 2022.....	53
Figure 43: NO <sub>x</sub> emission factors for after-treatment failures and normal trucks.....	54
Figure 44: The relationship between meteorological variables and NOx emission factors based on plume chasing measurements.....	55

Figure 45: Comparison of vehicle-specific NO <sub>x</sub> emission factors measured by PEMS and chasing concurrent test.....	56
Figure 46: The relative influence of drivers on NO <sub>x</sub> and BC emissions of HDTs based on GBM machine learning model.....	57
Figure 47: Boxplot of fuel-specific NO <sub>x</sub> and BC EFs of HDTs from China III to China V emission standards.....	58
Figure 48. Generalized addition model of fuel-specific NO <sub>x</sub> emissions based on ambient temperature and BC emissions based on speed for China III-V HDTs.....	59
Figure 49. Annual variations in NO <sub>x</sub> emissions of HDT fleet in China and comparison with regulatory and previous results in 2010–2019.....	60
Figure 50: Comparison of NO <sub>x</sub> emission measurements by means of RES type 3 and SEMS on three different vehicles.....	62
Figure 51: Results from RES type 3 NO <sub>x</sub> measurements on heavy-duty trucks in Prague/Brno 2022 – daytime vs nighttime measurements.....	63
Figure 52: Results from roadside inspections of suspected high-emitting heavy-duty trucks based on RES type 3 measurements.....	63
Figure 53: Average NO <sub>x</sub> and PN concentrations for cars A, B, C and D recorded in relation to ambient temperature.....	65
Figure 54: Trip NO <sub>x</sub> and PN emissions for cars A, B, C and D recorded in relation to ambient temperature.....	65
Figure 55: Maximum NO <sub>x</sub> and PN concentrations for cars A, B, C and D recorded in relation to ambient temperature.....	66
Figure 56: An example of NO <sub>x</sub> and PN concentration during an acceleration event from an urban area to highway.....	67
Figure 57: Example of NO <sub>x</sub> and PN emissions during an acceleration event from an urban area to highway.....	67
Figure 58: Pollutant mass fraction in the CEP of a vehicle driven at 50 km/h for LH and LD tailpipe configurations.....	69
Figure 59: Pollutant dispersion behavior of a vehicle driven at 30, 50 and 80 km/h with a LH tailpipe.....	70

## List of Tables

Table 1: Overview of RES type 3 measurements carried out in Europe. ....	27
Table 2: Key information of the test vehicles. ....	28
Table 3: Number of tests and average trip ambient temperature range in respect to each test vehicle. ....	29
Table 4: Overview of results of RES type 3 measurements carried out on heavy-duty trucks in various countries in Europe 2016-2021. ....	63
Table 5: Test data summarizing NO <sub>x</sub> and PN emissions as average and maximum concentrations together with the corresponding trip-based results. ....	66

## Introduction

Largely as a consequence of the dieselpgate scandal, revealed in 2014 [1], the efforts to further reduce air pollutant emissions from road traffic, and in particular NO<sub>x</sub> emissions, through stricter emission legislation have increased substantially in the last 5-10 years, not only in Europe but also in China and in the US. In Europe, the introduction of the Euro 6 standard and the associated stepwise Real Driving Emissions (RDE) Regulation are the clear examples of the new ambitions to strongly reduce emissions from vehicles when they drive on the road and not only in the legislative laboratory test cycles. With a few years backlog a similar tightening of the emission legislation has taken place also in China.

Still, air pollution – with road traffic as the main source – is a lingering health problem in many large cities all over the world – Europe, China and North America not exempted. For instance, in 2022 around 1 % of all the air quality monitoring stations in Europe, all of them traffic stations located in nine EU member states, recorded concentrations above the EU annual limit value for NO<sub>2</sub> of 40 µg/m<sup>3</sup>. On the contrary, 72 % of the stations, located in all the 27 EU member states, reported concentrations above the WHO NO<sub>2</sub> guidelines level of 10 µg/m<sup>3</sup>. A similar picture with regard to exceedances of air quality limit and guidelines values is seen for particulate matter, both PM<sub>10</sub> and PM<sub>2.5</sub>, with road traffic being a major source [2].

Reaching the new very strict WHO Air Quality Guidelines introduced in 2021 [3], will most likely require a near full-scale compliance of the in-use vehicle fleet with the recently implemented real driving-based emission legislation, which in turn will require, apart from the legislative testing for vehicle type approval and in-service conformity, also efficient road worthiness testing (PTI and I/M programs). An evolving complementary cornerstone to efficiently further reduce vehicle emissions and improve air quality is measurements of emissions from individual vehicles in real-world operation from the roadside or from chasing vehicles, more commonly referred to as remote sensing or remote emission sensing (RES).

This report compiles the work of the partners of IEA AMF Task 61 to summarize state-of-the-art and review the opportunities and limitations of applying RES for 1) direct enforcement of vehicles not complying with the increasingly stricter emission standards over the last 5-10 years in both Europe and China, and 2) air pollution policy purposes to more generally learn about real-world vehicle emissions in order to find the most effective ways to reduce them. In this work inclusion of data, results and experiences from extensive studies with onboard emission measurement techniques, i.e., PEMS, as well as advanced modelling of vehicle exhaust plumes have been a major and crucial asset.

## Objectives

The objective of Task 61 is to evaluate and propose how remote emission sensing (RES) can be used - for policy purposes as well as for direct enforcement - to detect high-emitting/gross-polluting vehicles in real-world traffic. The project will make use of:

- the on-going efforts in mainly Europe and China to further refine existing as well as develop new RES technologies for contactless and non-intrusive measurements of real-driving emissions on an individual vehicle level, and
- the large number of past, on-going, and planned remote emission sensing measurement campaigns in European cities in the coming years, primarily as a direct or indirect consequence of the dieselgate scandal emerging in 2014.

Task 61 comprises all vehicle categories, i.e., passenger cars, light commercial vehicles, and heavy vehicles (i.e., heavy trucks and buses), running on commonly used combustion fuels, i.e., petrol, diesel and CNG, but also biofuels, and designed to meet all adopted legislative emission limits (e.g., Euro 1 - Euro 6). However, special attention is paid to high-emitting vehicles designed to meet the most recent emission standards, e.g., Euro 6. Target pollutants are nitrogen oxides and particulate matter, for which exceedances of air quality standards still occur in many densely populated areas of the world, whereas air quality problems related to carbon monoxide (CO) and hydrocarbons (HC) today are almost negligible thanks to the introduction of efficient three-way catalysts on light-duty petrol cars more than 30 years ago.

Task 61 aims to evaluate and compare the performance and applicability of the following main types of RES technologies to identify high-emitting vehicles (see Figure 1):

- 1) Conventional RES (type 1) – this is in practice the technologies that are already offered to the market by commercial providers for emission measurement services.
- 2) Point sampling RES (type 2) – in terms of measurement strategy point sampling RES is quite similar to type conventional RES, but it is still under development, i.e., not yet commercialised, and has its main advantage for measuring PM emissions, both number and mass.
- 3) Plume chasing RES (type 3) – from a measurement strategy perspective rather different to type 1 and 2: Not as many vehicles can be measured per time unit, on the other hand the measurements on each vehicle have a longer duration than in the case of 1 and 2 → more straightforward to pinpoint high-emitters.

In the work of Task 61 to evaluate, compare and improve the performance of the three different RES types to identify high-emitting vehicles, research studies involving onboard emission measurements by means of PEMS and SEMS systems, as well as simulations of exhaust plumes – by means of further developed highly advanced state-of-the-art models – during typical real driving conditions, have been an underlying pillar for a better overall understanding of the very complex matter of road vehicle emissions.

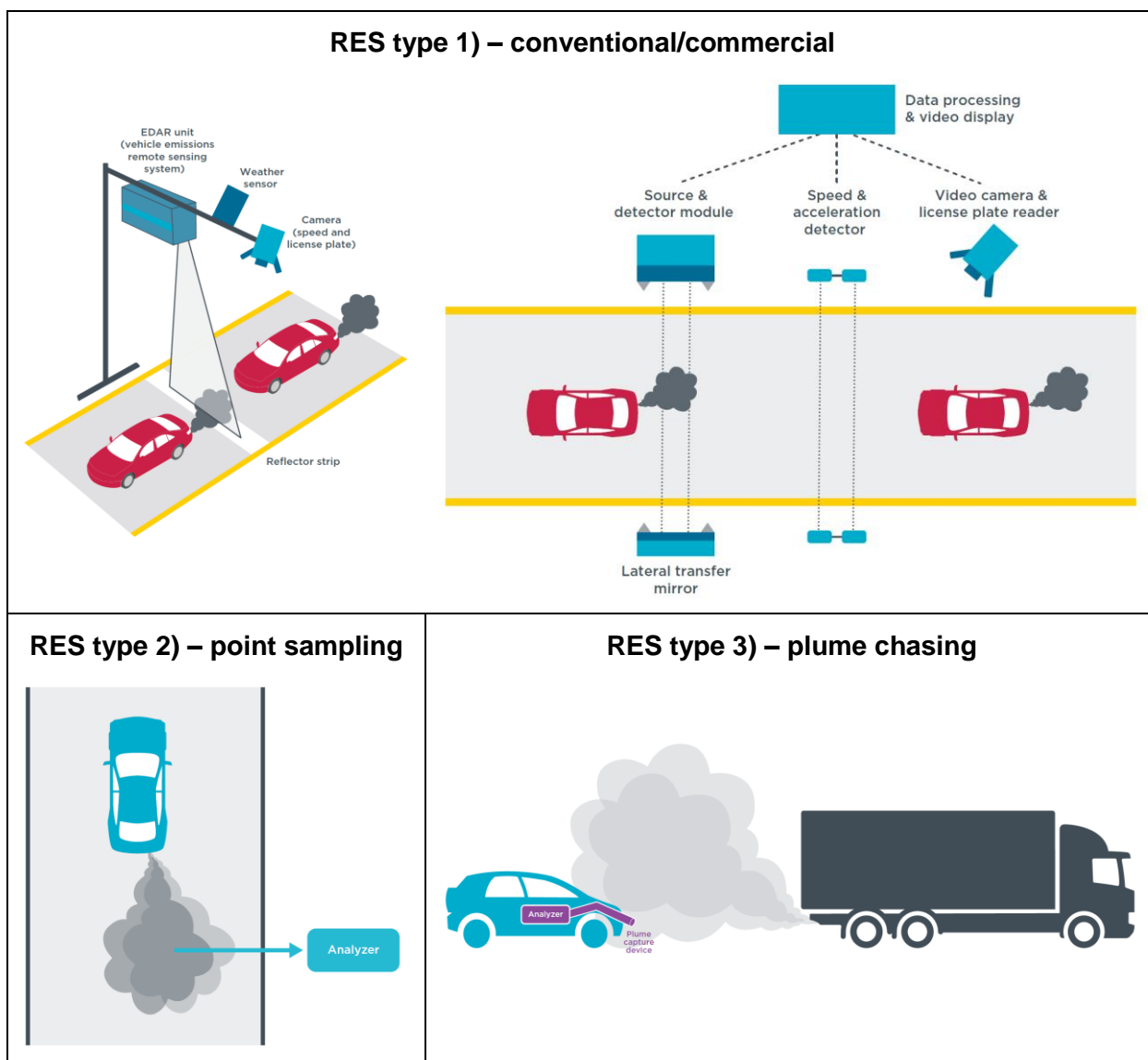


Figure 1: Overview of the three different types of remote emission sensing (RES) techniques.

Both for the comparison and evaluation of the performance of the different RES technologies and for responding to the project's objective to come up with proposals on how these can practically be used - for policy purposes as well as for direct enforcement - to combat excess real-world vehicle emissions, the project will make use of existing RES datasets in Europe, China and the US, and new datasets from upcoming RES measurement campaigns in the next few years to come (2020-22). Dataset examples are:

- The CONOX remote sensing database was originally developed and set-up in 2017 within the CONOX project, an initiative by the Swiss Federal Office of the Environment under the umbrella of ERMES (<https://www.ermes-group.eu/>). At present (April 2020) the database, now entitled CONOX+, holds data from RES measurements (type 1) on about 1.4 Mio vehicles. The database is hosted by IVL.
- The H2020-project CARES (<https://cares-project.eu/>), launched in summer 2019 and running until late spring 2023, in which three major RES measurement campaigns

were carried out in the cities of Prague, Milan and Krakow. All the three RES types were applied in these measurements, and in addition a dedicated controlled experiment campaign involving all three RES types and PEMS measurements on a small sample of untampered and tampered vehicles was carried out in June 2020. The CARES project is coordinated by IVL.

- Similar RES measurement campaigns as in the CARES project in two major cities in China in the framework of a project financed by the Ministry of Science & Technology, with a similar objective as and strongly associated with the CARES project (mutual collaboration and exchange of results and experiences).
- On-going major RES projects in Denmark and Switzerland (task sharing participants in this project), and in other countries such as Germany.
- On-going projects involving PEMS and chassis dynamometer measurements on in-use vehicles in several countries that are task sharing participants in this project.
- In China, Ministry of Science and Technology (MOST) supported two major projects (2018YEF0106800, in partnership with CARES, and 2017YFC0212100) on RES type 3 technology. A mobile plume chasing database of NO<sub>x</sub> and BC emission factors for more than 13000 heavy-duty trucks (HDTs) in China has been accumulated by June 2023. Concurrent comparison tests between plume chasing and PEMS were also conducted.

## Methodology

### RES type 1 - conventional/commercial RES

The first RES technology was developed already in the late 1980's by researchers at the University of Denver, commonly known as the Fuel Efficiency Automobile Test or FEAT [4]. The original FEAT instrument used NDIR (Non-Dispersive Infra-Red) spectroscopy to measure the concentrations of carbon monoxide (CO) and carbon dioxide (CO<sub>2</sub>) across the road in the dispersing exhaust plumes of passing vehicles from the roadside in less than one second (Figure 2). By determining the ratio of CO to CO<sub>2</sub> in the exhaust plume the instantaneous emission of CO expressed as grams per kg fuel burnt can be determined from the fuel combustion equation. The emission measurement is synchronized with a video camera taking a snapshot image of the rear or front license plate of the measured vehicle, in order to retrieve technical vehicle information from the vehicle registry for the further analysis of the emission data collected. The major advantage with RES Type 1 is the ability to measure the emissions from thousands of vehicles in a normal working day.

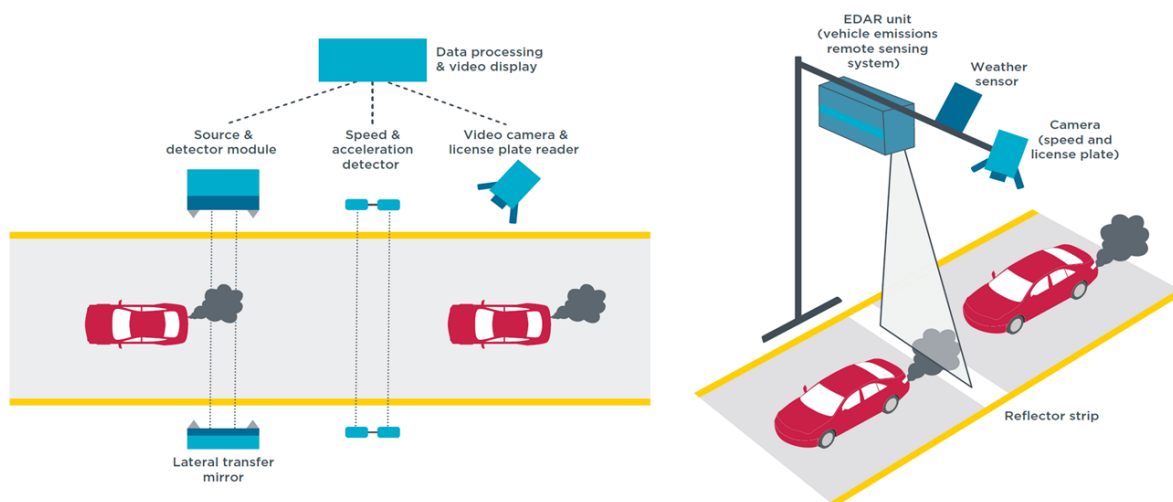


Figure 2: Schematic principle and set up for a RES type 1 instrument (left: original cross-road – horizontal – RES; right: the newer vertical RES).

Over the years RES type 1 has gone through a major development, enabling measurements of emissions of also HC, NO, NO<sub>2</sub> (i.e., NO<sub>x</sub>), NH<sub>3</sub>, CH<sub>4</sub> and particulate matter, of speed and acceleration (yielding vehicle specific power data in kW/ton), and deploying automatic license plate readers [5]. The first commercial instruments, building on the FEAT device, came to the market already in the early 1990's, and have been used for enhanced US state I/M programs since the mid-1990's [6] and for enforcement purposes also in China in the last ten years [7], but – so far – merely for research, demonstration or real-world emission evaluation purposes in Europe. Today there is one commercial provider of RES type 1 instruments in Europe ([opusrse.com](http://opusrse.com)), one in the US ([heatremotesensing.com](http://heatremotesensing.com)), and – at least – one in China (<http://subsites.chinadaily.com.cn/>).

More recently, methodologies to convert the directly measured g/kg fuel emissions by RES type 1 instruments to be expressed in g/km have been developed [8,9], which is practical for e.g., evaluating measurement results against emission standards given by law. These methodologies can also be applied to RES type 2 data.



## RES type 2 - point sampling RES

The RES type 2 principal shares many similarities with RES type 1, the main difference being that RES type 2 measures the concentrations of exhaust components from the roadside in one point through extractive sampling, thereby the name point sampling RES – see Figure 3.

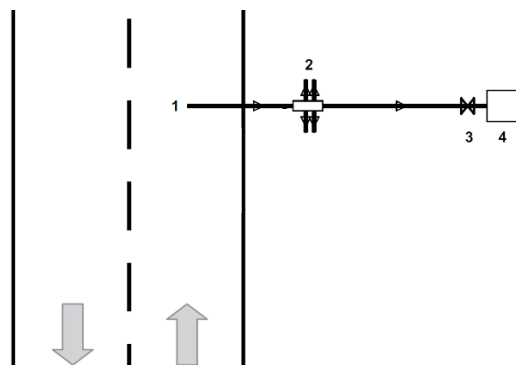


Figure 3: Schematic principle and set-up for RES type 2 instrument (adapted from reference 10).

(1) Sampling tube inlet located in the center of – alternatively close to – the lane, secured to the road surface or the pavement, (2) dilution volume with connectors for the CO<sub>2</sub> instrument and for connecting additional pollutant monitoring instruments, (3) valve for sampling flow regulation, (4) sampling pump.

To be able to measure the emissions from individual vehicles, the CO<sub>2</sub> instrument and the deployed air pollutant monitoring instruments must measure with a sufficiently high time resolution – 1 Hz or higher. An example of a measurement series is presented in Figure 4. The measured concentrations of any exhaust component are plotted against the measured concentrations of CO<sub>2</sub> in the plume peak and if a sufficiently strong correlation between the two is achieved, the ratio between the two can be used to derive the instantaneous emission factor of the pollutant measured expressed as gram per kg fuel burnt, similar to the principle for RES type 1 measurements.

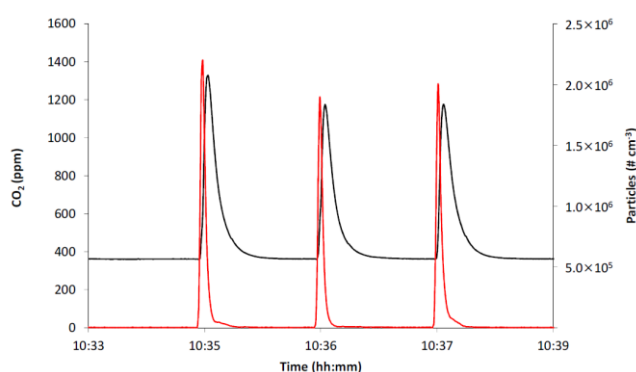


Figure 4: Example of measured concentrations with an RES type 2 instrument from three successive passages of the same vehicle, in this case a bus in acceleration mode (Ref 14). Measured particle number (red line) and CO<sub>2</sub> concentration (black line).

The first applications of the RES type 2 technology were made to measure particulate matter emissions with rather sophisticated, research-grade particle analyzers [10,11]. More recently, low-cost sensors to measure particle number and Black Carbon (BC) emissions have been developed for RES type 2 applications, as well as NO/NO<sub>2</sub>/NO<sub>x</sub> analyzers [12].

The fuel-based emission factor of individual vehicles can be calculated based on the concentration ratio of the target pollutant to CO<sub>2</sub>. The calculation in this study uses the simplified carbon balance method, which assumes all carbon in the fuel converts to CO<sub>2</sub>. The fuel-based emission factor for pollutants  $P$  ( $EF_P$ ) is shown in Equation 1,

$$EF_P = \frac{\Delta[P]}{\Delta[CO_2]} w_c \quad (1)$$

where  $w_c$  represents the carbon fraction of fuel and was set to 0.87 in this study. The  $\Delta[P]$  and  $\Delta[CO_2]$  are the increments of pollutant  $P$  and CO<sub>2</sub>, and calculated by the difference between peak maxima and background concentrations:

$$\Delta[CO_2] = CO_{2max} - CO_{2bg} \quad (2)$$

$$\Delta[P] = P_{max} - P_{bg} \quad (3)$$

The  $P_{bg}$  and  $CO_{2bg}$  are the background concentrations, which are calculated with a time interval of 5 minutes. The units for NO emission factor (NO-EF) and PN emission factor (PN-EF) are g/kg and #/kg, which refers to grams (g) of NO and numbers (#) of particle emitted by per kilogram of fuel burned. In this study, we selected the peak height method for calculating the emission factor instead of integrating the peak area to minimize the artifacts from instrument delay.

A correction factor for  $\Delta[NO]$  is required to count for the artifacts caused by the response time of NO sensor. The electrochemical NO sensor rises slower than the CO<sub>2</sub> analyzer. The rise time of a typical plume in this study is around 3 seconds, which is adequate for CO<sub>2</sub> and PN to give full response while only allow the NO sensor to give approximately 63% relative response. Therefore, the  $\Delta[PN]$  need no further correction while a semi-experimental correction coefficient of 1.59 (= 1/0.63) was used for  $\Delta[NO]$  in this study.

The limit of quantification (LOQ) for emission factor is determined by the concentration ratio between the detection limit of  $\Delta[P]$  and corresponding  $\Delta[CO_2]$ . Similar to Eq. 1, we estimate the limit of quantification (LOQ) of emission factor  $EF_{P,LOQ}$  as:

$$EF_{P,LOQ} = \frac{\Delta[P]_{LOD}}{\Delta[CO_2]} w_c \quad (4)$$

Where  $\Delta[P]_{LOD}$  is the limit of detection (LOD) of pollutant  $P$ . The LOD of different species are determined by three times of the standard deviations of the background signals, which is around 5 ppm, 10 ppb, and 1000 #/cm<sup>3</sup> for  $\Delta[CO_2]$ ,  $\Delta[NO]$  and  $\Delta[PN]$ . The  $EF_{P,LOQ}$  is principally dependent on  $\Delta[CO_2]$  instead of a fixed value, the relationship between them are presented in Figure 44b. During the experiment, the majority of  $\Delta[CO_2]$  in this study are within the range of 10-100 ppm. Therefore, the LOQ for NO emission factors (NO-EF) and PN emission factors (PN-EF) are roughly 2 g/kg and  $1 \times 10^{14}$  #/kg in relatively diluted plumes ( $\Delta[CO_2] = 10$  ppm), as detailed discussed in the Supporting Information. For the high emitter identification propose, the data below LOQ should not be ignored, but should be considered as the reference range between 0 and the LOQ. The k-means algorithm groups the objects into a specific number of clusters by their relative positions. The algorithm automatically adjusts the grouping until the mean distance between the cluster center and the belonging data points reaches the minimum. The position and distance in the k-means algorithm are virtual concepts. In this study, the positions are defined within a two-dimensional space, and the distances are calculated using  $\log(PN-EF)$  and  $\log(NO-EF)$  as the two dimensions.

### RES type 3 - plume chasing RES

Mobile plume chasing (RES type 3) uses a vehicle equipped with high-resolution pollutant analyzers to chase the prior vehicle and measure its on-road pollutant emissions (Figure 5). The plume emitted from the prior vehicle is rapidly diluted after entering the atmosphere and captured by the sampling inlet mounted at the front of the mobile platform. Based on the assumption that contaminants such as nitrogen oxides (NO<sub>x</sub>)/ black carbon (BC) are rapidly diluted with carbon dioxides (CO<sub>2</sub>) in equal proportions for a short time, the fuel-specific emission factor (g/kg-fuel) was established based on the carbon balance method by taking CO<sub>2</sub> as a fuel tracer (see Equation 4). Thus, characterizing the individual emission level and identifying high emitters among massive on-road vehicles.

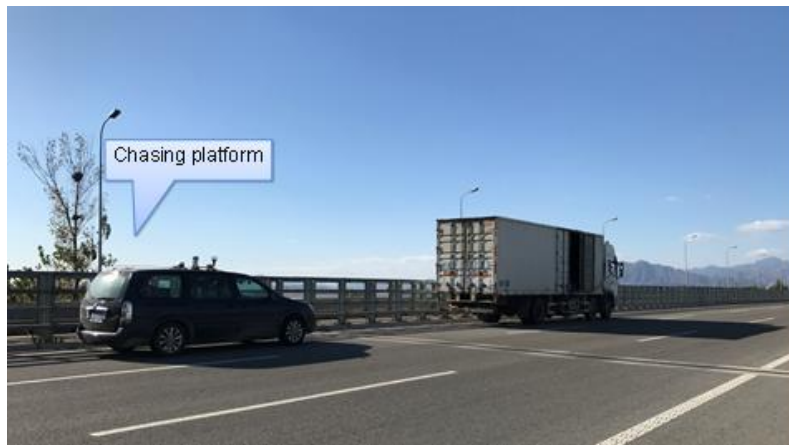


Figure 5: Field study of chasing – RES type 3 – tests.

$$EF_p = \frac{\Delta[P]dt}{\Delta[CO_2]dt \left( \frac{MW_C}{MW_{CO_2}} \right)} \cdot w_c \quad (4)$$

where  $\Delta[i]=[i]-[i]_0$ ,  $i=CO_2$ , P (NO<sub>x</sub>, BC),  $\Delta[i]$  represents the net concentration of pollutant  $i$ ;  $[i]$  represents the diluted exhaust concentration of  $i$  for the target vehicle ( $g\ cm^{-3}$ );  $[i]_0$  represents the background concentration of pollutant  $i$  ( $g\ cm^{-3}$ );  $EF_p$  is the emission factor of pollutant P in grams of pollutant emitted per kilogram of fuel consumed (g/kg-fuel);  $MW_C$  and  $MW_{CO_2}$  is the molecular weight of the carbon and carbon dioxide;  $w_c$  is the mass fraction of carbon in the fuel, it is 0.86 for diesel.

## On-board emission measurements – PEMS and SEMS

PEMS (Portable Emission Measurement System) are on-board emission measurement devices used for quantifying the emissions produced by light- or heavy-duty vehicles in real world conditions. The PEMS devices are simplified laboratory grade equipment that are connected to the tail-pipe of the test vehicle. The device itself may be installed on e.g., a vehicle towing hook or in the vehicle boot alternatively. Typical PEMS devices are able to measure following emission components: CO<sub>2</sub>, CO, NO<sub>x</sub> and PN. The PEMS devices are additionally able to monitor the momentary emissions produced by a vehicle, and therefore it enables to study in detail the emission performance in respect to a wide variety of variables. PEMS devices enables e.g., determining any situations or road conditions where high emissions may take place.

PEMS devices are currently used as a part of the type approval processes for determining the real driving emissions (RDE) for a specific vehicle model. The RDE test was introduced in four different RDE-packages between 2016 and 2018. The main objective for deployment of RDE was primarily monitoring of NO<sub>x</sub> and PN emissions in real-world environments, and thus to improve the correlation between vehicle emission performance between laboratory tests and real-world conditions. The European Union adopted the RDE procedure as a part of the type-approval (TA) process by the deployment of RDE 4, starting from 2017 [13]. The combined uncertainties caused by the PEMS-measurements in RDE were tackled by applying separate conformity factors (CF) for NO<sub>x</sub> and PN. The usage of CF resulted in separate RDE derived emission limits, i.e., not-to-exceed (NTE) limits. The RDE4 package was initially adopted with temporary, more lax conformity factors, before eventually entering fully in form in its final form in 2020. Vehicles type-approved within the temporary stage were called Euro 6 d-TEMP. In Euro 6 d-TEMP, the CF factors for NO<sub>x</sub> was 2.1 and for PN, 1.5 respectively. The corresponding final figures for Euro 6d (RDE4) were 1.43 for NO<sub>x</sub> and 1.5 for PN. Since the deployment of the RDE test, the RDE regulation has been supplemented and revised from multiple perspectives. For example, the CF factors have been revised and further reduced both for NO<sub>x</sub> and PN among others. In the most recent stage, Euro 6e, which was adopted in 2022, CF numbers for NO<sub>x</sub> was reduced to 1.1 and PN was reduced to 1.34 correspondingly.

The NTE limits are defined for NO<sub>x</sub> and PN following:  $NTE\text{-limits} = CF \times \text{EURO-6 limits}$ . For example, the NTE NO<sub>x</sub> limit for Euro 6 d-TEMP is  $2.1 \times 800 \text{ mg} = 1680 \text{ mg/km}$  and correspondingly for PN,  $1.5 \times 6 \times 10^{11} \text{ \#/km} = 9 \times 10^{11} \text{ \#/km}$ .

The RDE procedure is acting as a supplementary method for laboratory testing for determining and ensuring the robustness of the emission performance for the road vehicles. For vehicles produced prior to 2017, the emissions were solely determined explicitly in controlled laboratory conditions. Because of this, the absolute, vehicle specific correlation between the emissions determined in the laboratory and the real emissions produced in real world conditions may often remain unknown. However, several studies produced for vehicles produced prior to 2017 indicate that the real-world emissions were typically significantly higher in RDE compared to the TA values declared by the manufacturers in laboratory testing. Since the implementation of the RDE procedure, especially since CF factors have been reduced, the robustness of vehicle emission characteristics have in real world conditions drastically improved.

A SEMS (Smart Emissions Measurement System) is a smaller, simplified PEMS that measures the concentrations of NO<sub>x</sub>, PN, CO and CO<sub>2</sub> in the vehicle exhaust equally well as a PEMS, but doesn't measure the exhaust flow, which the PEMS does by means of a dedicated exhaust flow meter. Instead, the exhaust flow is often calculated from data taken from the vehicle's OBD system. However, a SEMS measures accurately the ratios – of pollutant emissions to CO<sub>2</sub> emissions, e.g., NO<sub>x</sub> to CO<sub>2</sub>, on a second-by-second basis,

which is a useful measure of the NO<sub>x</sub> emission performance for different conditions regarding e.g., driving behavior, vehicle load and ambient temperature. This ratio is often entitled NO<sub>x</sub>-Index and expressed in mg NO<sub>x</sub> per gram CO<sub>2</sub> emitted.

The main advantages of a SEMS compared to a PEMS are the hardware costs and the measurement costs associated with the mounting, since a SEMS may only take a few minutes to install. It also does not occupy as much space of the vehicle as a PEMS does.

Typical setups of PEMS and SEMS instruments are shown in Figure 6.



Figure 6: A typical PEMS (top) and SEMS setup (bottom).

## Exhaust plume modelling

Direct numerical simulations (DNS) and (wall-resolved) large eddy simulations (LES) are computationally too expensive for the flow around a vehicle ( $Re > 10^6$ ). Therefore, in the present work, the Unsteady Reynolds-Averaged Navier-Stokes (URANS) equations are used. In this way, turbulent scales are modeled, but large coherent vortex structures are resolved. These structures/eddies are coherent because they occur with some regularity. For this reason URANS is considered to be an eddy-resolving method [14]. This implies that the detachment of the flow around the vehicle creates not only a large number of small turbulent eddies, but also recurring large eddies. However, all turbulent fluctuations of the flow are treated by the turbulence model.

The following describes the setup of a simulation environment in OpenFOAM for the flow around a vehicle, which is emitting exhaust gases. Thus, temperature as well as density vary in space and time, since the exhaust is a high temperature multicomponent mixture. Therefore, the Navier-Stokes-Fourier system of equations containing the conservation equations of mass, momentum, energy and species are considered to simulate the mentioned flow problem.

$$\begin{aligned} \frac{\partial \bar{\rho}}{\partial t} + \frac{\partial (\bar{\rho} \tilde{u}_i)}{\partial x_i} &= 0 \\ \frac{\partial (\bar{\rho} \tilde{u}_i)}{\partial t} + \frac{\partial (\bar{\rho} \tilde{u}_i \tilde{u}_j)}{\partial x_j} &= - \frac{\partial \left( \bar{p} + \frac{2}{3} \bar{\rho} k \right)}{\partial x_i} + \frac{\partial}{\partial x_j} \left[ \underbrace{\mu_{\text{eff}} \left( \frac{\partial \tilde{u}_i}{\partial x_j} + \frac{\partial \tilde{u}_j}{\partial x_i} - \frac{2}{3} \frac{\partial \tilde{u}_k}{\partial x_k} \delta_{ij} \right)}_{\tau_{ij}} \right] + \bar{\rho} \tilde{g}_i \\ \frac{\partial}{\partial t} (\bar{\rho} E) + \frac{\partial}{\partial x_j} (\bar{\rho} \tilde{u}_j H) &= \frac{\partial}{\partial x_j} \left( \alpha_{\text{eff}} \frac{\partial \tilde{h}}{\partial x_j} \right) + \frac{\partial}{\partial x_j} \left( \tilde{u}_j \tau_{ij} + \underbrace{\sum_k \overline{h^k J_j^k}}_{\text{small influence, therefore neglected}} \right) + \bar{\rho} \tilde{g}_i \tilde{u}_i \\ \frac{\partial (\bar{\rho} \tilde{Y}_k)}{\partial t} + \frac{\partial}{\partial x_i} (\bar{\rho} \tilde{u}_i \tilde{Y}_k) &= \frac{\partial}{\partial x_i} \left( \bar{\rho} D_{\text{eff}} \frac{\partial \tilde{Y}_k}{\partial x_i} \right) \\ \bar{p} &= \bar{\rho} R_u \tilde{T} \sum_k \frac{\tilde{Y}_k}{W_k} \end{aligned}$$

The above described equations are implemented in the open source CFD platform OpenFOAM, making use of its existing solvers and various functionalities [15]. The PISO (Pressure Implicit with Splitting of Operators) algorithm is chosen to iteratively solve the coupled equations. Therefore, the continuity equation is not solved for the density but used to construct a pressure-poisson equation as presented in [16]. Thus, mass conservation is still ensured (through construction of the pressure-poisson equation) and the simulation runs very stable for low-Mach numbers. The time step is obtained by the Courant-Friedrichs-Lewy (CFL) condition and continuously updated to conform with  $\text{CFL} < 1$ . For further details please refer to [17].

To provide additional insights on the exhaust plume dispersion downstream a realistic vehicle and how this affects an on-road RES measurement, a parameter study deepening and extending the one by [18] was carried out to relate various properties of the exhaust plume to the given circumstances. Since the parameter study led to numerous simulations, this was another reason URANS was chosen instead of LES. However, a novel hybrid LES/RANS dual-mesh framework was developed for future investigations to further increase the accuracy of URANS simulations but reduce the computational cost of LES drastically [19].

## Activities and data

### RES type 1 measurements

#### Danish studies on roadside remote sensing

Measurements with RES type 1 were carried out in Denmark in 2019, focusing on the detection of high-emitting heavy-duty trucks [20]. The report presents results of field campaign studies with roadside remote sensing equipment for online detection of road traffic emissions of nitrogen oxides from individual vehicles. The project focused on control of SCR cleaning systems for removal of nitrogen oxides (NO<sub>x</sub>) in the exhaust from heavy-duty trucks and methods for identification of malfunctioning (manipulated and defect) SCR-systems.

The project was divided in the following activities:

1. Assessment of which RES type 1 RSD method that will be most suitable for control of SCR-systems on heavy-duty trucks in Denmark, and under which driving conditions the method can be applied.
2. Perform tests in a closed area with the aim of validating measurement methods, and determining emission levels beyond which heavy-duty trucks are most likely equipped with malfunctioning SCR-systems or particle filters. These emission levels are in the following termed emission thresholds. The tests include measuring emissions from heavy-duty trucks with well-functioning SCR-systems and particle filters followed by measurements on the same heavy-duty trucks where the SCR-systems and particle filters are deliberately switched off or removed. The reason for removing particle filters in some of the tests is that for some of the manipulation methods this is a necessity. In these situations, emissions will be enhanced for both nitrogen oxides and particles.
3. Selection of 1-3 field sites suitable for carrying out measurements with the RSD method in combination with subsequent police control of heavy-duty trucks suspected to be equipped with malfunctioning SCR-systems. The focus of the campaigns is to measure a large number of heavy-duty trucks, and subsequently to perform police roadside control of heavy-duty trucks with emissions exceeding the emission threshold. In addition, 11 emissions from all passenger cars that pass the measurement site are measured, which allows a large number of samples to be obtained from the Danish car fleet.
4. On basis of the above mentioned, the enhanced emissions of nitrogen oxides related to malfunctioning SCR-systems are estimated. This estimate is used for calculations of the increase in health effects related to enhanced emissions of nitrogen oxides.
5. Develop an outline for a method for routine control of SCR-systems based on measurements of the RSD method in combination with police roadside control of heavy-duty trucks for which the measurements show emissions exceeding the emission threshold indicative of malfunctioning SCR-systems.

## CONOX project - RES type 1 data pooling and comparison with PEMS data

In the so called CONOX project more than 700,000 emission data records from RES type 1 measurements carried out in Spain, Sweden, Switzerland and United Kingdom between 2011 and 2017, were pooled and analyzed, with a particular focus on the real-world NO<sub>x</sub> emission performance of Euro 5 and Euro 6 diesel passenger cars [8]. The results of were compared with PEMS data from national surveys conducted in the UK, the Netherlands, France and Germany. For Euro 5 comparison there were 128 PEMS tests and about 58,000 remote sensing measurements, whereas for the Euro 6 comparison there were 173 PEMS tests and about 16,000 remote sensing measurements.

## Swedish study focusing on early Euro 6 diesel cars

RES type 1 measurements with an Opus RSD 5000 instrument were carried out in summer 2018 outside Stockholm along a trunk road carrying a high share of commuters [21]. The objective of the study was to demonstrate and evaluate the potential of remote sensing to be used as a complementary tool, when e.g., targeting non-compliant and high-emitting vehicles, as individuals and/or certain types or groups of vehicles, in in-service conformity testing, in-use compliance programs and PTI (periodic technical inspection) programs. The use of a high-commuter site enabled repeat remote sensing measurements on a substantial share of passing vehicles. Based on the remote sensing Euro 5 and Euro 6 light-duty diesel vehicles, mainly early Euro 6 (Euro 6ab) passenger cars, were recruited for PEMS RDE tests as well as chassis dynamometer measurements over the legislative driving cycles (NEDC and WLTP). 30 vehicles were recruited, of which all were measured with PEMS

## RES type 1 measurements in the CARES project

CARES was a Horizon 2020 flagship project running from May 2019 through April 2023 (<https://cares-project.eu/>). Four major measurement campaigns involving RES type 1 instruments were carried out in the project in 2021 and 2022:

- Controlled characterization experiments at a vehicle test track in the Netherlands: Six vehicles (two passenger cars, an LCV, a heavy-duty truck, a scooter and a motorbike) were measured under different driving conditions on vehicles in both emission tampered and non-tampered mode, producing 1,400 passes past an Opus RSD 5500 instrument [22,23]. Also, RES type 2 and 3 as well as PEMS measurements were carried out simultaneously for instrument comparison purposes.
- City demonstration measurements in Milan [24]: Measurements were carried out with two vertical RES type 1 instruments (HEAT EDAR) deployed at two different sites, producing about 35,000 emission records. RES type 2 and PEMS measurements were carried out simultaneously for instrument comparison purposes. The primary aim of the measurements in Milan was to evaluate the potential of RES to track air quality policy effectiveness, e.g., to further develop and follow up the impact of the city's low emission zone (LEZ).
- City demonstration measurements in Krakow [24]: Measurements were carried out with several horizontal RES type 1 instruments (Opus) at a multitude of sites, producing more than 100,000 emission records. Parallel measurements with RES type 2 instruments were carried out at some sites. The primary aim of the measurements in Krakow was to evaluate the potential of RES to steer new policies, in this case to prepare for the implementation of the first LEZ in Poland.
- City demonstration measurements in Prague/Brno [24]: Measurements were carried out with several horizontal RES type 1 instrument (Opus) at a multitude of sites,



producing more than 100,000 emission records. RES type 2 and 3 as well as PEMS measurements were carried out simultaneously for instrument comparison purposes. The primary aim of the measurements in Prague and Brno was to evaluate the potential of RES to identify high-emitting vehicles.

### Other RES type 1 measurement campaigns in Europe of relevance for Task 61

During the three and a half years that Task 61 has been running, several other major RES type 1 measurement campaigns have been carried out across Europe from which it has had access to both data and results reports, mainly through the continued operation of the CONOX remote sensing database by IVL and different activities within the CARES project.

- Measurements in Flanders (2019): Two HEAT EDAR instruments were deployed at five different sites across Flanders in June 2019, providing nearly 190,000 valid emission records [25]. Two of the sites were at motorways with a speed limit of 120 km/h, which means that this was the first remote sensing study in Europe with a substantial share of high-speed driving conditions, providing more complete coverage of everyday vehicle use. Other objectives were to evaluate how high-emitters can be properly defined and identified and to estimate the occurrence of vehicle tampering (SCR and DPF fraud/malfunctions) by means of remote sensing.
- Measurements in Berlin (2019) and Frankfurt (2020): In these two major studies the first ever remote sensing measurements in Germany were conducted [26,27]. The two studies served similar objectives, such as the influence of ambient temperature and other ambient factors, the influence of vehicle ageing on NO<sub>x</sub> emissions, primary emissions of NO<sub>2</sub>, i.e., NO<sub>2</sub>/NO<sub>x</sub> ratios in the exhaust, validation of HBEFA emission factors and the underlying PHEM model, and identification of high-emitters. In Berlin two Opus RSD 5000 instruments were deployed along two streets in October and November 2019, resulting in more than 100,000 emission measurements on 50,000 unique vehicles. In Frankfurt both the HEAT EDAR and the Opus RSD instrument were deployed at different sites, resulting in 90,000 emission records. The analysis in the Frankfurt study also incorporated the data from the Berlin 2019 study, in order to increase the sample size and thus the statistical robustness of the results.
- Measurements in Brussels (2020): The study in Brussels represents one of the most extensive RES type 1 measurements in a European city, comprising more than 260,000 emission measurements on more than 130,000 unique vehicles at eight different sites using four Opus RSD instruments, of which two were the new RSD 5500 unit, with improved NO<sub>2</sub> capability compared to its predecessor the RSD 5000 [28]. Some of the measurements related to roadside tailpipe PN measurements for the upcoming PN testing in the Belgian PTI.
- Measurements in Switzerland (2021): In the national ReMOVES research project two HEAT EDAR and two Opus RSD 5500 instruments were deployed at eight different sites across Switzerland in June 2021 [29]. 138,000 valid emission measurements were successfully assigned to vehicles for further evaluation. Among the objectives were to compare the HEAT and Opus instruments and to verify their correlation with PEMS RDE measurements at a designated test track, to compare the RES results with HBEFA modeling results, and to evaluate whether remote sensing provides a sound basis for determining high-emitters.

Here should also be mentioned the yearly remote sensing measurements carried out by the Kanton of Zürich since 2002 using Opus RSD instruments and the last reported measurements that were carried out in 2021 [30].

## RES type 1 databases

The first database pooling data from RES type 1 measurements across Europe was the CONOX database developed in the CONOX project 2016-2018 - see above [8].

During and after the completion of the CARES project the CONOX database was gradually substituted with the new CARES database [31], presently holding more than 2 million emission records from about 10 European countries. A special feature of the CARES database is that some of the data is accessible for the public through dedicated apps, see e.g., <https://cares-public-app.azurewebsites.net/>. The most recent data in the CARES database is from the measurement campaign in Prague and Brno in the early fall of 2022.

## RES type 2 measurements

### China

Field experiments were conducted in a driving track located in the rural area of Yancheng, far away from the urban area and industry zones. The tests were carried out on several cloudy daytimes with moderate air temperature (~15-20°C), the prevailing eastward breeze helped the exhaust plumes to disperse steadily. During the field experiment, the sensor platform was placed at the curbside of the downwind direction to measure exhaust plumes from passing vehicles.

The tested vehicles are diesel trucks named as “China-VI”, “China-VI fail”, “China-V”, and “China-V fail”. The “China-VI” and “China-V” are China VI (equivalent to Euro VI) standard medium-duty diesel trucks (MDTs) and China V (equivalent to Euro V) standard heavy-duty diesel trucks (HDTs). The aftertreatment system for “China-V” only includes selective catalytic reduction (SCR), while the aftertreatment system for “China-VI” also includes diesel oxidation catalyst (DOC) and diesel particulate filter (DPF) to further reduce NO<sub>x</sub> and PN (Vressner et al., 2010). The “China-VI fail” and “China-V fail” are the exact vehicles as “China-VI” and “China-V,” but the entire aftertreatment systems were deliberately removed. Therefore, the “China-VI fail”, “China-V”, and “China-V fail” are associated with outdated or failed aftertreatment systems and are expected to be potential high-emitters. For clarity, we call these vehicles “designed high emitters”. Each vehicle drove 15 laps without extra loading, while “China-V” and “China-V fail” drove additional 15 laps with ~5000 kg cargo loading (30 laps each vehicle). The tested driving speeds were 10, 20, 40, 60, and 80 km/h. The total laps are 90 for the whole experiment.

To validate the performance of the sensor platform, the emission factors are compared with an onboard PEMS (OBS-ONE-PN, HORIBA, Japan). The PEMS data are averaged for 30 seconds near the sensor platform, when the vehicles maintained constant speeds.

### Europe

- The emissions of particles from 234 city buses were measured under real-world stop-and-go traffic conditions at a bus stop in Gothenburg, Sweden, in 2016 [32]. The total number of particles was measured with a CPC (Condensation Particle Counter) and the particle number size distribution in the range from 5.6 nm to 560 nm over 32 size channels with an Engine Exhaust Particle Sizer (EEPS) instrument. The measured buses comprised models fulfilling Euro III-VI and EEV (Enhanced Environmentally Friendly Vehicle) standards running on different fuels, such as compressed natural gas (CNG), diesel, Rapeseed Methyl Ester (RME) and Hydro-treated Vegetable Oil (HVO).

- The emissions of particles – as PN, PM and black carbon (BC) – from 556 heavy-duty trucks were measured at a roadside location in Gothenburg, Sweden, in summer 2018 [33]. The measured fleet comprised trucks complying with the Euro III to the Euro VI and the EEV standards.
- In the three city demonstrations (Milan, Krakow and Prague/Brno) in the CARES project in 2021 and 2022, RES type 2 measurements were carried out on in total ≈18,000 (for BC – Black Carbon), ≈13,000 (for PN – particle number) and ≈7,000 (for NO<sub>x</sub>) diesel and petrol passenger cars [24]. The measured vehicles ranged from Euro 2 to Euro 6d.

## RES type 3 measurements

### China

The Tsinghua team has launched large-sized plume chasing campaigns across several regions in China, including the Beijing–Tianjin–Hebei region (BTH region), Yangtze River Delta region (YRD region), Pearl River Delta region (PRD region), Fen–Wei region and Sichuan Basin region (see Figure 7). A database of NO<sub>x</sub> and BC emissions more than 13000 heavy-duty trucks (HDTs) in China has been established by 2023. The large sample test data of multiple test sites enable the comprehensive coverage of technological (e.g., emission standards) and operational conditions (e.g., ambient temperature and driving speed) for real-world HDT emissions. Figure 7 summarizes the vehicle specifications in each region. More than 1000 samples were tested randomly on-road for most region to increase the regional representativeness of the samples. The experimental routes were majorly selected on highways to avoid congested traffic conditions, where exhaust plumes from surrounding plumes can cause uncertainties. The driving speeds are from 10 km/h to 106 km/h and concentrated on 60-70 km/h (~65 km/h on average). These tests were conducted during the daytime (9:00-17:00) in all seasons and the ambient temperature measured at the chasing platform is from –3 C to +40 C.

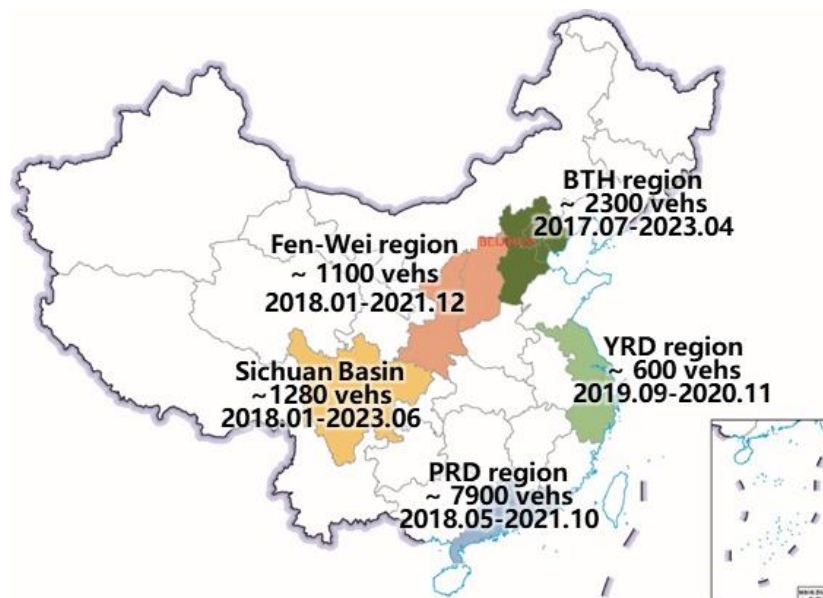


Figure 7: Sample distribution of plume chasing – RES type 3 – tests in China.

The vehicular information for the chasing test was mainly identified by field observation and remotely queried. The vehicular license number plate and mass load were obtained through field observation. Furthermore, 71% of tested vehicles were later identified to match the detailed vehicle specifications in official registration datasets remotely (e.g., Ministry of Ecological Environment, Ministry of Transport). The queried information included fuel type, gross vehicle weight (GVW), emission standard, and manufacture year (MY). The GVW of the tested HDTs was between 4.5 and 49 tonnes and mainly larger than 20 tonnes. As shown in Figure 8, 90% of the chased vehicles are fueled by diesel and 7% fueled by natural gas. Most of the HDTs complied with China III to China V standards. The proportion of China III, China IV, and China V HDT samples to the total tested HDTs was 10%, 31%, and 55%, respectively. A small amount of 4% HDTs complied with China VI emission standard.

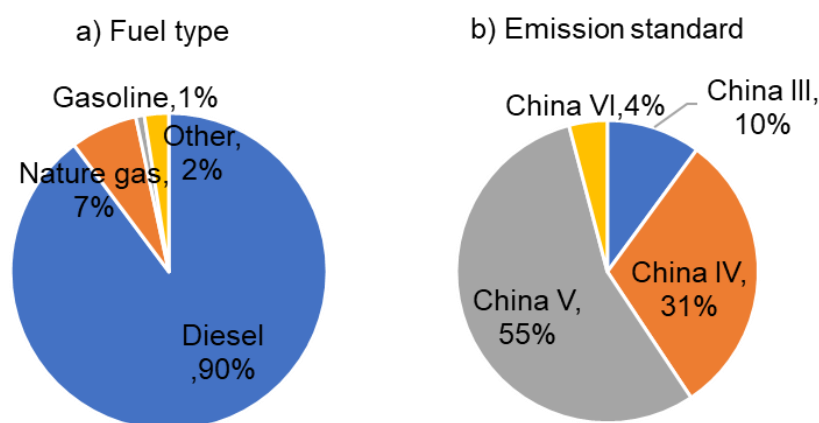


Figure 8: Fleet composition of chased vehicles.

## Europe

RES type 3 measurements were first carried out in Europe on heavy-duty trucks on German highways in 2016 by researchers at the University of Heidelberg. The same research group and its spin-off company Airyx (<https://airyx.de/>) have over the last five years expanded the plume chase measurements in Europe to countries such as Austria [35], further measurements in Germany [36], Switzerland [37], Denmark [38], Sweden [39,40] and Czechia [24] and also carried out measurements on buses and light-duty vehicles. The plume chase measurement technique has been validated against PEMS measurements [22,37] and also compared with RES type 1 and type 2 measurement techniques [22,23].

A summary of the main RES type 3 measurements carried out in Europe is given in Table 1.

Table 1: Overview of RES type 3 measurements carried out in Europe.

Country	Year	No. of HDVs measured	Reference (comments)
Germany	2016	250	[34]
“	2019	140	[36]
Austria	2018	215	[35] (only data for 185 HDVs was evaluated)
Switzerland	2019	39	[37] (comparison with PEMS measurements)
Denmark	2020	480	[38]
Sweden	2020	121	[39] (comparison with PEMS measurements)
“	2021	85	[40]
Czechia	2022	>900	[24] (also ≈1100 LDVs and buses measured)

## PEMS measurements

### RDE/PEMS measurements on light-duty vehicles in Helsinki in 2019

In 2019, VTT conducted a series of RDE/PEMS measurements for four diesel passenger cars. This work was conducted as a collaboration between partners in Finland and in Norway. The main objective of the experiment was to study the day-to-day variation of the emission performance of different Euro 6 class diesel vehicles in respect to vehicle exhaust aftertreatment technologies, vehicle age, and ambient and on-road conditions. More specifically, the purpose of the tests was to monitor how the emission performance of different vehicles within Euro 6, type-approved both outside and within the RDE regulation would perform in various real-world conditions, and thus demonstrate and quantify the variation in between vehicle to vehicle.

From the PEMS device, CO<sub>2</sub>, CO, NO<sub>x</sub> and PN emissions and exhaust mass flow were recorded. The most relevant data gathered from the PEMS tests were exploited and further processed to support the work described in this report. The main purpose of the processed data was to improve the understanding in which specific factors, such as e.g., road sections, ambient temperatures or other conditions would affect the momentary and overall emission performance of Euro 6 class diesel cars. Summarizing these factors would provide with important information regarding factors that should be taken into account when monitoring NO<sub>x</sub> and PN emissions using RES equipment. For this case study, any factors affecting NO<sub>x</sub> and PN emissions were explicitly analyzed. In this case, the overall emission performance regarding both NO<sub>x</sub> and PN were compared with maximum concentrations per trip. This enabled to demonstrate the natural emission behavior of the given vehicles and enabled to understand the magnitude and variation of emissions Euro 6 diesel vehicles may produce in typical daily use. Furthermore, road sections where typically highest emissions were produced were separately analyzed for gaining back-to-back comparison between the emission characteristics of individual vehicles.

The vehicles included in the tests represented family-size and medium size diesel vehicles typically used on the Finnish roads. The vehicle age varied from model year 2015 to 2018. The test fleet included vehicles that were type-approved both within (Euro 6-d TEMP) and outside (Euro 6b) the predominant RDE regulation. Because the non-RDE compliant vehicles (Euro 6b) were not type-approved within RDE, no on-road emission limits nor conformity factors were available nor had been defined by the manufacturers. The cars were equipped with engines that were comparable in terms of engine configuration and displacement. The engine aftertreatment system (EATS) depended on car type approval class yet varied mostly by the NO<sub>x</sub> reduction strategy. Cars A and B were equipped with lean-NO<sub>x</sub> traps (LNT), car C with a selective catalyst reduction (SCR) system and car D with twin LNT technology. All cars but car C were equipped with diesel oxide catalysts (DOC).

A more detailed description of the test vehicles is presented in Table 2.

Table 2: Key information of the test vehicles.

Car id.	Type	Model year	Emission class	Engine displacement [l]	NO <sub>x</sub> conformity factor	PN conformity factor	Transmission	EATS	Vehicle mileage [km]
Car A	Estate	2015	Euro 6 b*	1.6	-	-	M6	DOC+DPF + LNT	73 500
Car B	Estate	2017	Euro 6 b*	1.6	-	-	M5	DOC+DPF + LNT	24 800
Car C	Estate	2014	Euro 6 b*	1.6	-	-	M6	DPF + SCR	59 100
Car D	Hatchback	2018	Euro 6 d-temp	1.5	2.1	1.5	AT8	DOC+DPF + 2xLNT	2000

The data used for this case study was gathered with PEMS using different routes representing typical driving characteristics in mixed environments, including urban, rural and motorway environments. An example of a PEMS route used in the campaign is shown in Figure 9. The tests were conducted during daytime within a normally following the traffic stream. During the campaign, a total of 24 PEMS RDE tests were made. The tests were performed in ambient temperatures ranging from – 1.3 °C to 19.6 °C, as shown in Table 3. The test quantity and test conditions varied between cars.

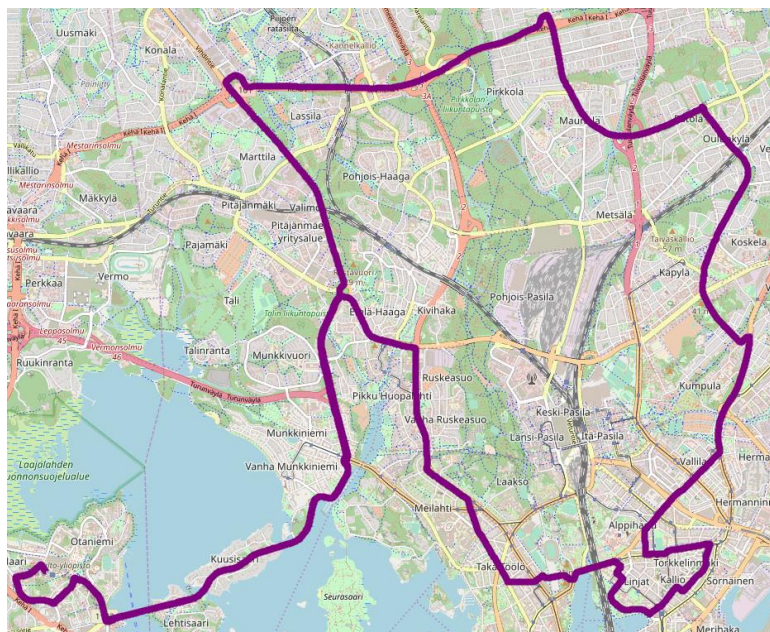


Figure 9: An example of a PEMS route in the Helsinki region

Table 3: Number of tests and average trip ambient temperature range in respect to each test vehicle.

Car	Number of PEMS tests	Average trip ambient temperature range [°C]
Car A	4	0.9 to 3.4
Car B	4	-1.3 to 5.7
Car C	9	2.7 to 19.2
Car D	7	6.2 to 19.6
Total	24	0.9 to 19.6

### SEMS measurements on a diesel van and heavy-duty trucks in Copenhagen in 2020

In this study the emissions from three heavy-duty trucks and one delivery van – all diesel powered Euro VI – were measured with a SEMS to assess real driving emissions of mainly NO<sub>x</sub> from vehicles delivering goods in urban areas, to find out under which conditions the SCR-system was fully functioning/not fully functioning with respect to engine load, engine temperature, SCR-efficiency, driving conditions, outdoor temperature, and load/weight of the vehicle [41]. Also, emissions of PN and CO were measured.

## Exhaust plume modelling

1. The homogeneity of the plume was first studied. Since the dispersion in the wake is mainly determined by turbulence, the molecular diffusion of each species plays an insignificant role and can hence be neglected. Therefore, within the plume, all species are homogeneously distributed and can be represented as one compound.
2. Since OpenFOAM is based on the finite-volume-method for unstructured meshes, such a mesh needs to be created. Therefore, the meshing utility *snappyHexMesh* supplied with OpenFOAM is used to create hexahedra-dominant meshes.
3. When creating the computational mesh, particular attention was paid to a balance between necessary computational time and accuracy in the sense of a sufficiently high resolution. For the investigation of several influencing parameters, more than 100 simulations were performed; therefore the computation time per simulation had to be limited. After several iterations of the mesh generation, the mesh shown in Figure 10 was obtained and selected.

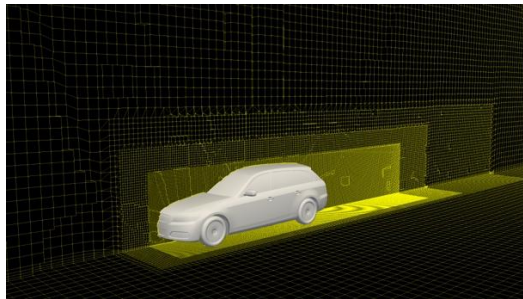


Figure 10: Computational mesh for exhaust plume simulations.

4. The pressure-based URANS solver was developed in OpenFOAM making use of the pre-existing solver *rhoReactingFoam*.
5. The described solver was used to simulate flow around the vehicle at different driving and ambient conditions. The chosen parameters are, on one hand, vehicle-related characteristics such as velocity as well as the position and orientation of the exhaust tailpipe. To study the individual effects of each parameter, the exhaust gas mass flow was kept constant. Additionally, wind is included in the study as a general external effect, distinguishing between orientation and wind velocity. Furthermore, how a vehicle upstream affects the exhaust plume dispersion of a vehicle further downstream was studied.
6. Possibilities of comparing exhaust plume simulation results with RES measurements of any type were investigated. However, due to the unpredictable nature of such measurements (ambient/driving conditions) a comparison was deemed unreliable and insufficient to draw further conclusions.
7. To address the modeling assumptions of URANS that come with inaccuracies, a consistent framework for hybrid turbulence modeling was adopted for future studies. This framework involves solving the filtered and Reynolds-averaged equations concurrently across the entire domain. This means conducting both LES and RANS simulations on two separate meshes. To ensure consistency between the two solutions regarding velocity, pressure, and turbulent properties, additional drift terms to the respective equations are introduced. This approach effectively ensures clean conditions at the interfaces between LES and RANS and is often referred to as tight coupling of LES and RANS.



## Results

### RES type 1

#### Truck tampering studies in Denmark

##### *Experimental set-up using road-side remote sensing*

In the Danish project *Control of SCR-systems using roadside remote sensing* carried out in 2019 [20], Remote Sensing Devices (RSD) were placed along the roadside to measure individual vehicle exhaust emissions as the vehicles passed the remote sensing devices. The remote sensing devices take a “snapshot” of the emissions from the exhaust tailpipe during less than a second. They can therefore be used to carry out measurements of emissions close to normal driving conditions.

In order to account for air pollution contributions from other sources than the targeted vehicle, two identical sets of measurements are carried out. One measurement was performed immediately before the vehicle was passing and another measurement was performed just after the vehicle had passed. The difference between the two measurements was taken as the contribution from the vehicle passing the instrument.

The measurements take only few seconds to carry out, and the results are available immediately after these are completed. The equipment can therefore be used to determine emissions from a large number of heavy-duty trucks in short time at roadsides when measured in accordance with certain technical guidelines. Measurements are thus ideal as basis for a fast selection of heavy-duty trucks with potentially manipulated or defect SCR-systems.

##### *Controlled tests of malfunctions of SCR-systems and particle filters*

One of the major tasks in the project was to carry out tests of RSD measurements within a closed area. A series of tests with deliberately manipulated SCR-system were performed. The overall aims of this part were to:

- Characterize NO emissions from vehicles with SCR-systems deliberately switched off using manipulation devices.
- Characterize PM emissions from vehicles with dismantled particle filter.
- Characterize other parameters and their effects on emissions.

The reason for testing PM emission with dismantled particle filter is that the particle filter normally needs to be removed when the SCR-system is manipulated.

Other parameters that were tested included: engine temperature, weather, speed, acceleration and the presence of a trailer.

The main outcome of these tests was to establish threshold concentrations of pollutants. The intention was to apply these at a later stage to discriminate between normal functioning SCR-systems and malfunctioning SCR-systems for roadside inspections.

The most important conclusions from these tests were (with NO emissions expressed as NO<sub>2</sub> equivalents):

- Average NO emissions equaled 0.8 g/kg fuel for active SCR, 24 g/kg fuel for inactive SCR and 18 g/kg fuel for active SCR-system with the SCR switched off. Thus, NO emissions differ by a factor of 20 between well-functioning SCR and malfunctioning SCR-systems. The difference between the malfunctioning SCR-systems is within the uncertainty of the measurements.

- NO emissions from Euro V heavy-duty trucks featuring an inactive SCR-system averaged 32 g/kg fuel. This is 35% higher than for Euro VI measured under similar conditions and about a factor of 2 higher than for Euro VI with the SCR-system switched off. Unfortunately, it was not possible to test Euro V with well-functioning SCR-system for which reason it has not been possible to make a comparison between Euro V and Euro VI with SCR switched off.
- For Euro VI heavy-duty trucks, the present findings suggest a threshold concentration of NO, at which the SCR-system is probably malfunctioning, at around 7 g/kg fuel (330 ppm NO). However, the results clearly show that a high NO emission could just as well be ascribed to an inactive SCR, e.g., arising from a cold engine.
- For Euro V heavy-duty trucks, the tests results suggest a threshold concentration, at which the SCR-system is probably malfunctioning, which is higher than for Euro VI. This is based on the fact, that Euro V heavy-duty trucks with inactive SCR in average has 2 times higher NO emissions compared to the average for Euro VI heavy-duty trucks with SCR switched off. The test themselves therefor point at a threshold of NO of about 14 g/kg fuel (660 ppm).
- The three different brands showed relatively large differences with respect to emissions of NO and impact of NO following removal of the particle filters. It is not known whether these differences can be ascribed to general differences between the brands or whether it is due to differences between the specific heavy-duty trucks under test.
- Removal of the particle filter in connection with switching off the SCR-system increased the PM emissions about a factor of 2 for two of the tested brands, while the third brand was unaffected. The reason for this is not known at the moment, and it may be ascribed to problems with a specific heavy-duty truck under test.
- A supplementary test of a Euro V heavy-duty trucks based on the onboard diagnostic equipment showed low emissions of NO in the exhaust. Moreover, these tests showed that onboard diagnostic equipment may provide interesting information that could be used for further projects on malfunctioning SCR-systems on heavy-duty trucks.
- The measurements of NO during the tests were very robust towards variations in speed and acceleration. This means higher flexibility with respect to testing at closed areas and makes it possible to use shorter testing roads as previously thought.
- The weather conditions did not change significantly between the two days of testing the same heavy-duty trucks for which reason it was not possible to test to what extend weather conditions influenced the measurements. However, it is clearly not possible to measure during rain since the droplets scatter the light beam and thus influence the measurements.
- A number of other practical test were carried out (for example test of the requirements for calibrations) that enables us to make a more consolidated suggestion for a routine control method to identify malfunctioning SCR-system in heavy-duty trucks.

### *Measurements at Padborg and at the Great Belt*

In the project, the police conducted extensive roadside control involving 52 heavy-duty trucks in parallel with the measurement campaigns at Padborg and the Great Belt Bridge. In total, 44 Euro V and 8 Euro VI heavy-duty trucks with NO emissions exceeding 800 ppm (comparable to 17 g/kg fuel) were selected. The police identified malfunctioning SCR-systems among 61% of the selected heavy-duty trucks. As described in detail in the report it is assumed that the remaining 39% showing high emissions are due to cold engines leading to inactive SCR-systems (in the main report this assumption is elaborated further). These observations document that remote sensing in combination with roadside control is an efficient way to target control of malfunctioning SCR-systems within the fleet of heavy-duty trucks.

A total of 2,942 heavy-duty trucks and 3,306 passenger cars were measured in the campaigns at the Great Belt Bridge and Padborg. Based on these measurements, it was estimated that about 10% of the Euro V and Euro VI heavy-duty trucks are equipped with malfunctioning SCR-systems. This estimate has been applied for the calculations of health effects related to enhanced emissions from malfunctioning SCR-systems. It should be noted that this estimate (10%) is highly uncertain, since the measurements do not demonstrate a major jump in emissions between well-functioning and non-functioning SCR-systems, but also because the results demonstrate that the heavy-duty trucks with cold engine may have similarly high emissions as heavy-duty trucks with malfunctioning SCR-systems.

### *Method for routine control of SCR-systems on heavy-duty trucks using remote sensing*

The project has demonstrated that using the remote sensing method is an efficient method for identifying heavy-duty trucks for subsequent roadside control by the police. Combining measurements and roadside control makes it possible to focus the police resources towards controlling heavy-duty trucks with the highest likelihood of malfunctioning SCR-systems. Simultaneously, the combination of measurements and roadside control will have a preventive effect, since the measurements will make it possible to identify a much larger number of heavy-duty trucks with malfunctioning SCR-system than the police is able to find by control based on random selection for roadside control.

## CONOX project

The main results and conclusions from the CONOX project, based on RES type 1 measurements measured across Europe up until 2017, were:

- Average NO<sub>x</sub> emissions from diesel passenger cars (by Euro standard, make, brand, model, engine family, etc.) as measured by RES type 1 agree well with corresponding emissions measured on-board vehicles, e.g., by means of PEMS (cf. Figure 11). Thus, remote sensing has been proven as a powerful tool for market surveillance and for complementing conventional test methods aiming at capturing real driving emissions.
- With help of remote sensing all top selling models can be measured. Despite large efforts and resources spent on PEMS tests following dieselgate, these did not cover the market sufficiently, and high NO<sub>x</sub> emitters were effectively escaping the tests (cf. Figure 12).
- The real-world NO<sub>x</sub> emissions from diesel passenger cars remain virtually unchanged by the EU emission legislation from Euro 1 through Euro 5, meaning that in real-world driving the average European diesel Euro 5 car emits 5-6 times more NO<sub>x</sub> in excess of the Euro 5 standard.
- Euro 6 diesel passenger cars emit on average about half as much NO<sub>x</sub> as Euro 5 diesel cars, still the Euro 6 diesel cars emit on average about 5 times more NO<sub>x</sub> in excess of the Euro 6 standard.
- The introduction of effective diesel particulate filters (DPFs) along with the Euro 5 standard has effectively reduced the real-world emissions of particulate matter from Euro 5 and 6 diesel passenger cars down to very low levels (cf. Figure 13).

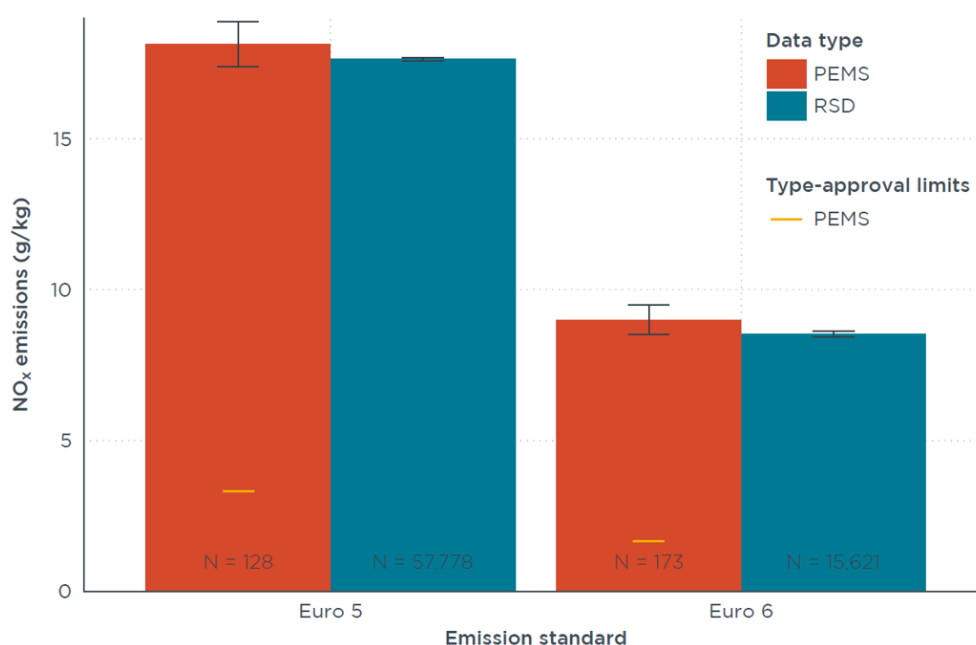


Figure 11: Average real driving NO<sub>x</sub> emission factors (in g/kg fuel burned) for Euro 5 and Euro 6 diesel passenger cars according to PEMS (red bars) and remote sensing measurements (blue bars), respectively [8].

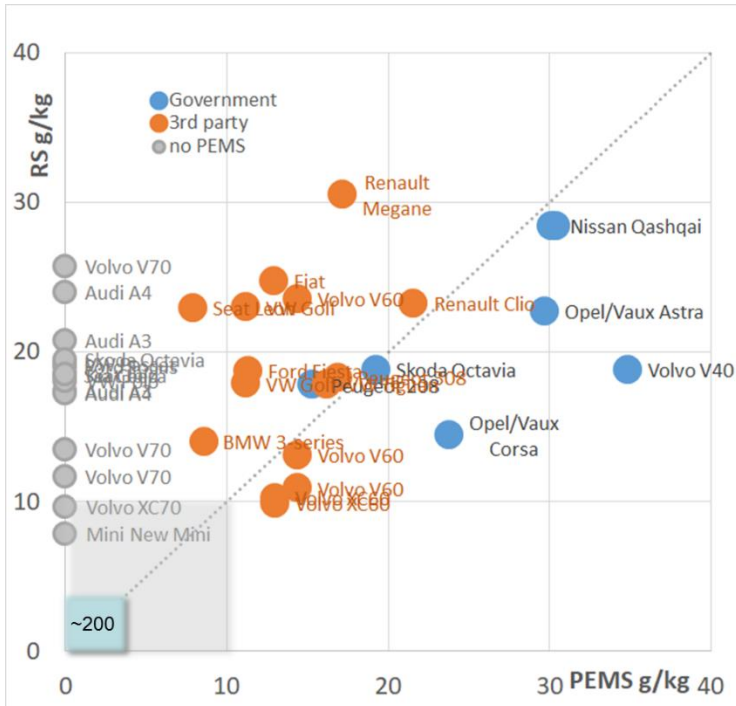


Figure 12: Comparison of NO<sub>x</sub> emission factors (in g/kg fuel) derived from RES type 1 measurements and governmental (blue circles) and 3rd party PEMS testing (orange circles), respectively, by vehicle model (Euro 5). Grey circles represent models captured in the RES type 1 measurements but not in the PEMS tests [8].

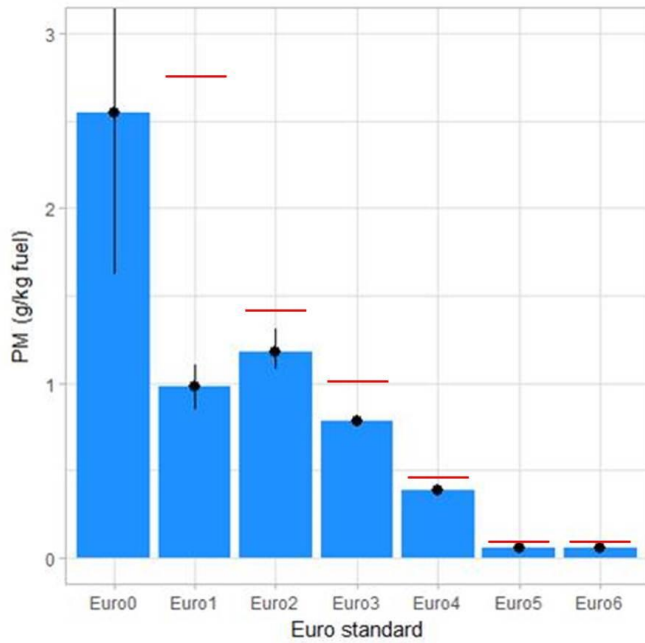


Figure 13: Average PM emissions (in g/kg fuel burned) by Euro standard for diesel passenger cars as measured by remote sensing in four European countries. Red lines indicate the emission standard [8].

## Light-duty diesel vehicle on-road emission performance study in Sweden

The main results from this RES type 1 study [21], carried out in 2018, were:

- A good agreement between remote sensing and PEMS in terms of real-world diesel LDV NO<sub>x</sub> emission reductions from Euro 5 to the various steps of Euro 6, i.e., both methods and the various datasets showed a 50% reduction for Euro 6ab and an 80% reduction for Euro 6c, cf. Figure 14. PEMS measurements (on four cars) showed a further substantial reduction for Euro 6d-temp compared to Euro 6c, but this was not seen in the remote sensing data (measurements on 138 cars).
- For early Euro 6 diesel cars, i.e., Euro 6ab, there was a good agreement in NO<sub>x</sub> emissions between remote sensing and PEMS also when data were broken down on vehicle model level, and particularly on engine alliance level (cf. Figure 15), with regression coefficients of  $\approx 0.6$  and  $\approx 0.9$ , respectively.
- Even on an individual vehicle level there was a fair agreement between remote sensing and PEMS, indicating that remote sensing is capable of identifying diesel cars exceeding the Euro 6 RDE NO<sub>x</sub> limit with a factor of three or more, with reasonably low estimated errors of omission and commission, cf. Figure 16.

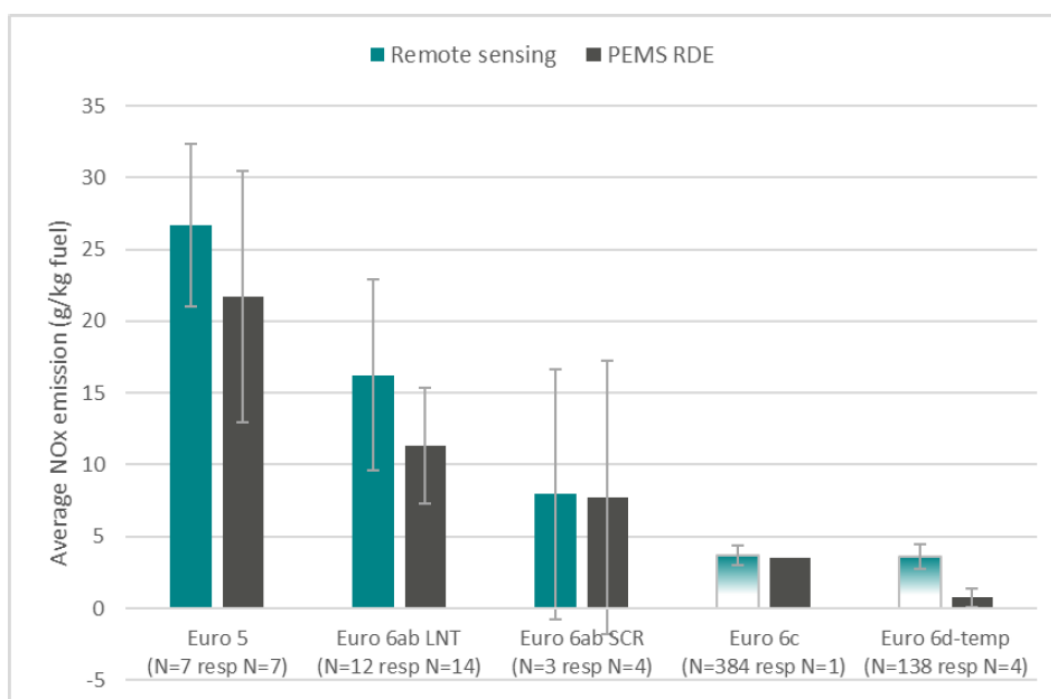


Figure 14: Average NO<sub>x</sub> emissions by Euro standard and Euro 6ab emission control technology for diesel passenger cars as measured by PEMS (full RDE test) and the same car individuals measured by RES type 1, except for the Euro 6c and Euro 6d-temp [21].

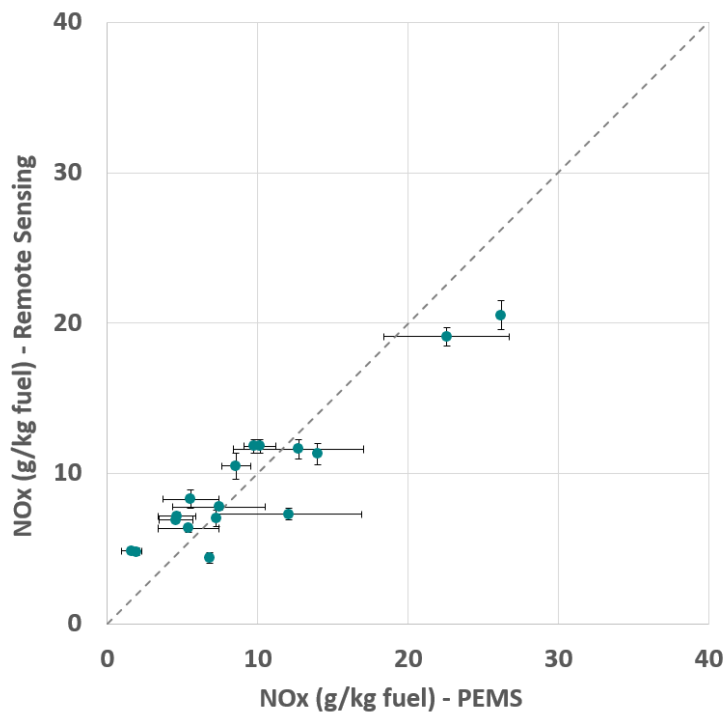


Figure 15: Average NOx emissions for common Euro 6ab diesel engine families as measured by PEMS RDE and by remote sensing [21]. Error bars represent the standard error (95% CI).

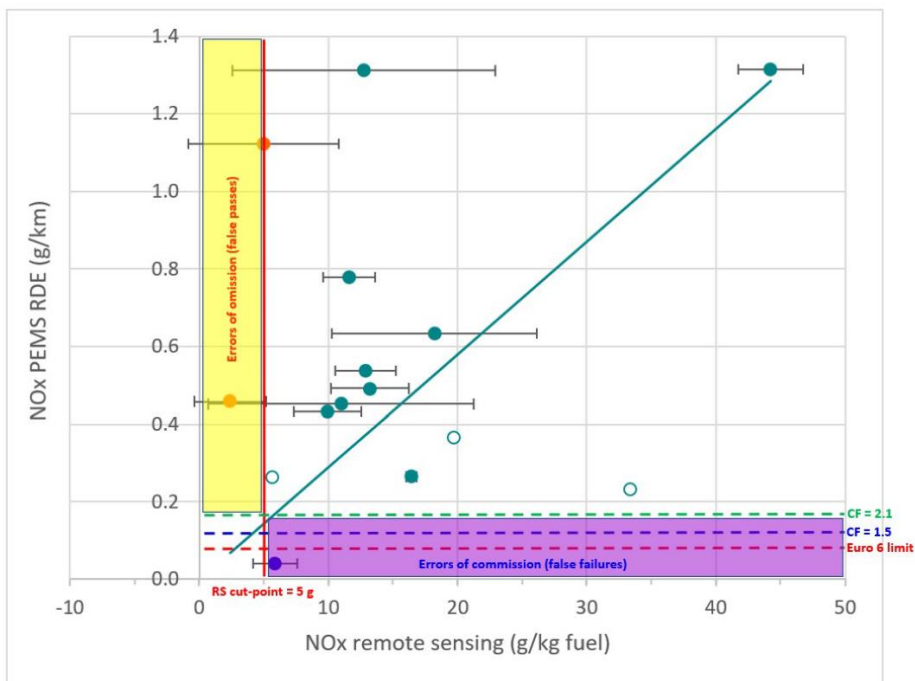


Figure 16: PEMS RDE NO<sub>x</sub> (in g/km) emissions vs NO<sub>x</sub> emissions as measured by RES type 1 (in g kg/fuel) for 15 Euro 6ab light-duty diesel vehicles [21].

## RES type 1 measurements in the CARES project

A cross-campaign comparison of NO<sub>x</sub> emissions by Euro standard for diesel, petrol and LPG light-duty vehicles as measured by RES type 1 in Milan, Krakow and Prague is shown in Figure 17. Overall, the results demonstrate that light-duty vehicles measured in all three cities are emitting NO<sub>x</sub> at comparable levels, and that the two different commercial RES type 1 instruments (HEAT EDAR and OPUS RSD) do not show large discrepancies as regards NO<sub>x</sub> emissions. Both median and mean NO<sub>x</sub> emissions from light-duty diesel vehicles measured in all three cities showed a good agreement. Notably, diesel cars have achieved comparable NO<sub>x</sub> emission performance with petrol cars after the introduction of RDE testing (Euro 6d-TEMP and Euro 6d). Those of petrol vehicles certified to Euro 5 and earlier, however, reaffirmed the likely presence of vehicles with defective or tampered three-way catalysts in the Prague measurements, largely indicated by the higher mean and median NO<sub>x</sub> emissions. The CARES measurements also generated emission factors for LPG cars, commonly found in Milan and Krakow, which showed higher NO<sub>x</sub> emissions than their petrol counterparts, which was a new finding. Figure 18 demonstrates the capability of RES type 1 to reveal large differences in NO<sub>x</sub> emission performance also for the most recent Euro 6 categories of diesel cars that are to comply with the RDE regulation (6d-temp/6d).

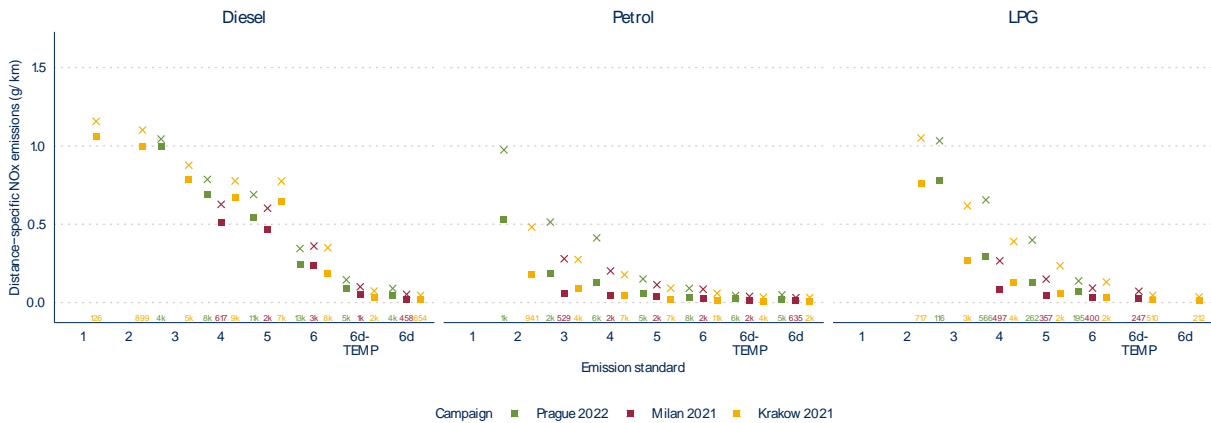


Figure 17: Average NO<sub>x</sub> emissions (in g/km, converted from the RES g/kg fuel data) for diesel, petrol and LPG passenger cars as measured by RES type 1 in Prague, Milan and Krakow in the CARES project [24]. Crosses represent mean values and squares represent median values.

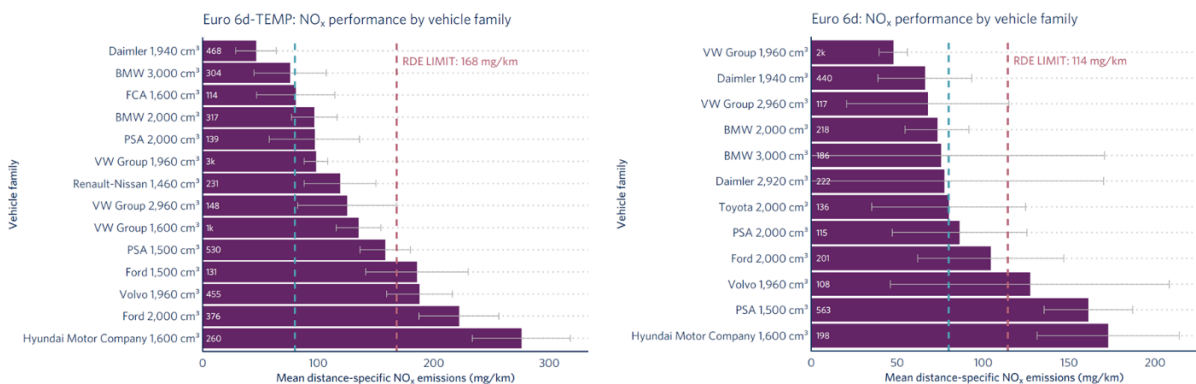


Figure 18: Average NO<sub>x</sub> emissions (in mg/km) by engine family for Euro 6d-temp (left) and Euro 6d (right) diesel passenger cars according to RES type 1 measurements in the CARES project [24].



## Other RES type 1 measurement campaigns in Europe of relevance for Task 61

### Measurements in Flanders 2019

The RES type 1 measurements in Flanders in 2019 were the first that comprised a large number of cars certified to the Euro 6d-temp standard [25]. In all about 5,000 Euro 6d-temp diesel cars were measured, having NO<sub>x</sub> emissions that were about 50% lower compared to the non-RDE compliant Euro 6 diesel cars, see Figure 19.

Since a large share of the measurements were made on motorways, a large number of heavy goods vehicles (HGV) were measured. The results show that the NO<sub>x</sub> emissions of Euro 6 HGVs were almost 80% lower compared to the emissions of Euro 5, see Figure 20.

The Flanders study focused also on identifying and quantifying the fractions and contributions of high-emitting vehicles, both light- and heavy-duty, to NO<sub>x</sub> and PM emissions, by means of the RES type 1 measurements, see Figure 21. When suspicious trucks, based on the RES measurements were pulled over for roadside inspection by the federal police, the tampering detection success rate increased from 9% to over 83%.

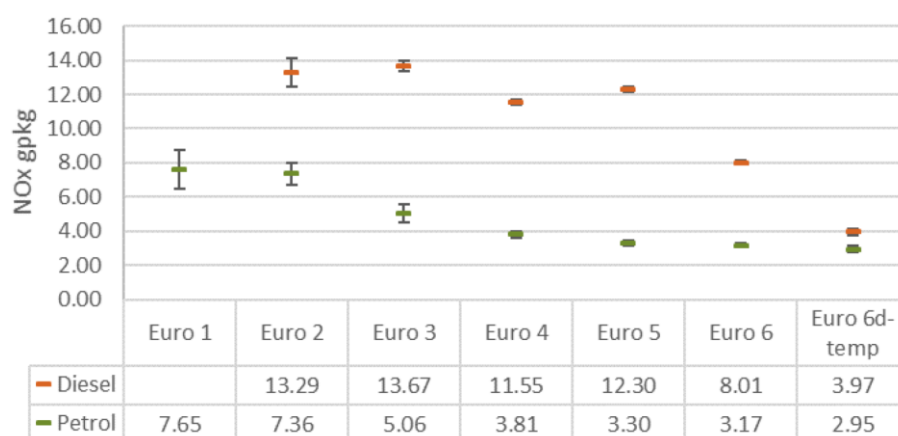


Figure 19: Overview of the evolution of NO<sub>x</sub> emissions (in g/kg fuel) by Euro class for passenger cars as measured by RES type 1 in Flanders 2019 [25]. The results show the averages for petrol (green) and diesel (orange), for which a spread is given representing the 95% confidence interval.

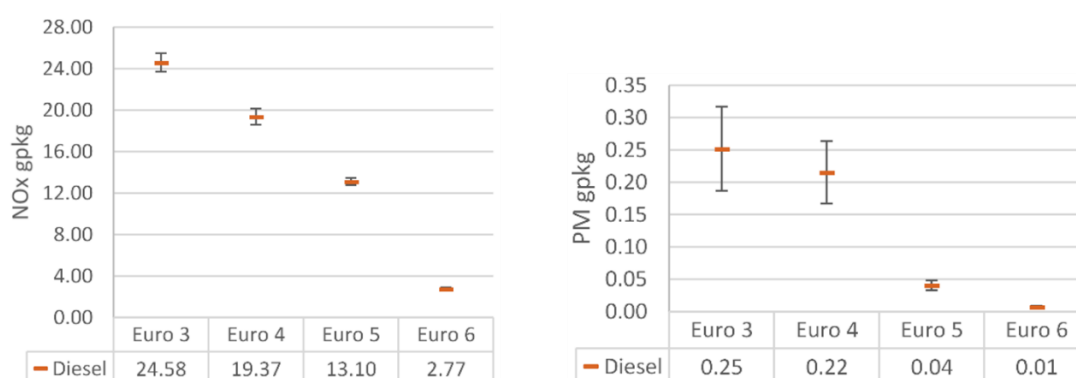


Figure 20: Overview of the evolution of NO<sub>x</sub> (left) and PM (right) emissions by Euro class for heavy goods vehicles as measured by RES type 1 in Flanders 2019 [25].

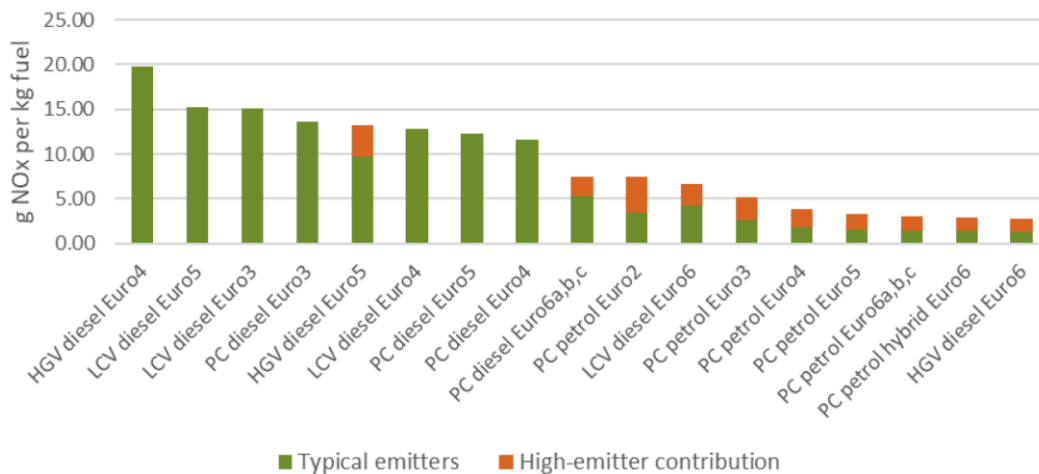


Figure 21: Average NO<sub>x</sub> emissions (in g/kg fuel) by different vehicle categories according to RES type 1 measurements in Flanders in 2019 [25]. The contribution from high-emitters is indicated by the orange bars.

### Measurements in Berlin (2019) and Frankfurt (2020)

The measurements in Frankfurt in 2020, were the first involving Euro 6d cars, although the number of measurements was quite small, since Euro 6d was not mandatory until January 2021 [27]. The measured NO<sub>x</sub> emission levels of Euro 6d are equal to those of Euro 6d-temp, see Figure 22. Compared to Euro 6abc, NO<sub>x</sub> emissions levels are reduced by about 50% with Euro 6d-temp/6d, for both diesel and petrol cars.

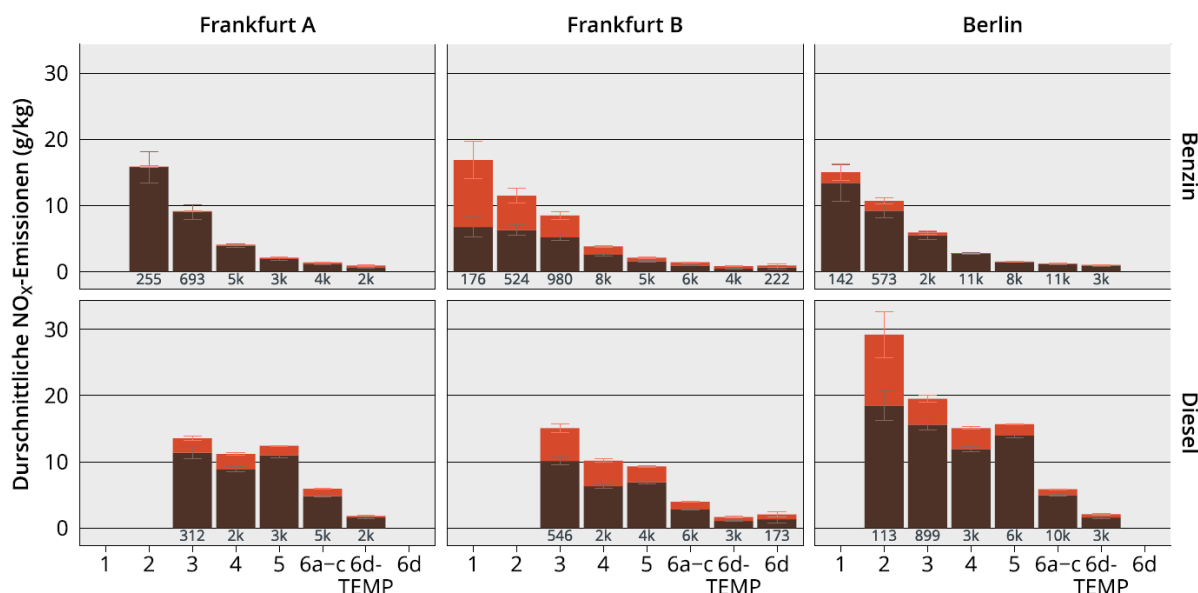


Figure 22: Average NO<sub>x</sub> emissions (in g/kg fuel) by Euro standard for petrol ("benzin") and diesel passenger cars according to RES type 1 measurements Berlin 2019 and Frankfurt 2020. The Frankfurt A measurement campaign was conducted with the HEAT EDAR system, while the Frankfurt B and the Berlin campaigns were conducted with the Opus RSD 5000 system [27].

Other important results from the Berlin and Frankfurt studies are:

- RES type 1 offers a very good means to derive relationships between vehicle age and emissions for various Euro classes, see Figure 23. The results from the Frankfurt measurements are coherent with earlier RES type 1 studies, with a clear increasing trend of all the regulated gaseous pollutants with vehicle age for petrol cars up to Euro 5/early Euro 6, whereas for diesel cars no clear trend as regards CO and HC emissions, seemingly a downward trend as regards NO<sub>x</sub> emissions for Euro 4, a downward trend for Euro 5, and an upward trend for Euro 6abc.
- Just as for vehicle age, RES type 1 also presents a very good means to derive relationships between (hot engine) emissions and ambient temperature by Euro class (Figure 23). Petrol car NO<sub>x</sub> emissions are independent of ambient temperature (in the range of ≈5 to ≈30 degrees C) for all Euro classes, whereas diesel car NO<sub>x</sub> emissions increase with decreasing ambient temperature for Euro 4 and Euro 5 in the range of ≈5 to ≈20 degrees C, and then increases with increasing temperature. For Euro 6 diesels no clear relationship with ambient temperature could be seen. No influence of other ambient parameters, i.e., air humidity and air pressure, on emissions was observed.
- According to RES type 1 measurements in London, Paris, Berlin and Frankfurt, the share of NO<sub>2</sub> of NO<sub>x</sub> in the exhaust of diesel Euro 5 cars has steadily decreased from 25% in 2012 to 11% in 2020. For the much cleaner Euro 6 diesel cars, this ratio is fluctuating around 20%.
- The hit-rate of detecting high-emitting vehicles by means of RES type 1 can be substantially improved by repeat measurements on the same individual vehicles. The fraction of true high-emitting passenger cars in the two studies seems to be max 1%.
- A surprisingly good agreement between RES type 1 measurements and PHEM modeling results was observed for NO<sub>x</sub> emissions for both diesel and petrol passenger cars, when taking into account ambient temperature and vehicle ageing effects in the PHEM modeling, see Figure 24.

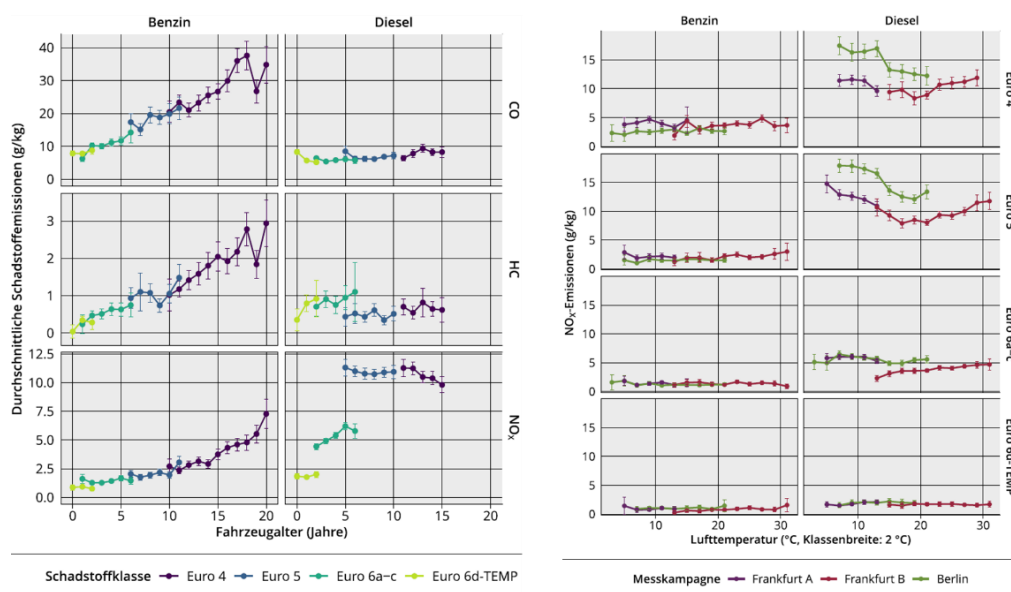


Figure 23: NO<sub>x</sub> emissions (in g/kg fuel) for petrol and diesel passenger cars as a function of vehicle age (left) and ambient air temperature (right), as measured by RES type 1 in Frankfurt [27].

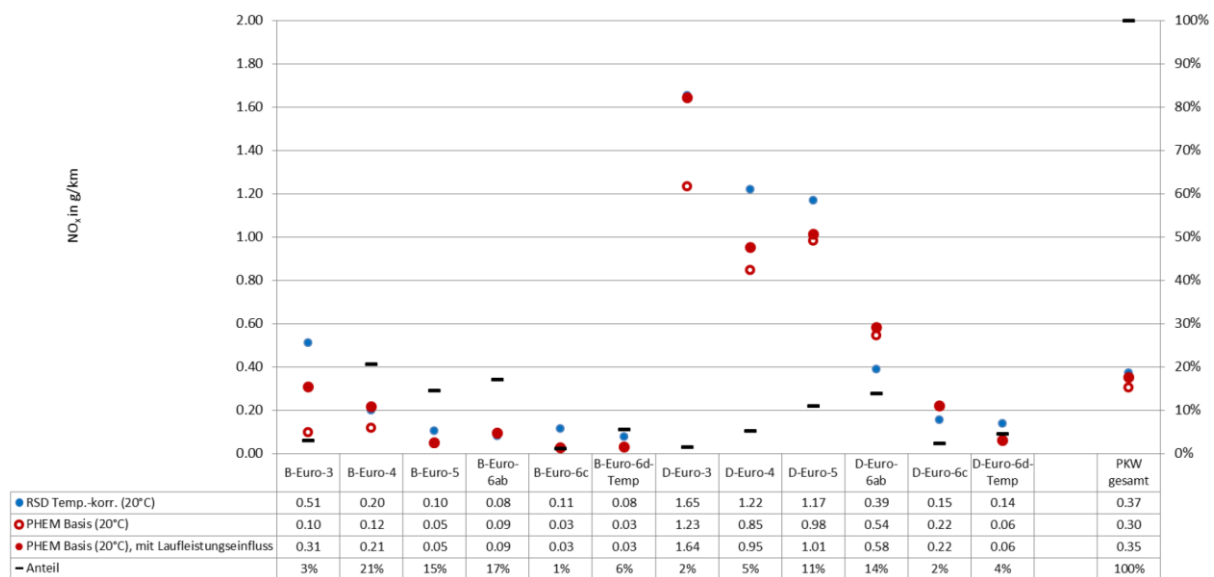


Figure 24: Average NO<sub>x</sub> emissions (in g/km) for petrol (B) and diesel (D) passenger cars according to RES type 1 measurements in Berlin 2019 and PHEM modeling results, respectively [26]. The filled red circles represent PEMS results when the age influence on the emissions was taken into account in the PHEM modeling.

### Measurements in Brussels (2020)

With the measurements carried out late in 2020, this campaign managed to collect a large number of emission data for Euro 6d passenger cars – in total almost 7,000 measurements, of which almost 3,000 were diesels [28]. It was also the first study that pulled over cars measured by the RES type 1 instrument to the roadside to go through a PN tailpipe test.

The key findings of this study were:

- The NO<sub>x</sub> emissions of Euro 6d-TEMP and 6d diesel cars are 63% and 74% lower, respectively than those of vehicles certified to previous stages of the Euro 6 standard. However, average emissions from Euro 6d-TEMP diesel cars remain 60% greater than those of petrol vehicles certified to the same standard. See Figure 25.
- Approximately 17% of Euro 6d-TEMP diesel vehicle families exceeded the on-road type-approval not-to-exceed limit, suggesting that the RDE regulation does not sufficiently cover all typical urban driving conditions.
- Approximately 2% of the light-duty diesel vehicles measured in Brussels that were equipped with a diesel particulate filter (DPF) were found to have PM emissions indicative of some level of failure of the emission control system. These findings were consistent with the results of the dedicated tailpipe PN test program, where PN emissions levels for 5% of the tested DPF-equipped diesel fleet well exceeded those expected of vehicles with properly functioning exhaust aftertreatment systems. It was estimated that this small group of very high-emitting vehicles to be responsible for more than 90% of total particles emitted from the test group.
- A wide, non-programmed screening of vehicle PM emissions with RES type 1 may identify DPF-faulty vehicles that should be checked with the new PN counting test at an unanticipated vehicle inspection, see Figure 26.

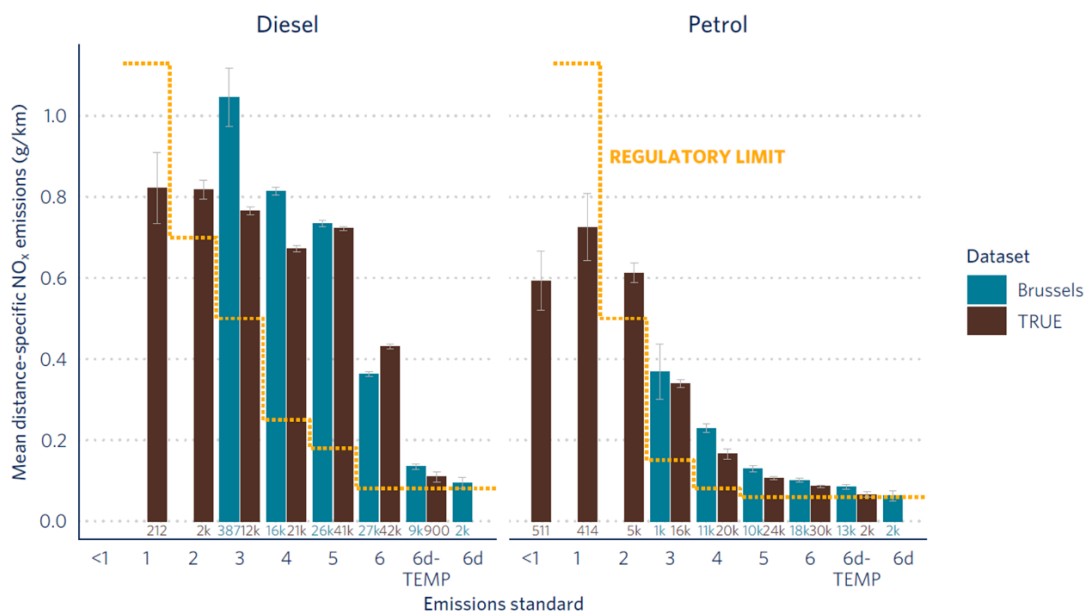


Figure 25: Mean estimated distance-specific NO<sub>x</sub> emissions from diesel and petrol passenger cars by emissions standard for Brussels and TRUE remote sensing data [28]. The number of measurements is presented below each bar. Whiskers represent the 95% confidence interval of the mean. Only results for groups with at least 100 measurements are shown.

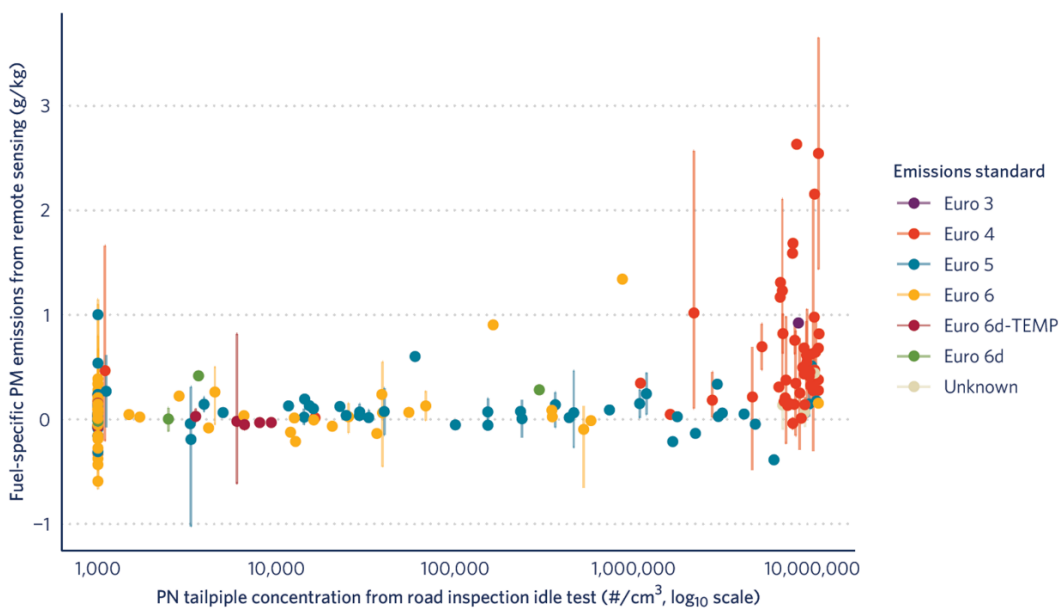


Figure 26: Mean fuel-specific PM emissions for light-duty diesel vehicles from remote sensing compared to PN concentration from road inspection at idle, by Euro standard. The range represents the min-max range when a vehicle was measured more than once with remote sensing [28].

### Measurements in Switzerland 2021 (ReMOVES project)

The key findings of the dedicated test track experiments in the major Swiss 2021 RES type 1 study [29], where two different RES type 1 instruments (Opus RSD 5500 and HEAT EDAR, respectively) were compared with an onboard instrument (SEMS), measuring the NO<sub>x</sub> emissions from a small sample of diesel powered light- and heavy-duty Euro 5 and 6/VI vehicles, were:

- RES type 1 instruments are capable of correctly measuring NO<sub>x</sub> emissions, coherent with SEMS measurements, particularly for vehicles with high emissions, e.g., Euro 5 diesel passenger cars and heavy-duty trucks under load (Figure 27 and Figure 28).
- RES type 1 poses some shortcomings when it comes to measuring NO<sub>x</sub> emissions from low-emission vehicles, e.g., the majority of petrol cars and Euro 6d-temp/6d diesel cars, since the detection limit of e.g., the Opus RSD instrument is estimated to 0.75 g/kg fuel for a single measurement (corresponding to about 0.04 g/km).
- Thus, for RES type 1 to be capable of more adequately separating vehicles not complying, from vehicles complying with the emission regulation, two or more measurements should be carried out on each vehicle.

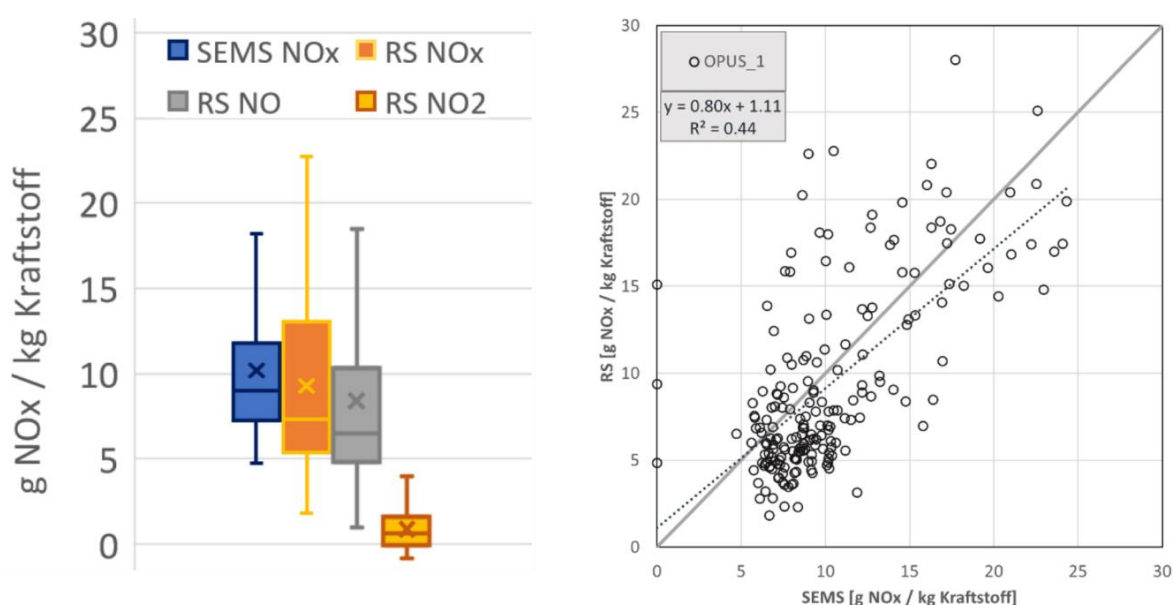


Figure 27: Comparison of repeat NO<sub>x</sub> emission measurements by means of RES type 1 (Opus RSD 5500) and SEMS on a Euro 5 diesel car on a test track in Switzerland in 2021 [29]. Left: average (x), median (-) and percentile ranges; right: individual vehicle passes (second-by-second data).

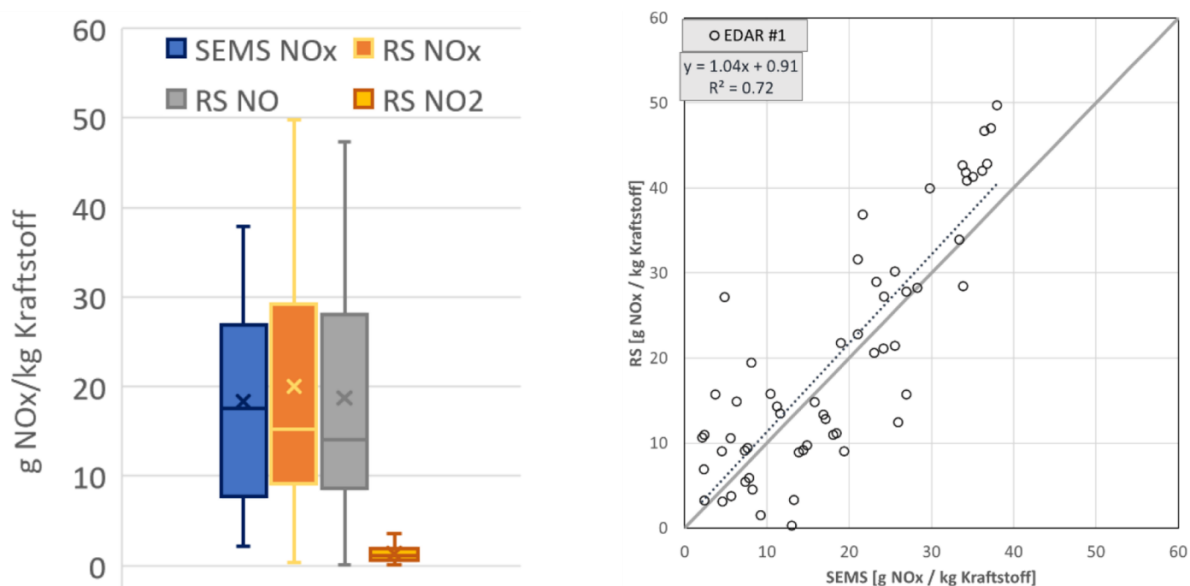


Figure 28: Comparison of repeat NO<sub>x</sub> emission measurements by means of RES type 1 (HEAT EDAR) and SEMS on a Euro VI heavy-duty diesel truck with trailer on a test track in Switzerland in 2021 [29]. Left: average (x), median (–) and percentile ranges; right: individual vehicle passes (second-by-second data).

The key findings of the measurements carried out in Swiss real-world settings were:

- As regards the average NO<sub>x</sub> emissions by Euro class, measured by both the HEAT EDAR and the Opus RSD 5500 instrument, there was a good agreement with other recent RES type 1 measurements studies in Switzerland and elsewhere, when considering the different driving conditions. See Figure 29.
- Compared with modelling results of HBEFA 4.2 applied to the rural sites (with speeds below 80 km/h), the RES results agreed generally well for NO<sub>x</sub> from petrol cars but were substantially higher for diesel Euro 6d-temp and 6d cars. When HBEFA was applied to the motorway sites (speeds above 80 km/h), the RES results were higher for petrol cars for all Euro classes and for Euro 6d-temp and 6d diesel cars, but lower for all the other diesel Euro classes. See Figure 29 and Figure 30.
- RES type 1 can be used to identify suspected high-emitting vehicles, both light- and heavy-duty, type approved for the EU RDE regulation (Euro 6d and 6d-temp). For heavy-duty vehicles a threshold value of 3.5 g NO<sub>x</sub>/kWh, for cars 300 mg/km is recommended. To lower the number of “false positives” and “false negatives”, it is recommended to operate at least two RES type 1 instrument in series, to retrieve repeat individual vehicle measurements.

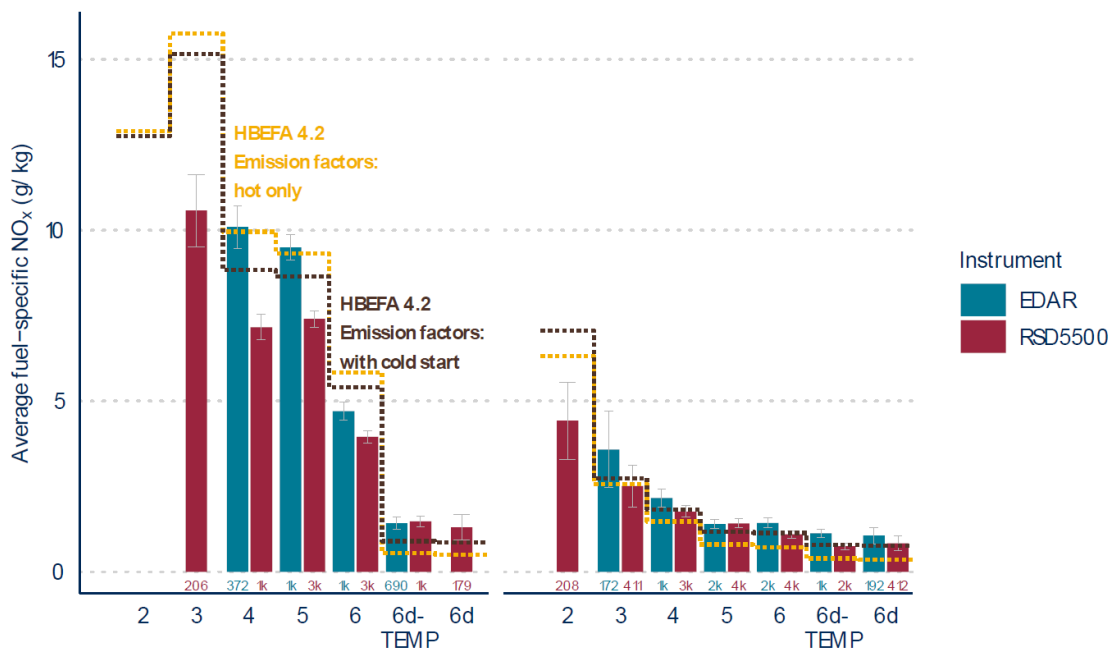


Figure 29: Average fuel-specific NO<sub>x</sub> emissions from measurements at speeds in rural areas (below 80 km/h) by instrument, fuel type and emission standard. The yellow dashed lines indicate the HBEFA 4.2 NO<sub>x</sub> emission factors for rural driving, the brown dashed lines indicate those that take into account the effects of cold starting [29].

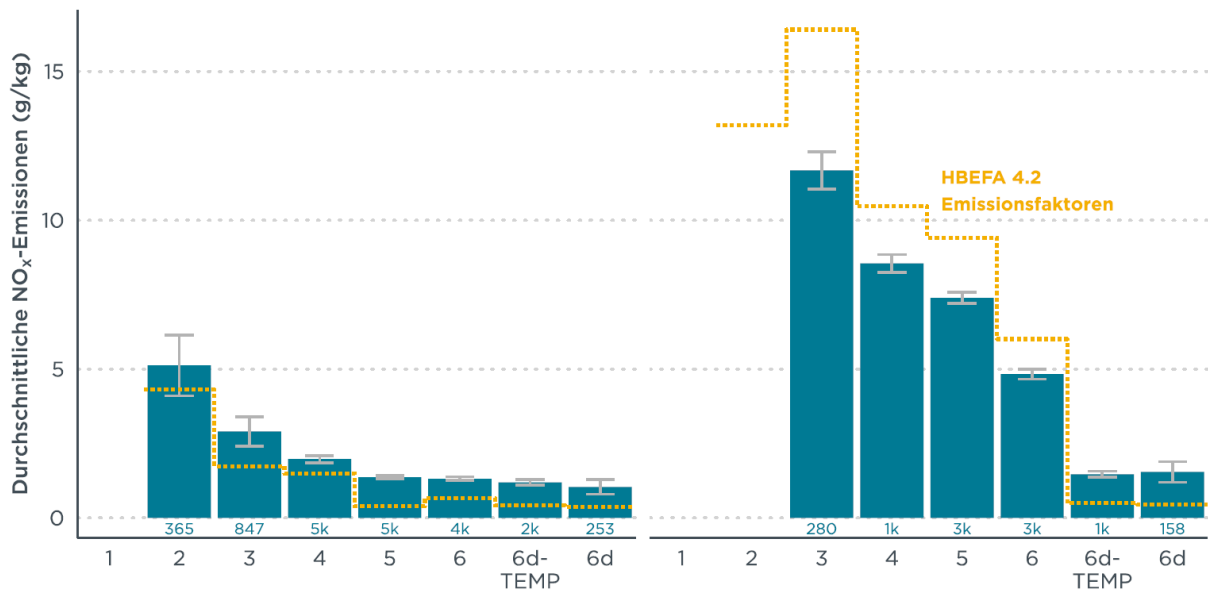


Figure 30: Average fuel-specific NO<sub>x</sub> emissions from measurements at highway speeds (above 80 km/h) by fuel type (left: petrol; right: diesel) and emission standard for passenger cars. The yellow dashed lines show the HBEFA 4.2 NO<sub>x</sub> emission factors when driving on the highway [29].



## RES type 2

### China

#### Plume Detection

The CO<sub>2</sub>, NO and PN could give evident responses simultaneously when tested vehicles drive by. As shown in Figure 31, the signals of different species rise simultaneously after the emitter drives by. The peaks usually appear within 2-8 seconds after each drive by. Typical peaks only take 3 seconds to rise to the maxima and start falling immediately, the falling takes about 5 to 10 seconds until the signals fall back to background level. The duration of the PN peak is relatively shorter, followed by CO<sub>2</sub> and NO, which is similar to previous studies and is likely to result from the different response times of instruments.

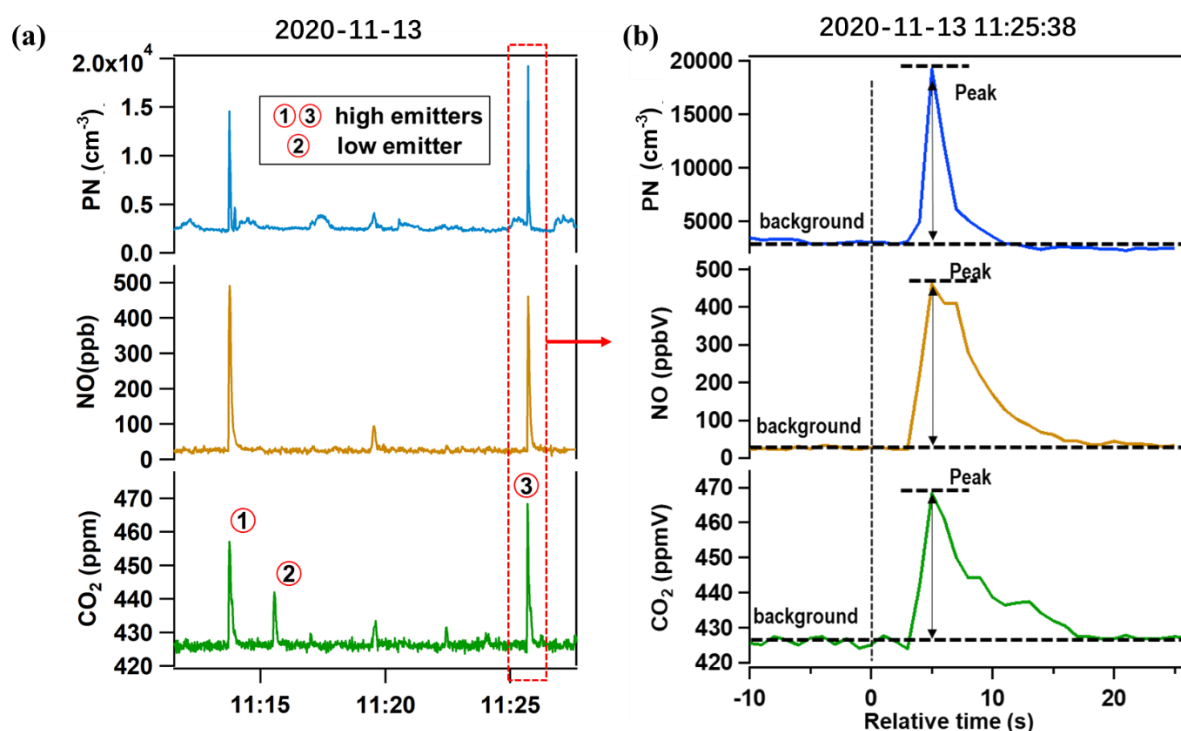


Figure 31: Time series of pollutant signals for continuous driving throughs (a) and a selected single drive-through (b). The vertical dashed line in (b) indicates the time a vehicle passing the sensor platform.

During the experiment, 97% of plumes have been successfully detected by apparent CO<sub>2</sub> increments, while the frequency of successful detection of each pollutant depends on their concentration in the highly diluted plumes. The distribution of  $\Delta$  [CO<sub>2</sub>] is relatively narrow (~10-100 ppm), which is associated with the synergistic influence of driving speed on tailpipe CO<sub>2</sub> and dilution ratio (~200-15000). For the pollutant species, the NO and PN usually give evident responses to designed high emitters but rarely respond to the low emitters. The typical  $\Delta$ [NO] and  $\Delta$ [PN] are 10-2000 ppb and 1500-40000#/cm<sup>3</sup>. In contrast, the PM<sub>2.5</sub>, CO and NO<sub>2</sub> increments are usually too low to be separate from the background signal; only 32%, 0% and 17% of plumes have derivable  $\Delta$ [PM<sub>2.5</sub>],  $\Delta$ [CO] and  $\Delta$ [NO<sub>2</sub>]. The low plume concentration and detection frequency suggest those species neither have significant environmental impact nor are useful for high emitter identification in this experiment. Therefore, PN and NO can be used for high emitter identification.

### High Emitter Identification

The sensor platform successfully distinguishes the potential high-emitters (“China-V”, “China-VI fail”, “China-V fail”) from the low-emitter (“China-VI”) by NO and PN emission factors. Figure 32 presents the NO-EF and PN-EF of the tested vehicles. In general, the majority data points are located in the right-top part of the plot (‘red zone’) while the rest points are gathered at the left-bottom of the plot (‘blue zone’). A k-means algorithm further separates all data points into two representative clusters: Cluster-1 represents high emitters, which includes all data points from designed high emitters (“China-V”, “China-VI fail” and “China-V fail”) and few points from the low-emitter “China-VI”. Cluster-2 represents low emitter, with all points in this cluster coming from the low-emitter “China-VI”. In addition to cluster analysis, the experiential thresholds exist between the designed high emitters and low emitters. All plumes from the potential high emitters have NO-EF > 2 g/kg and PN-EF >  $1 \times 10^{14}$  #/kg at the same time, which is approximately power-based emission factors of 0.71 g/kWh and  $2.3 \times 10^{13}$  #/kWh for NO<sub>x</sub> and PN when assuming brake specific fuel consumption as 231.5 g/kWh. Such thresholds may provide a simple approach for classifying high emitters.

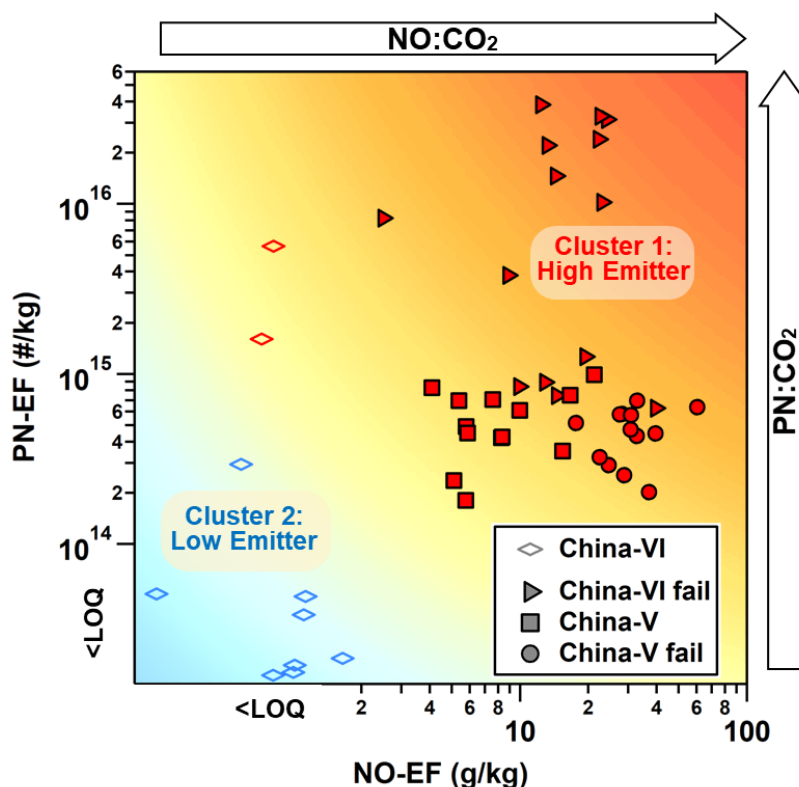


Figure 32: Distribution of PN and NO emission factors for tested vehicles. The marker colors represent the clusters by the k-mean algorithm. The “China-VI,” “China-VI fail,” “China-V,” and “China-V fail” refers to the name of four tested vehicles. The emission factors below LOQ are subject to a larger uncertainty but no more than exceed the LOQ.

In addition, the result suggests the importance of using NO-EF and PN-EF jointly for high emitter identification. In general, all plumes from designed high emitters present both high NO-EF and PN-EF, while the low-emitting China-VI standard vehicle occasionally presents high PN-EF at low NO-EF. Such result suggests that, on the one hand, the PN-EF can supplement NO-EF to identify potential high emitters with higher credibility. The NO-EF could separate the China-VI standard low-emitter from the designed high emitters high emitters with an experiential threshold of 2.0 g/kg fuel, such value is about 1.5 times of the Euro-VI and China-

VI limit (0.46 g/kwh) in dynamometer test. The data points close to the threshold can be further separated by PN-EF to increase the identification determinacy. On the other hand, the PN-EF can additionally identify “temporary high emitters” in real-world driving. The slightly different behavior between PN-EF and NO-EF is likely due to the DPF regeneration process rather than the measurement uncertainties. If the regeneration process significantly increases the PN-EF, some designed low-emitters may become “temporary high emitters” and causing adverse climate and health effects. It is crucial to identify them out for further inspection. Therefore, combining both NO-EF and PN-EF would identify real-world high emitters with higher determinacy for future application on public roads.

### Comparison with PEMS

A comparison with PEMS confirms that the sensor platform is reliable for NO measurement while serving as an indispensable commentary for PN measurement, as shown in Figure 33. The NO-EF by our sensor platform agrees well with PEMS with a high Pearson correlation coefficient ( $r = 0.93$ ) and low systematic bias (around 10%). Such consistency indicates the sensor platform has competitive performance compared with previous roadside measurements in well-controlled tracks [42] and chasing measurement on public roads [43]. It should be noted that a small fraction of NO could oxidize into  $\text{NO}_2$  in the atmosphere, which could lead to slightly different NO-EF between roadside and tailpipe. The roadside PN-EF is about an order of magnitude higher than PEMS. It is reasonable because they represent different particle populations. The PEMS follows Particle Measurement Programme (PMP) protocol to measure solid particles with a cut-off diameter of 23 nm [44,45,46], which is closely related to existing emission regulations, while our sensor platform counts all particles with a cut-off diameter of 10 nm, whose environmental effects are more straightforward. The difference between these two methods could be related to prominent nucleation during the dilution process by gaseous and semi-volatile precursor and have been widely investigated by previous experiments [47,48,49] and measurements [32,50,51]. Furthermore, the variate of roadside PN emission factors is more extensive, indicating the complexity of such nucleation process. Such results further support the necessity of using NO and PN jointly for high emitter identification.

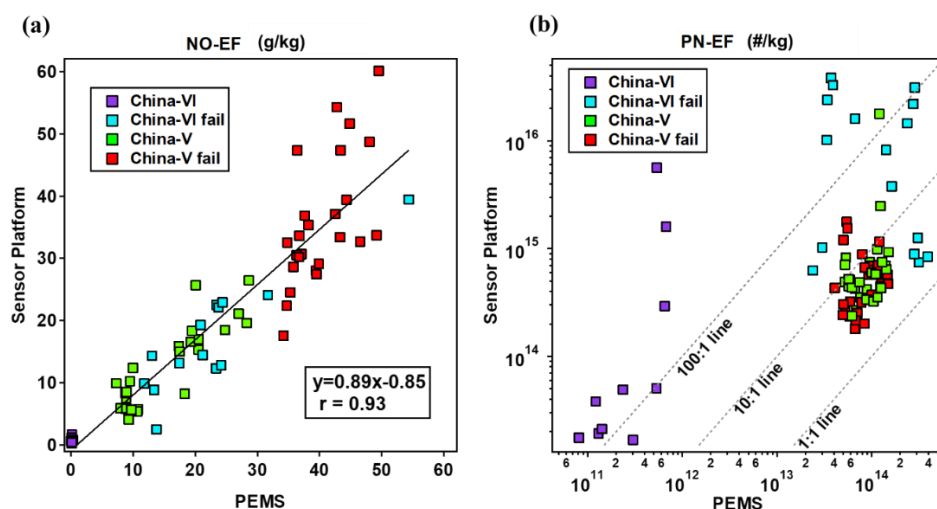


Figure 33: Comparison between roadside sensor platform measurement and PEMS measurement for NO-EF (a) and PN-EF (b).

### Characterize the Emission Factors

The sensor platform verifies that emission factors are significantly different among the tested vehicles. As illustrated in Figure 33, the “China-VI” has the lowest NO-EF among all vehicles ( $< 2.0$  g/kg), followed by “China V” (10.3 g/kg), “China VI fail” (14.5 g/kg fuel), and “China V fail” (32.8 g/kg). Meanwhile, the “China-VI” also shows the lowest PN-EF with the majority of data points below LOQ ( $< 1 \times 10^{14}$  #/kg). The rest vehicles have significantly higher PN-EF, the median values are  $9.2 \times 10^{15}$ ,  $4.9 \times 10^{14}$ , and  $5.2 \times 10^{14}$  #/kg fuel for “China-VI fail”, “China-V” and “China-V fail”.

## Europe

### Swedish city bus study (2016)

This study demonstrated the ability of RES type 2 to measure the real-world emission performance with regard to particulate matter (PM and PN) of city buses operating on different fuels, hybrid electric buses and retrofitted buses with older engines [32]. The study showed that replacing diesel fuel with RME and HVO fuel reduced the emissions of particulate matter from Euro V buses equipped with SCR by 60-70%, see Figure 34.

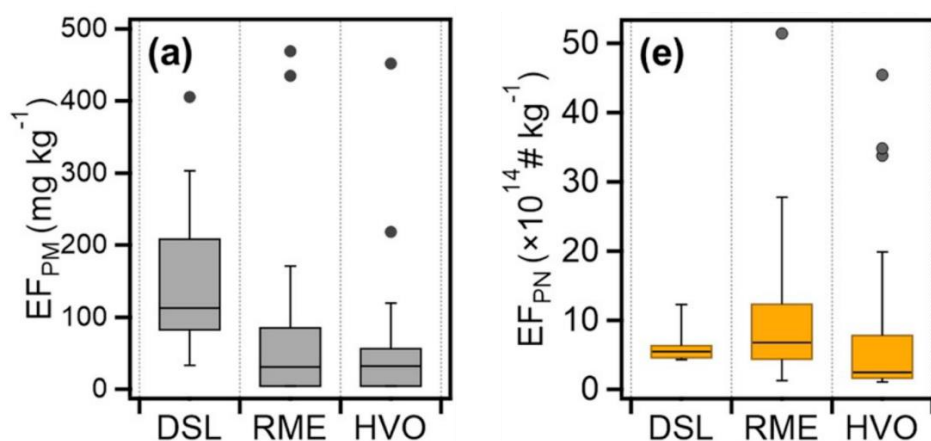


Figure 34: EFs for PM (a) and PN (e) for Euro V-SCR buses operating on different fuels (DSL=diesel, RME=Rapeseed Methyl Ester, HVO= Hydro-treated Vegetable Oil) as measured by RES type 2 [32].

### Swedish heavy-duty truck study (2018)

This study demonstrated the ability of RES type 2 to measure the real-world emission performance with regard to particulate matter (PM, PN and BC, i.e., Black Carbon) of heavy-duty trucks for urban driving conditions [33].

Euro VI heavy-duty trucks showed a very strong reduction of the real-world emissions of PM ( $\approx 99\%$ ) and black carbon ( $\approx 98\%$ ) compared to Euro III, cf. Figure 35. It was also observed that a small number of high-emitters contributed to a large fraction of the total emissions. The top 10% emitters were responsible for about 70% of 65% of total PM and total PN. Euro III trucks were the dominant top 3% emitters for PM and BC emissions, whereas Euro VI trucks were the dominant top 3% emitters for PN.

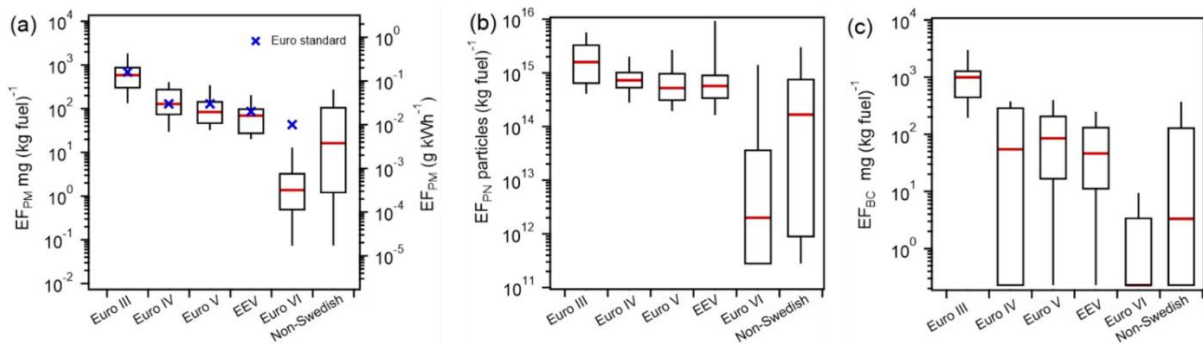


Figure 35: Average emissions of PM (a), PN (b) and BC (c) for Swedish Euro III to Euro VI and non-Swedish heavy-duty trucks as measured by RES type 2 [33]. The top and the bottom line of the box are 75th and 25th percentiles of the data, the red line inside the box is the median, and the top and bottom whiskers are 90th and 10th percentiles. Note that the median emissions of BC of Euro VI trucks overlaps with the bottom of the box.

### Measurements in the CARES project (2021-2022)

#### Controlled test track experiments

The capability of RES type 2 to detect whether a vehicle's SCR system or the DPF is working normally or is tampered with was investigated in the CARES controlled test track experiments [23]. The results are presented in Figure 36 and Figure 37, respectively.

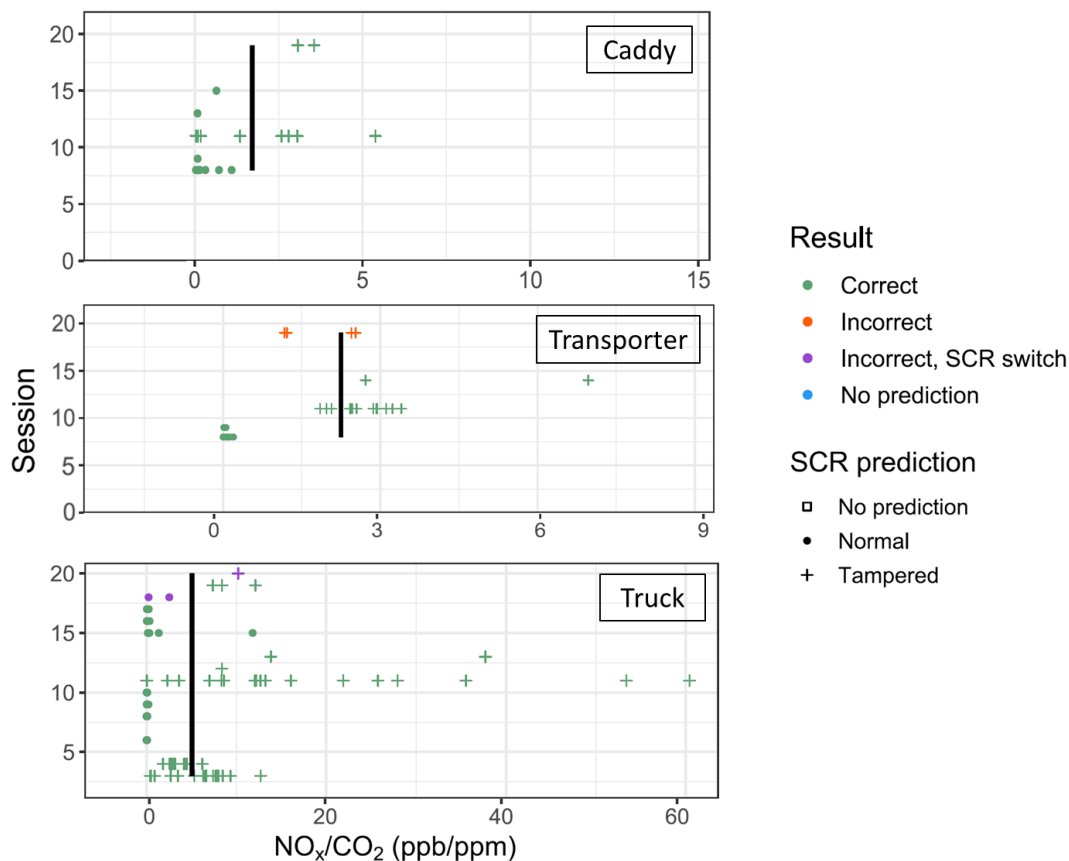


Figure 36:  $\text{NO}_x/\text{CO}_2$  ratios (ppb/ppm) for three light- and heavy-duty diesel vehicles, measured by RES type 2 grouped by test session in the CARES controlled test track experiments [23]. The data point shape corresponds to the predicted state of the SCR system and the data points are colored according to whether the prediction was correct. The solid lines show the 'tampered' emission thresholds.

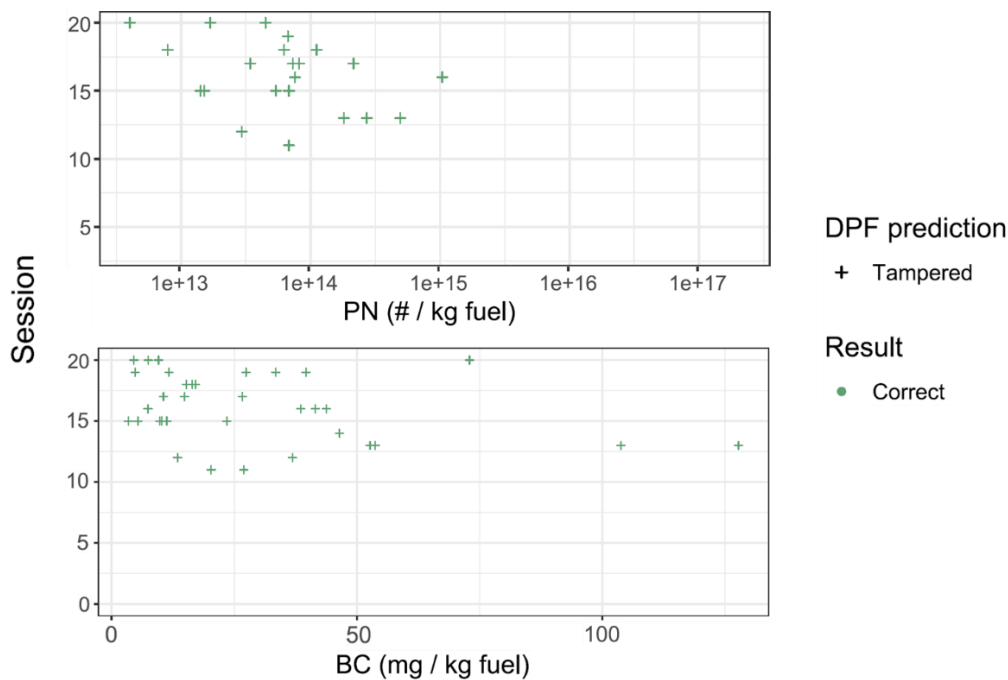


Figure 37: PN and BC emission factors (in #/kg fuel and mg/kg fuel, respectively) measured by RES type 2 grouped by test session in the CARES controlled test track experiments [23]. The data point shape corresponds to the predicted state of the DPF and the data points are colored according to whether the prediction was correct.

It is clear from Figures 36 and 37 that RES type 2 is quite successful in detecting diesel vehicles, the SCR systems and DPFs of which have been tampered with.

An important factor that affects the ability of different techniques to detect vehicle tampering is sample size. Based on the data collected in the CARES controlled test track experiments, simulations were made to evaluate the effect of sample size on estimated NO<sub>x</sub> emissions for RES type 1 and RES type 2. To calculate the mean and 95% confidence intervals at different sample sizes, chunks of data with different sample sizes were sampled at random, 1000 times per sample size. For example, for a sample size of 10, 10 values were randomly sampled from the data and the mean calculated. This process was repeated 1000 times to provide 1000 estimates of the mean emission and the 95% confidence interval in the mean. The process was repeated for a range of sample sizes as shown in Figure 38.

The dashed lines in the figure show the mean NO<sub>x</sub>/CO<sub>2</sub> ratios measured by RES type 1 and RES type 2 for the three diesel vehicles, when the SCR system is switched on (green) or off (orange). The shaded areas show the relationship between the 95% confidence intervals in the means and the number of PS and RS measurements for each vehicle and after-treatment state. As expected, for both RES techniques, the 95% confidence interval in the mean gets narrower as the sample size increases. This demonstrates that as more repeat measurements of the same vehicle are collected, the certainty to which the SCR system can be defined as on or off increases.

The proportion of valid PS measurements collected during the week of characterization experiments was lower than the proportion of valid RS measurements obtained. However, it is important to consider how the 'information value' of these two sets of measurements compare. Fewer RES type 2 measurements assigned as valid are available, but also fewer repeat valid measurements are needed to distinguish SCR on or off with a 95% degree of confidence, compared to RES type 1.

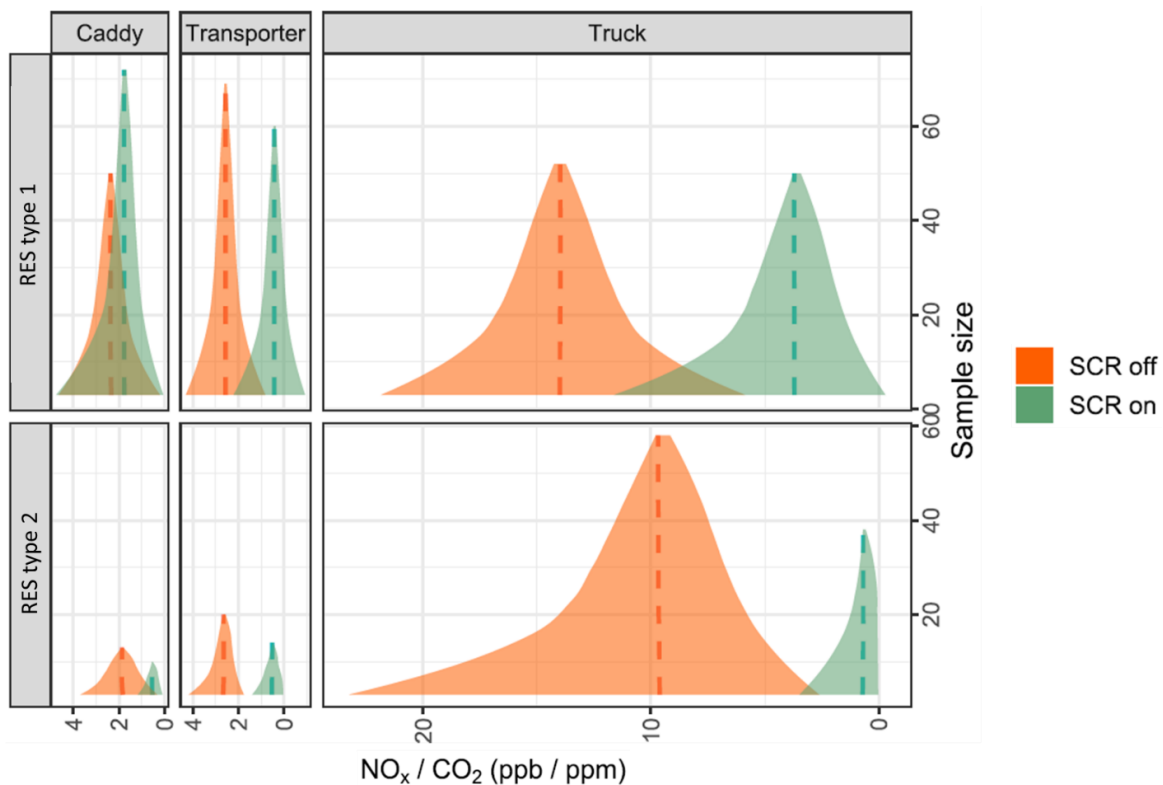


Figure 38: Mean  $\text{NO}_x/\text{CO}_2$  emission ratios for three light- and heavy-duty diesel vehicles, measured by point sampling and remote sensing [23]. The dashed horizontal lines show the average emissions for SCR on (green) and off (orange). The shaded areas show the relationship between the 95% confidence interval in the mean and the point sampling and remote sensing sample sizes, for both SCR on and SCR off.

### Measurements in real-world settings

The CARES city demonstrations in Milan enabled direct comparisons of measurements of the particle and  $\text{NO}_x$  emissions from two diesel passenger cars (a Euro 4 and a Euro 6b) by means of RES type 1, RES type 2 (the HEAT EDAR instrument) and PEMS under real-world driving conditions [52]. The results for particulate matter (PN and BC) are presented in Figure 39 and for  $\text{NO}_x$  in Figure 40.

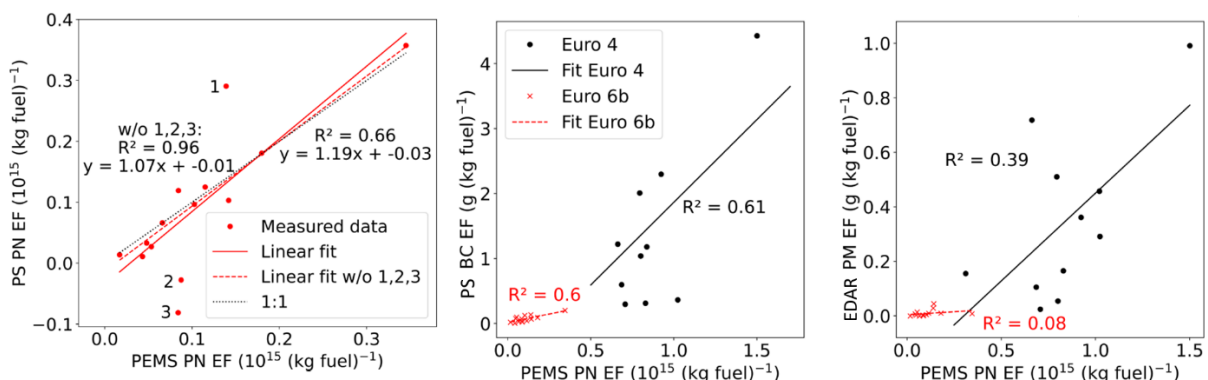


Figure 39: Left: Comparison of the PN emissions of the Euro 6b diesel car measured with RES type 2 (PS = point sampling) and PEMS. Middle: RES type 2 BC (black carbon) emissions vs PEMS PN emissions for the Euro 4 and 6b diesel cars. Right: RES type 1 (HEAT EDAR) PM emissions vs PEMS PN emissions [52].

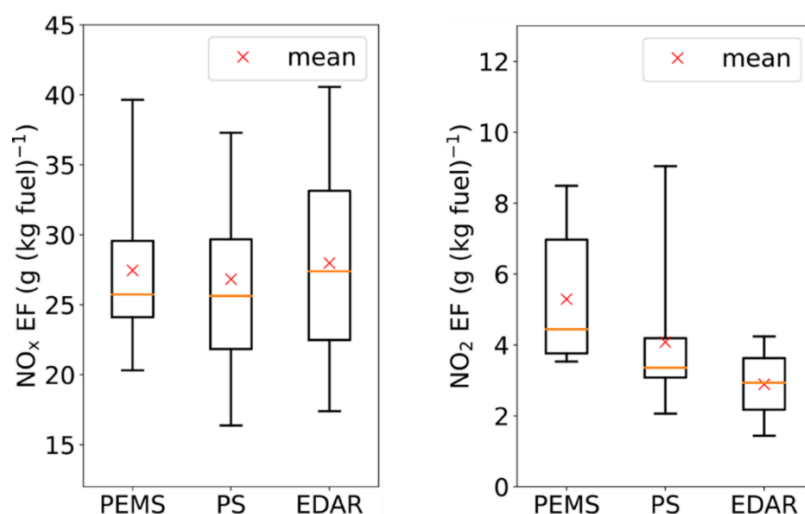


Figure 40: Comparison of average NO<sub>x</sub> (left) and NO<sub>2</sub> emissions of the test vehicles measured with PEMS, RES type 2 (PS = point sampling) and RES type 1 (HEAT EDAR) in Milan. Left: Boxplots of the measured fuel-based EFs. Comparison of NO<sub>2</sub> EFs of the test vehicles measured with PEMS, PS and EDAR. Left: Boxplots of the measured fuel-based EFs. Right: Deviation of PS and EDAR measurements compared to PEMS [52].

As seen by Figure 39, there was a very good agreement between RES type 2 and PEMS in the case of the Euro 6b diesel car PN emissions, especially when the three suspected outliers were removed ( $R^2 = 0.96$ ). Also, there was quite a good correlation between RES type 2 BC emissions and PEMS PN emissions for both the Euro 4 and the Euro 6b diesel car ( $R^2 = 0.6$ ). There was also a fair agreement between the RES type 1 instrument and the PEMS in the case of the Euro 4 car, but a very poor agreement for the Euro 6b car, due to the problems associated with optical measurement methods to measure low fine particle emissions from DPF equipped diesel cars.

As seen by Figure 40, the average NO<sub>x</sub> emissions of the two diesel cars measured with the three types of instruments agreed extremely well, within 5%, while on the other hand there were rather large discrepancies in the measured NO<sub>2</sub> emissions, with the PEMS values being the highest and the RES type 1 being the lowest. The observed differences were explained by losses in the RES type 2 sampling system due to humidity, large underestimations by RES type 1 due to measured concentrations below the instrument's detection limit, and/or inaccuracies in the PEMS measurements and calculations which include a correction factor for NO<sub>2</sub>.

Figure 41 and Figure 42 summarize the main findings of the RES type 2 city demonstration measurements in Prague and Brno in the Czech Republic in September 2022, which were the most extensive RES type 2 measurements carried out in the CARES project and focusing on diesel passenger cars [53]:

- Due to the introduction of extremely efficient diesel particle filters, mandatory from Euro 5, the real-world emissions of BC and PN from diesel passenger cars have on average been reduced by 90-95% when comparing Euro 3 with Euro 6 (Figure 41).
- The number of diesel cars (Euro 5 and 6) with seemingly non-performing or poorly performing DPFs, giving rise to emissions of particulate matter at the same level as Euro 3 cars, are few, but still appear even among Euro 6d-temp cars.
- The RES type 2 instruments developed in the CARES project were very successful in detecting the high-emitters, as proven by roadside idle PN tests conducted on cars with suspected high emissions according to the RES measurements, see Figure 42.



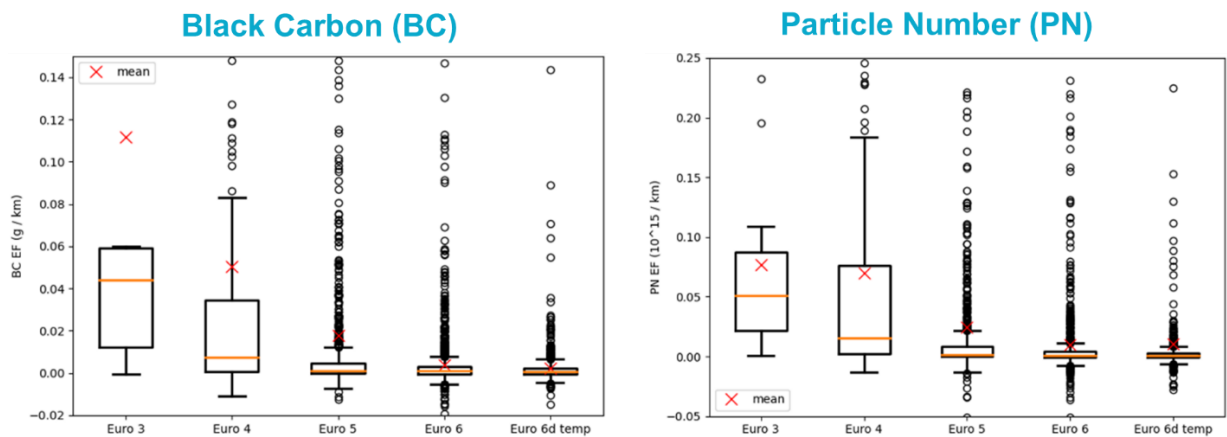


Figure 41: Average emissions of BC (Black Carbon) and PN (particle number) from diesel passenger cars by Euro standard by means of RES type 2 instruments in Prague/Brno in 2022 [53].



Index	Vehicle	Registration Year
1	FIAT	2007
2	FORD Transit	2008
3	MAN TGL 12.250	2011
4	DACIA Logan	2015
5	FIAT Dobolo	2014
6	FORD Transit	tbd
7	SKODA Octavia	2007
8	FORD Galaxy	2012
9	FORD S-Max	2006
10	SKODA Octavia	tbd
11	PEUGEOT 407	2008
12	SKODA Superb	tbd
13	IVECO Daily	2011
14	VW Transporter	2009
15	HYUNDAI i30	tbd
16	AUDI A3	tbd
17	MERCEDES BENZ	2001

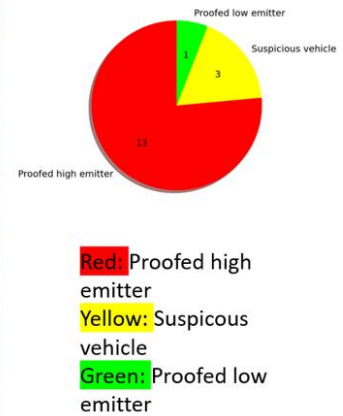


Figure 42: RES type 2 measurements for the detection of particle high-emitting diesel cars in Prague/Brno 2022. Of the 16 out of 17 cars with high PN emissions according to the RES measurements, 13 cars were confirmed as true high PN emitters and three cars as suspicious high PN emitters in the roadside idle PN test. Only one car was a false failure according to the RES measurements [53].

## RES type 3

### China

This study verified the accuracy and reliability of the plume chasing test for measuring emission factors based on conjoint PEMS and chasing test. The data from regulatory PEMS tests were used as the “actual emission factors” (i.e., comparison benchmarks), and the accuracy evaluations were conducted by comparing the emission factors from PEMS and plume chasing tests. The comparative tests of heavy-duty vehicles by using concurrent plume chasing and PEMS were conducted on a well-controlled track (7 vehicles) and real-world highways (12 vehicles). The track tests focused on evaluating the testing effectiveness of plume chasing tests on low-emitters (comply with China VI emission standard) and high-emitters (with failure aftertreatment). The on-road tests focused on evaluating the accuracy of emission factor of heavy-duty vehicles under real road conditions.

We conducted concurrent PEMS and chasing test with controlling the aftertreatment conditions on driving track at Chongqing and Yancheng in 2020 fall. The recruited test vehicles included 2 China V diesel trucks, 3 China VI diesel trucks, and 2 China VI natural gas vehicles. The mean and variance of vehicle-specific emission factors was calculated for comparing the plume chasing and PEMS test results. As shown in Figure 43, the results of NO<sub>x</sub> emissions from plume chasing are nicely comparable to that of PEMS test, especially in terms of the emission difference between aftertreatment normal and failure vehicles. For example, the NO<sub>x</sub> emission factors from these two methods for trucks with failure selective catalytic reduction (SCR) aftertreatment were around 50-60 g/kg-fuel, while the NO<sub>x</sub> emission levels can be controlled to 15 g/kg-fuel under high-speed conditions for SCR normal trucks; During aftertreatment normal status, the NO<sub>x</sub> emissions of the China VI diesel Truck (vehicles #C-E) didn't exceed 5 g/kg fuel. This indicated that low-emitting China VI vehicles can be effectively captured by plume chasing. When the aftertreatment failed, both plume chasing and PEMS test results showed that it will exceed by 1-2 orders of magnitude.

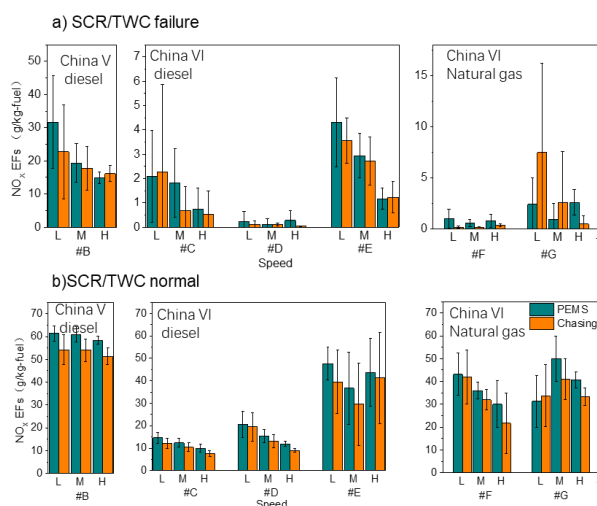


Figure 43: NO<sub>x</sub> emission factors for after-treatment failures and normal trucks.

A relationship that links the accuracy of NO<sub>x</sub> emission factors (EFs) calculated from chasing measurements to meteorological variables was developed based on PEMS-plume chasing test on track. To quantitatively evaluate this relationship, we postulated an “effective ratio” (ER) concept based on the momentum wake theory. The two methodological scenarios for chasing test are shown in Figure 44 (a). The effective ratio is considered a function of

meteorological variables in the vehicle wake (see Equation 2-4). To evaluate the effect of the effective ratios on  $EF_{\text{chasing}}$ , the calculated  $EF_{\text{chasing}}$  was separated into four groups based on the corresponding data intervals of the effective ratios and compared to  $EF_{\text{PEMS}}$ . Figure 44 (b) shows the comparison of the grouped  $EF_{\text{chasing}}$  from the baseline approach and  $EF_{\text{PEMS}}$  with all tested vehicles combined. For the  $EF_{\text{chasing}}$  that was calculated with effective ratios less than 1, the scattered data points were distributed close to the  $y = x$  line with  $R^2$  larger than 0.94. The average values of the slopes and the intercepts of the two regression lines were  $\sim 0.91$  and  $\sim 1.4$ , respectively. For the effective ratios larger than 1, the linear regression lines of the  $EF_{\text{chasing}}$  vs  $EF_{\text{PEMS}}$  showed the value of the slope less than 0.54 with  $R^2$  less than 0.58. This is evidence that the effective ratio could be a good parameter that quantifies the relative deviation of  $EF_{\text{chasing}}$ . Based on this relationship, the effective ratio can be further used to identify erroneous chasing measurements and improve the accuracy of  $EF_{\text{chasing}}$  [54].

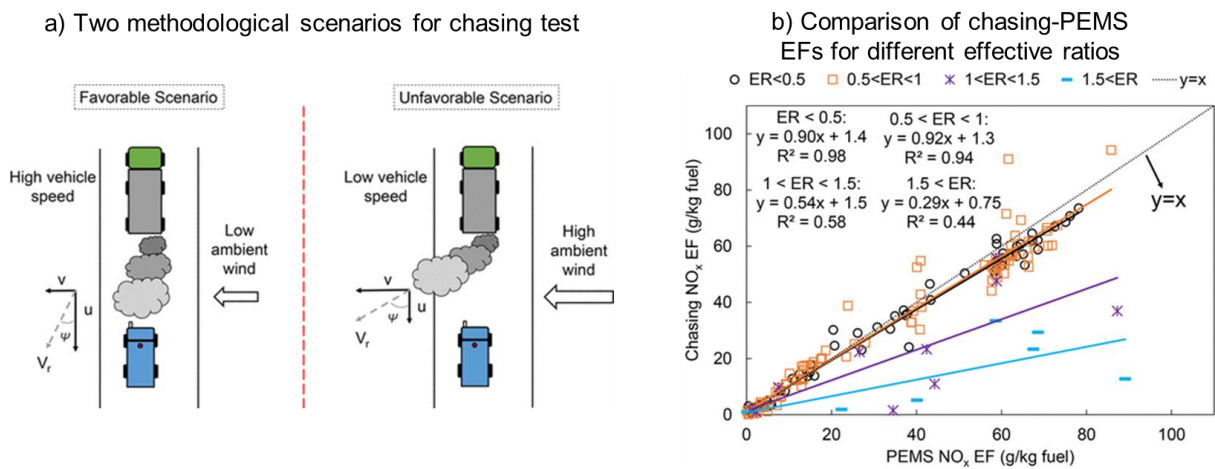


Figure 44: The relationship between meteorological variables and NOx emission factors based on plume chasing measurements.

$$\text{Effective ratio} = \left( \frac{\bar{v}}{\bar{u}} \right) \times \left( \frac{\sigma_u}{\sigma_v} \right) \quad \text{Equation 2}$$

$$\sigma_u = \sqrt{\frac{1}{T} \int_0^T (u(t) - \bar{u})^2 dt} \quad \text{Equation 3}$$

$$\sigma_v = \sqrt{\frac{1}{T} \int_0^T (v(t) - \bar{v})^2 dt} \quad \text{Equation 4}$$

Here, we define the vehicle driving direction as  $u$  and the direction that is normal to the driving direction as  $v$ . where  $\bar{u}$  and  $\bar{v}$  are the average wind speed (m/s) in  $u$  and  $v$  directions, respectively, during one plume-chasing event.  $\sigma_u$  and  $\sigma_v$  are the standard deviations of the wind speed fluctuation (m/s) in the  $u$  and  $v$  directions, respectively. The  $t$  in the basket and the overbar stands for the instantaneous and time average wind speed measurements in different wind directions, respectively. The capital  $t$  ( $T$ ) in the equations is the time interval that is used to calculate the  $\sigma_u$  and  $\sigma_v$ . To pair the measurement of pollutant concentrations (5 s average) and the turbulence measurements, the time interval applied to  $\sigma_u$  and  $\sigma_v$  calculations was set as 5 s.

The on-road chasing and PEMS concurrent test was conducted by in China for reliability verification of real-world plume chasing. The emission factor calculation method is optimized by a combination of the integral method for highways and the linear regression method for local roads. The integral method obtains the net pollutant concentration after subtracting the road background concentration and further calculates the emission factor based on the moving average carbon balance method. It requires measuring the road background concentration before and after this chasing test. The linear regression method assumes that the dilution of CO<sub>2</sub> and NO<sub>x</sub> from the exhaust pipe to the chasing platform is equivalent, and a linear regression can be used to describe the relationship between CO<sub>2</sub> and NO<sub>x</sub> emitter by target vehicles. The slope of the linear regression is used to calculate the average fuel-based emission of the plume during the chasing test. And the intercept of the linear fit represents the road background concentration during the chasing period, i.e., without an additional measurement of the road background data before and after the chasing test. The results of combining the two emission factors methods showed that the accuracy of a single vehicle in the chasing test is over 80% and the average accuracy of the fleet is over 95%, indicating good agreement of NO<sub>x</sub> emission factors between plume chasing and PEMS (see Figure 45) [43].

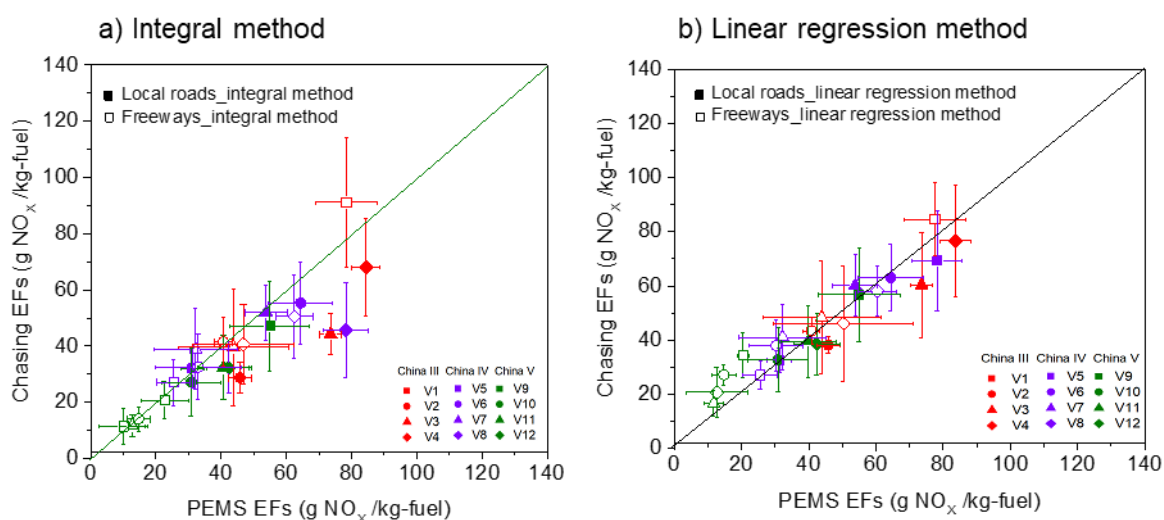


Figure 45: Comparison of vehicle-specific NO<sub>x</sub> emission factors measured by PEMS and chasing concurrent test.

Plume chasing measurements benefit from large-scale samples for exploring the impacts of drivers (technological and operational conditions) on NO<sub>x</sub> and BC emissions for HDTs. Based on the emission measurements on a large sample of heavy-duty diesel trucks in China by using mobile plume chasing, this study introduced a machine learning model, i.e., gradient boosting machine (GBM), to explore the key drivers of NO<sub>x</sub>/BC EFs for detailed analysis (as shown in Figure 46). The results indicated that ambient temperature was the leading driver for NO<sub>x</sub> emissions instead of emission standards. Unlike the importance ranking of NO<sub>x</sub> emissions, the emission standard was the leading driver for BC emissions of HDT, followed by driving speed.

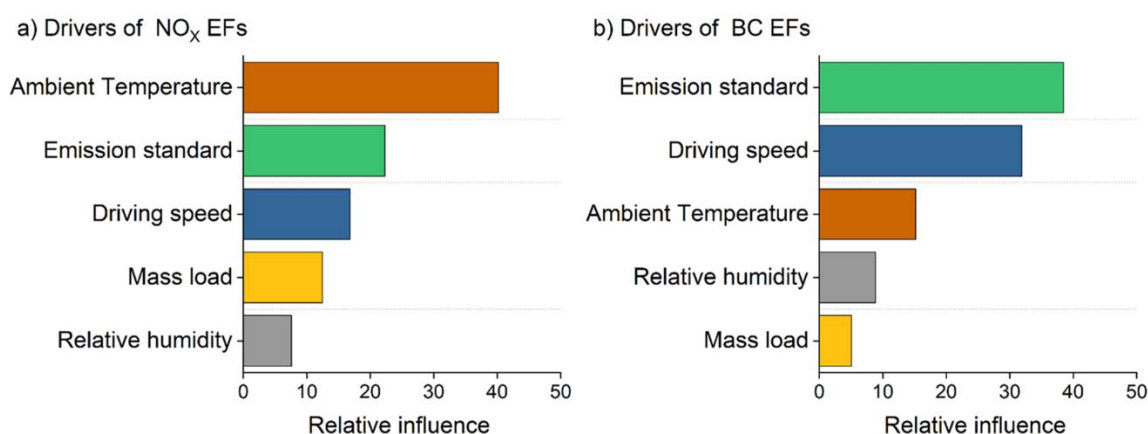


Figure 46: The relative influence of drivers on (a) NO<sub>x</sub> and (b) BC emissions of HDTs based on GBM machine learning model.

Figure 47 (a) shows the NO<sub>x</sub> emission trends of HDTs with the tightening of emission standards. The average NO<sub>x</sub> EFs from China III to China VI HDTs of this study were 42.6, 43.6, 31.8 and 6.1 g/kg-fuel, respectively. No significant improvement in fleet-wide NO<sub>x</sub> EFs was observed for China IV HDTs compared with China III trucks, which almost all claimed to have been equipped with SCR. Thus, the mobile measurements revealed that the China IV emission standard failed to deliver the emission reduction benefit as expected as the regulation limits reduction (–30%, 5.0 g/kWh for China IV and 3.5 g/kWh for China III). The average NO<sub>x</sub> emission factor of China V HDTs was found to be reduced by 27% compared with that of China IV HDTs. This modest reduction was also less satisfactory than the reduction in emission limits between China IV and China V (–43%, 3.5 g/kWh for China IV and 2 g/kWh for China V). Although the exact causes of high on-road NO<sub>x</sub> emissions could not be confirmed via mobile plume chasing tests, tampering and improper use of SCR may be important causes. Previous measurements also found typical tampering and cheating practices such as defeating the temperature sensor or adding water instead of urea liquid [55,56]. Furthermore, an 80% reduction from China V to recent China VI was observed and proved the effectiveness of the latest emission standards. It is worth noting that China launched the Three-year Action Plan on Blue-sky Defense during 2018-2020 [57]. This action plan prioritized the pollution control on diesel vehicle emissions by implementing a series of stringent measures, including enhancing the emission supervision and management for both newly-produced and in-use vehicles (such as compliance inspection and phase-out programs). It was found that HDTs manufactured in 2018 and 2019 could reduce NO<sub>x</sub> emissions by 11% and 38%, respectively, compared with the earlier China V HDTs based on 553 China V samples (see Figure 47a). The tightening of supervision since 2018 has achieved significant benefits in improving China V NO<sub>x</sub> emission levels.

The average BC EFs from China III to China VI HDTs were 0.87, 0.33, 0.23 and 0.14 g/kg-fuel, respectively (see Figure 47b). The significant reduction of BC EFs was 62% from China III to China V HDTs and 30% from China IV to China V HDTs. A 40% reduction was also observed from China V to China VI. This trend showed a progressive decline with more stringent emission standards. However, the fleet-average BC EFs were significantly higher than the median values (1.6–2.3 times) due to the high-emitters existing in China III to China VI fleets. The cumulative curve of BC emissions showed that the potential benefits for phasing out these top 5% and 10% high-emitters in fleets would be 39% and 53% for the total BC emissions, respectively. The identification and supervision of these high-emitters in BC emissions will achieve large, expected emission reduction benefits.

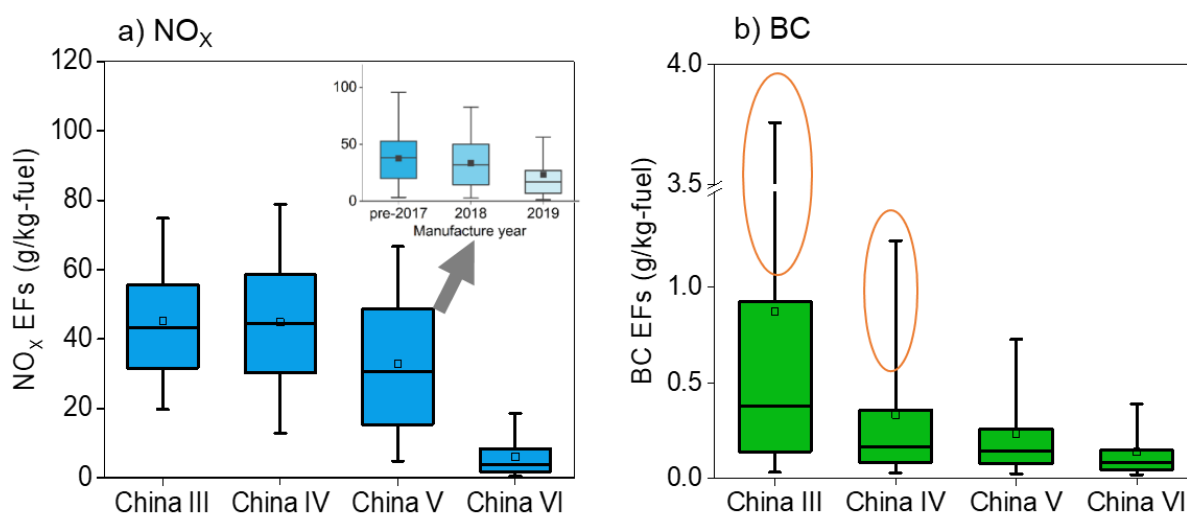


Figure 47: Boxplot of fuel-specific (a)  $\text{NO}_x$  and (b) BC EFs of HDTs from China III to China V emission standards.

Note: On each boxplot, the solid square, the central line, and the bottom and top edges of the box represent the mean value, the median value, the 25<sup>th</sup>, and 75<sup>th</sup> percentiles, respectively. The bottom and top whiskers out of the box represent the 5<sup>th</sup> and 95<sup>th</sup> percentiles, respectively.

Figure 48 depicts the sensitivity of  $\text{NO}_x$  and BC emissions for these two types of vehicles to ambient temperature and driving speed, respectively. Due to limited data from the China VI samples, only the trends from China III to China V trucks were analyzed. The samples are divided into two categories, namely,  $\text{HDT}_{1-3}$  (GVW<31 tons) and  $\text{HDT}_4$  (GVW>31 tons). In general,  $\text{NO}_x$  emissions from  $\text{HDT}_4$  were less dependent on ambient temperature than  $\text{HDT}_{1-3}$ . For  $\text{HDT}_{1-3}$ , the low-temperature penalty of  $\text{NO}_x$  emissions for China III to China V  $\text{HDT}_{1-3}$  was +32% (+12.1 g/kg-fuel), +38% (+12.7 g/kg-fuel), and +137% (+28.2 g/kg-fuel), respectively as the ambient temperature decreased from +35°C to -3°C.  $\text{NO}_x$  emissions of China V  $\text{HDT}_{1-3}$  that adopted SCR demonstrated a stronger temperature dependence compared with China III and China IV vehicles. The considerably greater ambient temperature sensitivity of China V  $\text{HDT}_{1-3}$  provided evidence for the better efficiency of SCR after-treatment of these trucks. It is important to realize that the ambient temperature dependence of  $\text{NO}_x$  emissions results could help improve the regional and seasonal accuracy of HDTs'  $\text{NO}_x$  emissions modeling and air quality simulations.

To construct the key correction module of ambient temperature in the emission model, the annual mean temperature in 2019 in China of 15°C was used as the reference temperature to calculate the correction coefficient of  $\text{NO}_x$  emissions. It was acknowledged that the closest correction coefficient was used to represent temperature conditions outside of -3 to +35 °C in this study. However, in colder climates, the low-temperature penalty of  $\text{NO}_x$  emissions for HDTs may be more extreme in the real-world based on these trends.

As indicated in Figure 48b, BC emissions showed an upward trend with decreasing vehicle speed. This may be related to the insufficient diesel combustion of engines at low speed [58]. For  $\text{HDT}_1$  to  $\text{HDT}_3$ , under a low driving speed (20 km/h), the BC emission factor of HDTs from China III to China V will increase by 106%, 82%, and 388%, respectively, to high speed (100 km/h). The low-speed trend of BC emissions for  $\text{HDT}_4$  was even more important. BC EFs for  $\text{HDT}_4$  at low-speed (20 km/h) will cause a 284%, 349%, and 150% increase, respectively, compared to that under high-speed conditions (100 km/h). Therefore, the speed increase of the HDTs through traffic control measures can considerably reduce BC emissions. The BC emission prediction was applied to speeds from 20 km/h to 100 km/h. It was estimated that

this finding of the low-speed penalty of BC emissions for HDTs may be more extreme at a much lower speed, such as under congested traffic.

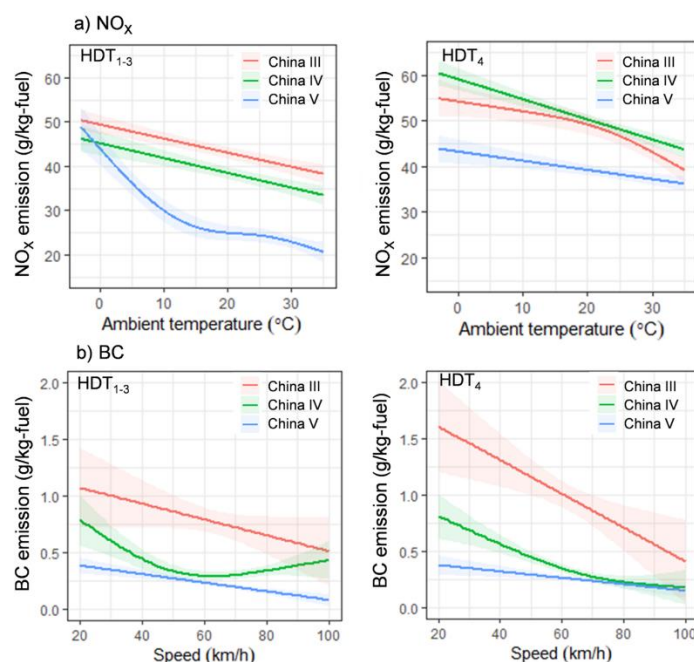


Figure 48: Generalized addition model (GAM) of fuel-specific (a) NO<sub>x</sub> emissions based on ambient temperature and (b) BC emissions based on speed for China III, China IV, and China V HDTs. The shaded zones represent the GAM standard error for the prediction.

The national NO<sub>x</sub> emission inventory of HDTs was revisited by unchanging the total vehicle activity level but adopting the updated EFs. Figure 49a shows the comparison between the previous study, regulatory limits, and this study. The new results showed that NO<sub>x</sub> emissions of HDT fleet in China increased from 3.4 Gg/yr to 4.1 Gg/yr from 2010 to 2014. Then, it appeared to have reached a plateau and decreased to 3.5 Gg/yr in 2019. The estimated total NO<sub>x</sub> emissions of HDTs indicated that the previous studies underestimated 18% of annual NO<sub>x</sub> emissions compared to the updated emission inventory in 2019, mostly attributed to the updating of EFs for China IV and V HDTs. The results of this study were compared with those calculated on the basis of the regulatory limits for different vehicle categories. It was revealed that real-world NO<sub>x</sub> emissions considerably exceeded the regulatory limit, and the gap has been widening since the promotion of China IV HDTs. The excessive NO<sub>x</sub> emissions above the regulation limits increased from 0.9 Gg/yr in 2010 to 1.7 Gg/yr in 2019, and roughly 26% and 48% of real-world NO<sub>x</sub> emissions were in excess of certification limits, respectively. Furthermore, the revised estimate of NO<sub>x</sub> emissions of HDTs will also challenge the NO<sub>x</sub> control of national heavy-duty vehicles and especially the regulation of high-emitters.

Considering the high dependence of NO<sub>x</sub> emission on ambient temperature, the ambient temperature correction module was constructed based on real-world plume chasing data as well as seasonal and provincial ambient temperature. Figure 49b shows the seasonal and regional heterogeneity of predicted NO<sub>x</sub> EFs for HDTs based on the metric of annual mean temperature (15 °C). The results showed that NO<sub>x</sub> emissions of HDTs in summer will decrease by 7%–12% compared with the baseline temperature. Meanwhile, the low-temperature sensitivity has caused a 9%–29% increase in NO<sub>x</sub> emissions in winter in the major regions of China, except for the southern region with a 3% NO<sub>x</sub> emission increase where the winter

temperature was still slightly higher than 15 °C. The regions located in the higher latitude with colder meteorological conditions were burdened with higher NO<sub>x</sub> emissions in winter and had suffered more significant seasonal discrepancy, which is most prominent in the northeastern areas of China. The existing emission model without the ambient temperature correction module may underestimate the NO<sub>x</sub> emission in winter and overestimate that in summer in major regions in China. This highlights the importance of considering real-world vehicle emission measurements to improve air quality management [59].

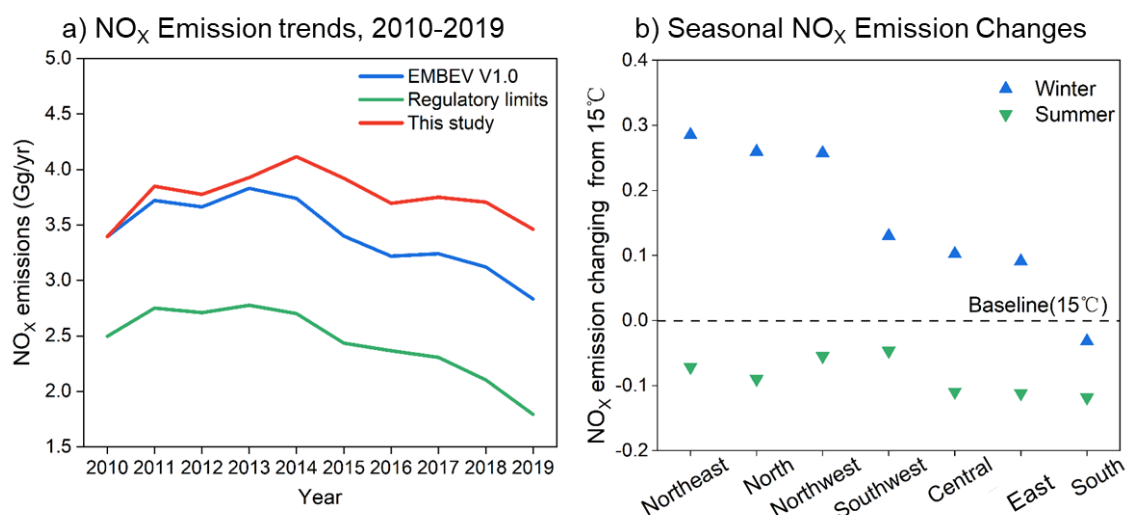


Figure 49: (a). Annual variations in NO<sub>x</sub> emissions of HDT fleet in China and comparison with regulatory and previous results in 2010–2019; (b). Changes in NO<sub>x</sub> emission of HDTs when considering winter and summer were considered throughout the major regions in China in 2019.

Note: The provinces included are as follows: Liaoning, Jilin, Heilongjiang (Northeast); Beijing, Tianjin, Hebei, Shanxi, Inner Mongolia (North); Shaanxi, Gansu, Qinghai, Ningxia, Xinjiang (Northwest); Sichuan, Guizhou, Yunnan, Xizang (Southwest); Henan, Hubei, Hunan (Central); Shanghai, Jiangsu, Zhejiang, Anhui, Fujian, Jiangxi, Shandong (East); Guangdong; Guangxi; Hainan (South).



## Europe

### Results from measurements prior to the CARES project 2016-2021

An overview of the results of RES type 3 measurements carried out on Euro V and Euro VI heavy-duty trucks across Europe during the period 2016-2021 is given by Table 4. It's quite clear that a substantial share of the trucks equipped with SCR systems to reduce NO<sub>x</sub> emissions drive around on European roads with their SCR systems tampered with or are not operational for other reasons. The share of high-emitters is higher among Euro V trucks than Euro VI trucks and among foreign (non-domestic) trucks than domestic trucks, with non-domestic in this case mainly comprising trucks from Eastern Europe.

On average, for Euro V – very roughly – 25-30% of the non-domestic and 15% of the domestic trucks drive around with non-functional or poorly operating SCR systems, whereas the corresponding shares for Euro VI are 20-25% and 10-15%. It's clear that this has a large impact on the mobile source NO<sub>x</sub> emissions in Europe.

Table 4: Overview of results of RES type 3 measurements carried out on heavy-duty trucks in various countries in Europe 2016-2021.

Country	Year	Share of manipulated/not working SCR				Reference (comments)
		Euro V		Euro VI		
		Foreign	Domestic	Foreign	Domestic	
Germany	2016	26%	0%	19%	7%	[34]
“	2019	26%	8%	20%	10%	[36]
Austria	2018	36%	25%	25%	19%	[35] Domestic also include trucks registered in Germany and the Netherlands
Switzerland	2019	See comment	0%	See comment	0%	[37] 38% for foreign trucks Euro V and VI taken together (split could not be made)
Denmark	2020	5-25%	8-23%	4-9%	1-5%	[38] The max and min reflect the probability of truly manipulated/not working SCR*s*
Sweden	2020	29%	30%	36%	13%	[39]
“	2021	50%	67%	26%	16%	[40] Shares are very uncertain for Euro V since only eight Euro V were measured

\* The indicated range of the share of vehicles with tampered/non-functional SCR is due to the fact that in this study two different limit values for NO<sub>x</sub> in the plume chase measurements were used to identify trucks whose SCR systems were: *highly likely* to be tampered/non-functional (min value) or *suspected* tampered/not working (max value).

In 2019, a comprehensive comparison between RES type 3 measurements and PEMS measurements was carried out on three heavy-duty trucks of different Euro classes – Euro II, V and VI – in Switzerland [37]. The measurements showed a good agreement, with a correlation of  $0.89 < R < 0.93$  over a NO<sub>x</sub> emission range from 200 mg/kWh to 10,000 mg/kWh. In 2021, a comparison between RES type 3 and PEMS was made on a Euro VI heavy-duty truck in an ISC test carried out in Sweden [40]. The comparison was made in two RDE tests, one with the vehicle in normal operation mode, and one with only water in the AdBlue tank. The two instruments showed a good agreement.

## Results from measurements in the CARES project (2022)

The controlled RES characterization experiments at a vehicle test track in the Netherlands included combined RES type 3 and onboard (SEMS) NO<sub>x</sub> emission measurements on three vehicles – a passenger car, a light-duty commercial vehicle and a heavy-duty truck, all diesel fueled [22]. The results are summarized in Figure 50. There was a good agreement between the two instruments, especially for the heavy-duty truck, having the highest emissions (a Euro VI operating in both normal mode and with the SCR switched off).

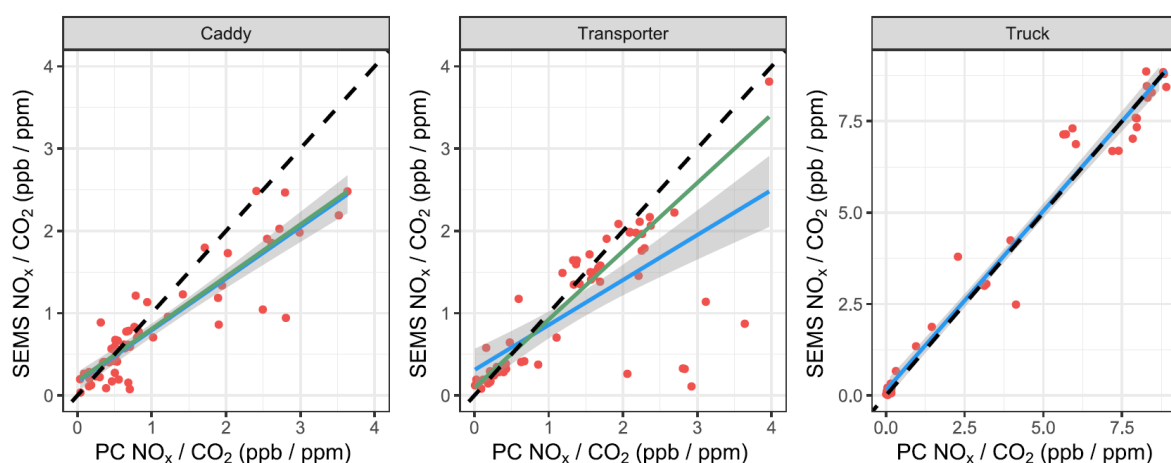


Figure 50: Comparison of NO<sub>x</sub> emission measurements by means of RES type 3 and SEMS on three different vehicles (Caddy: N1, diesel, Euro 6; Transporter: M1, diesel, Euro 6; Truck: heavy-duty, diesel, Euro VI) at a test track in the Netherlands in 2021 [22]. The blue line shows the linear model fit and the green line shows the median fit. The 1:1 line is represented by the dashed black line.

The measurements within the CARES project in Prague/Brno in September 2022 represent the most recent and comprehensive RES type 3 measurements in Europe carried out and published so far, with more than 900 heavy-duty trucks measured, of which 17 trucks (2% of the measured fleet) were pulled over to the roadside by the police and were subject to qualified inspections [24]. The key findings of these activities were:

- By applying a threshold in the RES measurements of 3500 and 2200 mg NO<sub>x</sub>/kWh for Euro V and Euro VI heavy-duty trucks, respectively, 40% of the Euro V trucks and 6% of the Euro VI trucks measured were flagged as high-emitters in the measurements carried out during daytime, see Figure 51.
- In the RES measurements carried out during nighttime, all Euro V trucks measured and 19% of the Euro VI trucks measured were flagged as high-emitters (Figure 51).
- The roadside inspection of 13 trucks flagged as high-emitters and 4 trucks flagged as suspicious high-emitters in the RES measurements showed that (Figure 52):
  - A reason for the high emissions could be found for all inspected trucks.
  - Trucks with very high emissions were more often manipulated (by adoption of Adblue emulators).
  - The share of trucks with manipulated SCR systems is higher for Euro V than for Euro VI trucks, whereas defects/errors and software issues are more common for Euro VI.
  - The software related issues were due to missing the mandatory update of the OEM (Original Engine Manufacturer) software of one OEM (Volvo). It appears to be a lack in the legislation that mandatory software updates are not made if trucks are not maintained at an authorized manufacturer workshop.

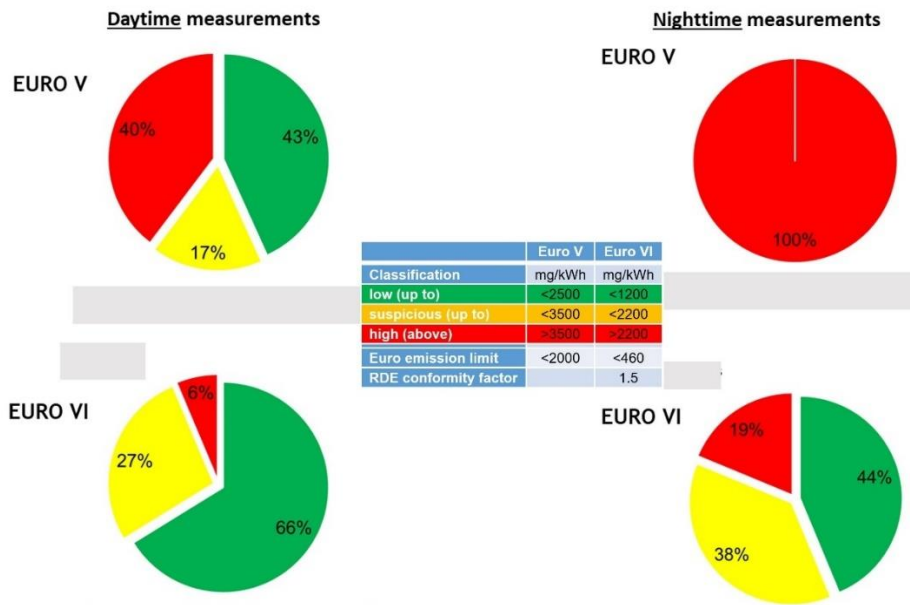


Figure 51: Results from RES type 3 NO<sub>x</sub> measurements on heavy-duty trucks in Prague/Brno 2022 – daytime vs nighttime measurements [24]. The embedded table displays the threshold for NO<sub>x</sub> emissions in mg/kWh units applied to categorize the measured trucks as low, suspicious or high emitters.

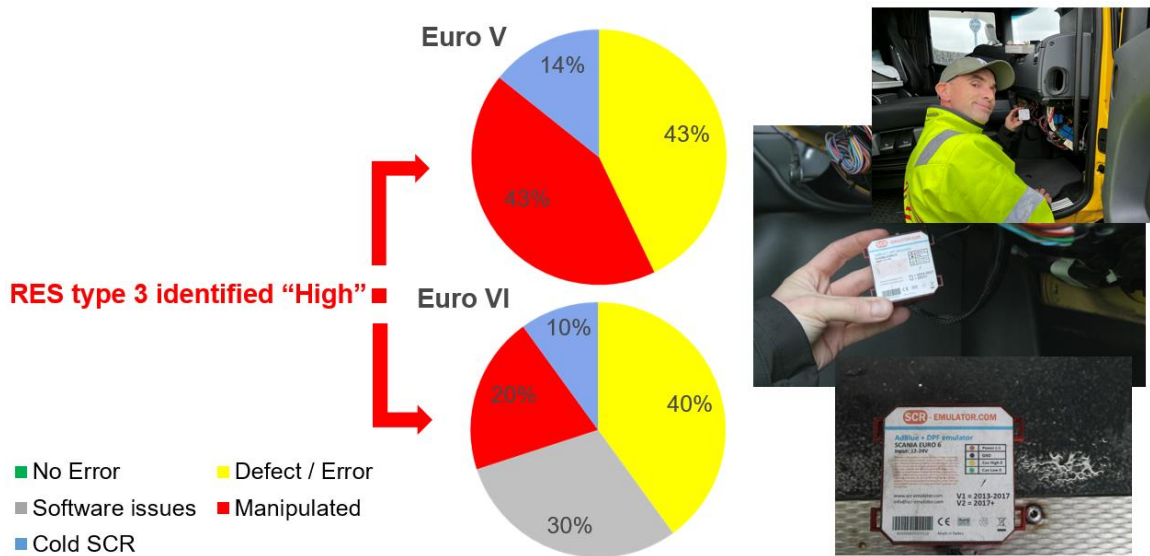


Figure 52: Results from roadside inspections of suspected high-emitting heavy-duty trucks based on RES type 3 measurements [24].

## PEMS/SEMS

### PEMS RDE measurements of Euro 6 diesel passenger cars

The collected and processed PEMS data from each trip related to NO<sub>x</sub> and PN data was organized in subsets per car, based on ambient temperature starting from lowest to highest as shown in Table 5. The table includes corresponding average and maximum NO<sub>x</sub> and PN emission concentrations for given car and trip. Further, to compare the emission performance of each vehicle with the predominant Euro 6 type approval and its corresponding RDE limits, the trip emissions are additionally displayed in the same table.

Table 5: Test data summarizing NO<sub>x</sub> and PN emissions as average and maximum concentrations together with the corresponding trip-based results.

Test #	Car id.	Average ambient temperature [°C]	Average NO <sub>x</sub> concentration [ppm]	Max momentary NO <sub>x</sub> concentration [ppm]	Trip NO <sub>x</sub> emissions [mg/km]	Average PN concentration [# /cm <sup>3</sup> ]	Max momentary PN concentration [# /cm <sup>3</sup> ]	Trip PN emissions [# /km]
1	Car A	0.9	62.3	2177	147.1	669	372172	5.8E+08
2	Car A	0	71.6	1963	144.8	803	204496	6.1E+08
3	Car A	1	55.2	1656	140.6	893	39347	8.0E+08
4	Car A	3.4	105.1	1562	416.7	1070	9357520	7.6E+08
5	Car B	-1.3	68.0	1740	257.7	983	29404	8.4E+08
6	Car B	-0.6	115.6	1458	267.8	868	35834	6.3E+08
7	Car B	0.8	152.7	966	284.1	774	60055	4.7E+08
8	Car B	5.7	145.7	1046	354.2	26626	40011	3.6E+10
9	Car C	2.7	12.7	388	34.1	17101	660413	2.3E+10
10	Car C	4.8	19.1	573	72.7	73131	11597200	1.2E+11
11	Car C	5.7	7.2	380	16.3	21211	4243350	2.4E+10
12	Car C	6.9	10.3	347	48.8	6149	56240	1.1E+10
13	Car C	13.1	19.1	444	43.2	69344	924741	7.9E+10
14	Car C	15.8	54.0	680	160.2	124096	733270000	1.9E+11
15	Car C	15.8	16.5	432	70.6	845	10604100	9.7E+08
16	Car C	17.1	9.0	577	27.0	5681	203489	8.6E+09
17	Car C	19.2	11.3	656	54.2	2091	5190330	3.4E+09
18	Car D	6.2	6.4	1976	20.1	333195	11629400	2.9E+11
19	Car D	10.7	11.4	1455	30.8	13855	16358500	2.4E+10
20	Car D	13.9	60.3	2364	133.9	201278	31736	1.8E+11
21	Car D	16.5	50.8	2329	107.1	161652	17053200	1.6E+11
22	Car D	17.8	19.9	2324	81.2	2049	380820	4.2E+09
23	Car D	18.5	31.3	3058	76.2	1232	346396	2.5E+09
24	Car D	19.6	39.4	2776	79.5	1335	249640	1.8E+09

The collected data suggest that the NO<sub>x</sub> performance of the test vehicles were rather dependent on either ambient temperature and/or type-approval class (Euro 6 sub class) and individual vehicle. This can be clearly seen by comparing the average trip NO<sub>x</sub> concentration in Figure 53 and from the trip based NO<sub>x</sub> emissions shown in Figure 54. The NO<sub>x</sub> emissions were clearly highest for the trips and cars, which were tested in sub 5 °C temperatures. These were jointly emitted by the two single LNT equipped cars, A and B. Car B was the only car failing to fulfill the NTE limits in any test. Because cars A and B were type approved as Euro 6b, the NTE nor RDE limits do not apply. Car A produced abnormally high NO<sub>x</sub> emissions in one test, which was caused by a regeneration event. However, due to the unequal ambient temperature conditions during the tests compared to cars C and D, a direct comparison might be arguable. Nevertheless, the NO<sub>x</sub> emissions produced by the Euro 6b class SCR equipped car, car C, in sub 5 °C conditions were far lower compared to results for cars A and B in corresponding conditions. The NO<sub>x</sub> performance of the Euro 6d-TEMP class, twin LNT equipped car D, was found generally similar compared to car C. Despite the uncomparable trip conditions, car C produced most stable NO<sub>x</sub> emissions throughout the varying ambient conditions, typically resulting in the range of sub 20 ppm NO<sub>x</sub> on average.

Similar temperature related effects on PN was not found, because all cars performed far beyond the requirements set by the predominant Euro 6 limits ( $6 \cdot 10^{11}$  #/km). PN concentrations varied between  $670 \text{ #/cm}^3$  to  $333195 \text{ #/cm}^3$  and were relatively well aligned with the average emission concentrations. No direct relation between trip conditions and PN emissions were distinguished.

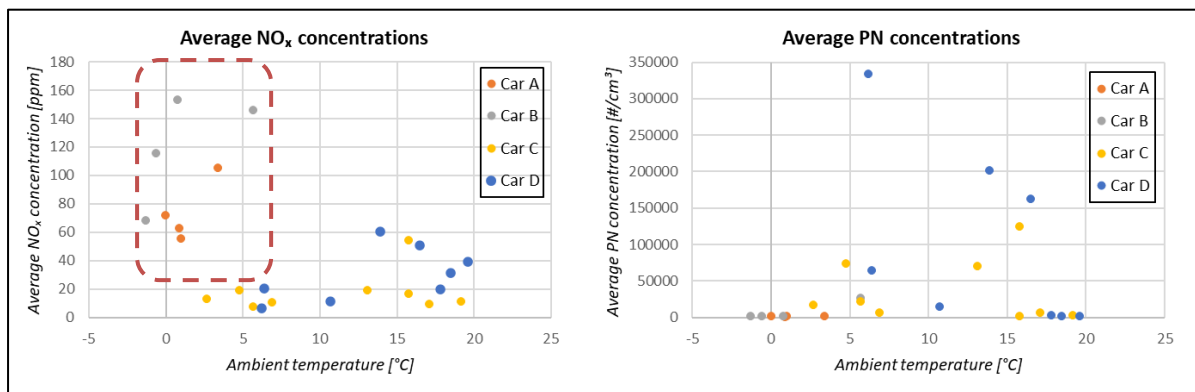


Figure 53: Average NO<sub>x</sub> and PN concentrations for cars A, B, C and D recorded in relation to ambient temperature.

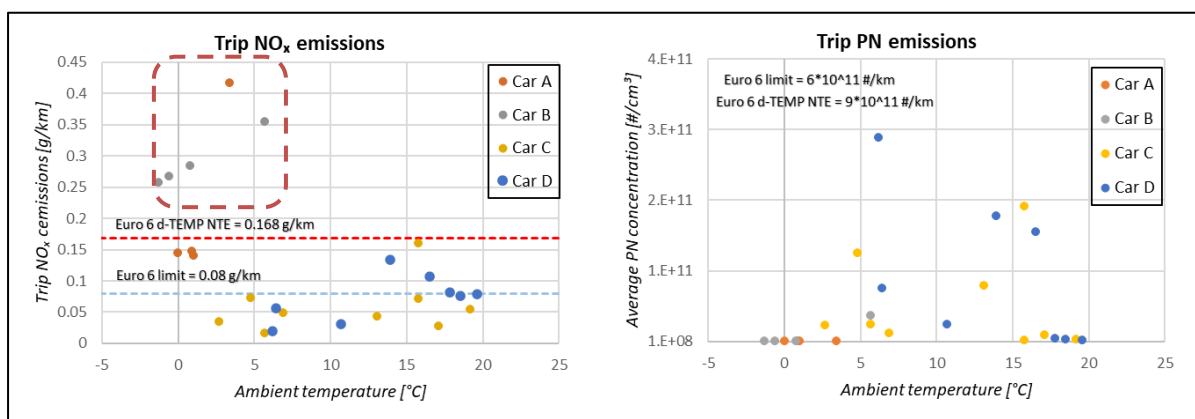


Figure 54: Trip NO<sub>x</sub> and PN emissions for cars A, B, C and D recorded in relation to ambient temperature.

The maximum NO<sub>x</sub> concentration recorded during each trip was clustered and clearly distinguishable per car individual as seen in Figure 55. For example, the NO<sub>x</sub> characteristics of car C seemed somewhat unaffected by trip conditions, and maximum NO<sub>x</sub> never exceeded 700 ppm in any test. This car was the only individual equipped with a SCR system, suggesting that SCR device was less sensitive to produce momentarily NO<sub>x</sub> spikes compared to its LNT counterparts. The maximum NO<sub>x</sub> emission for cars A and B, equipped with single LNT were found higher compared to car C, but the datasets were relatively well clustered together with concentrations ranging from ca. 1000 ppm to above 2000 ppm. Interestingly, regardless being tested in higher ambient conditions compared to e.g., Cars A or B, and despite performing overall well in terms of NO<sub>x</sub> emissions, Car D (twin LNT) produced highest momentary NO<sub>x</sub> peaks from the test group, with maximum concentrations varying between 1500 ppm and up to 3000 ppm depending on test. It should also be noted that car D was the only Euro 6d-TEMP car, meanwhile the others were type-approved as Euro 6b. These findings demonstrates that car individuals which tend to produce low NO<sub>x</sub> concentrations overall and even comply with the limit set in the RDE regulation may still occasionally produce significant spikes of NO<sub>x</sub>

emissions. This is especially crucial information for roadside RES monitoring, because any potential momentary spikes in NO<sub>x</sub> emissions recorded during a short period with RES may result in misleading conclusions. For example, a momentary 3000 ppm NO<sub>x</sub> peak is typically considered as a significant NO<sub>x</sub> concentration, and thus may cause a RES system to flag a car for ineffective EATS. In reality, the data obtained from these PEMS tests proves that this specific individual is in fact performing overall well better than required by the predominant regulation. Another challenge, which was identified from the data, was that no direct correlation between mean NO<sub>x</sub> concentrations and the maximum NO<sub>x</sub> values were found for any car. This means that a direct assumption based on momentary NO<sub>x</sub> emissions and overall NO<sub>x</sub> performance for any vehicle may be challenging to withdraw.

The recorded data of PN peaks was found relatively random, especially for cars C and D. The PN peaks were typically below 1\*10<sup>8</sup> #/cm<sup>3</sup> and a no direct relation between trip and maximum PN concentration could be found. The data proves that Euro 6 class diesel vehicles, which are equipped with DPF:s are highly efficient on particulate filtering, and thus no great variation in performance takes place even in varying trip conditions.

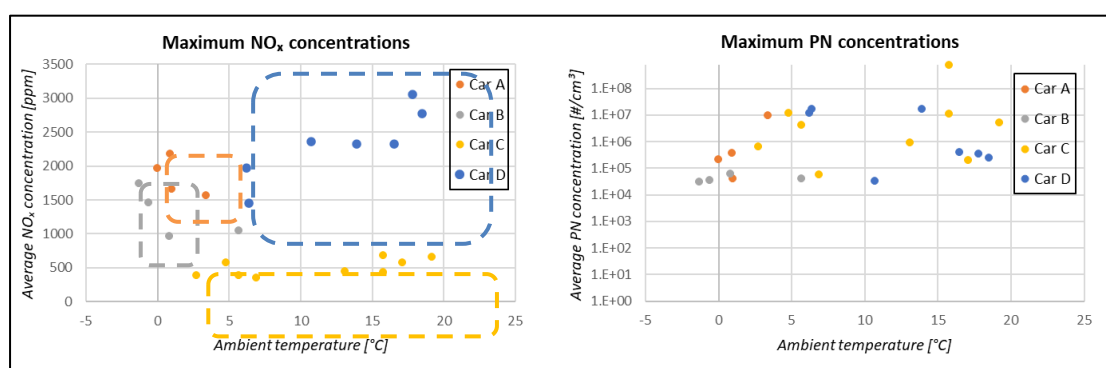


Figure 55: Maximum NO<sub>x</sub> and PN concentrations for cars A, B, C and D recorded in relation to ambient temperature.

Last, a specific road section from one of the RDE trips was further examined for providing additional information for back-to-back case study comparison. The section was a traffic junction, where cars are entering and accelerating from an urban, low speed area to a rural road with a speed limit of 80 km/h. This junction was selected for further examination because this location could potentially be suitable for either conventional roadside RES or point sampling RES monitoring, and was simultaneously identified as a sector, which caused highest abnormal NO<sub>x</sub> characteristics for multiple test cars.

Figure 56 shows examples of momentary NO<sub>x</sub> and PN concentration produced by each car in this specific location. Figure 57 depicts the corresponding NO<sub>x</sub> mass produced by each vehicle during the acceleration. The momentary NO<sub>x</sub> traces for the cars equipped with single LNT, cars A and B were comparable (with peaks of ca. 900 – 1000 ppm), meanwhile the twin LNT counterpart produced even higher NO<sub>x</sub> peaks during acceleration, ca 1400 ppm at most. Car C, which was equipped with SCR, resulted in producing NO<sub>x</sub> concentration below 100 ppm during the corresponding event. The data suggests that large variation between vehicle NO<sub>x</sub> characteristics takes place, especially between EATS technologies. The variation is particularly enhanced when analyzing momentary events, such as in this example, during rapid acceleration. On contrary, car C produced evidently higher PN emissions during the same event, most likely as a result of the urea injection for the SCR. No significant increase in PN was seen for any LNT car during the acceleration.

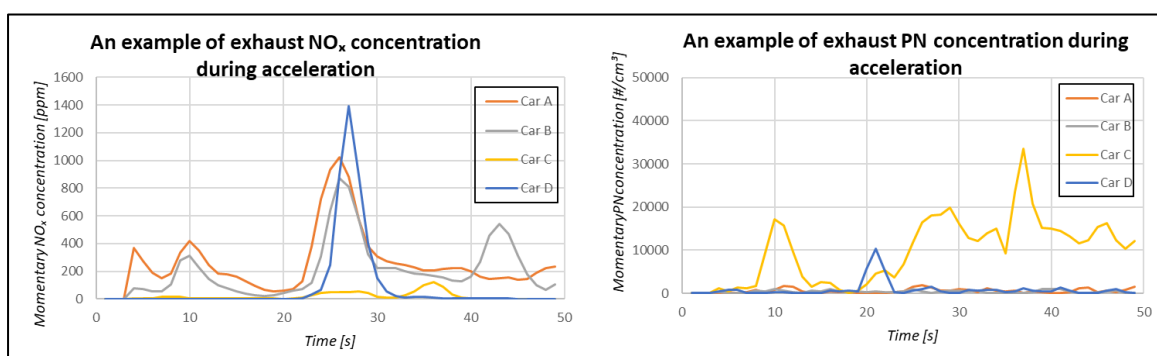


Figure 56: An example of NO<sub>x</sub> and PN concentration during an acceleration event from an urban area to highway.

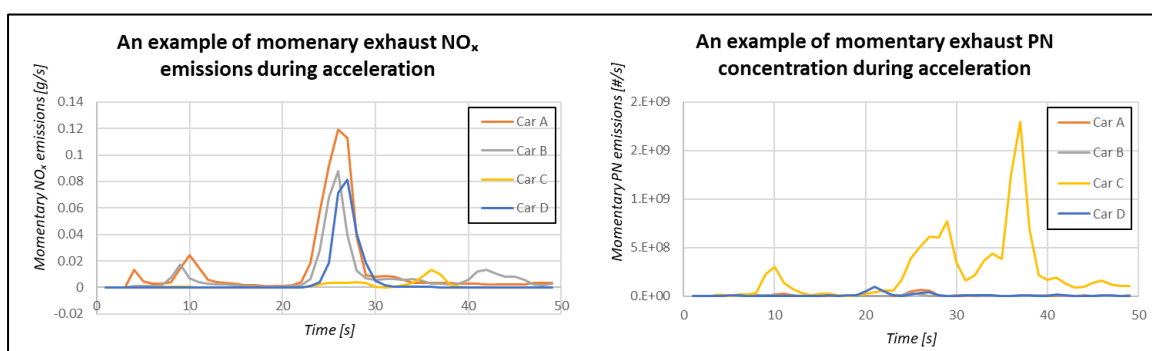


Figure 57: Example of NO<sub>x</sub> and PN emissions during an acceleration event from an urban area to highway.

The results obtained from the PEMS tests suggest that the emission performance of Euro 6 diesel cars, especially for NO<sub>x</sub> emissions, are highly reliant on the driving conditions, implemented EATS technology, vehicle model year and hence, its type approval class. The results demonstrate that the revisions related to the implementation of RDE testing in the Euro 6 regulation have resulted in significant improvements in overall NO<sub>x</sub> suppression during real-world driving. For example, the Euro 6 d-TEMP car, car D, which was equipped with the twin LNT performed based on a trip-based analysis similarly compared to the SCR vehicle. Nevertheless, the data also shows that diesel cars type approved outside the mandatory RDE testing may perform well in real-world conditions and even fulfill the corresponding Euro 6d-TEMP NTE limits. On the contrary, the data also demonstrates that despite the NO<sub>x</sub> performance may be overall good, high momentary NO<sub>x</sub> peaks may take place, especially during rapid accelerations, meaning that correlation between the overall NO<sub>x</sub> performance and momentary NO<sub>x</sub> spikes were concluded non-existing. This factor may produce challenges for conventional road-side or point sampling-based RES monitoring intended for determining the NO<sub>x</sub> emission performance for individual cars. However, this issue would be less evident for plume chasing because the emission performance may be monitored during longer distances and various conditions. Then, momentary spikes in NO<sub>x</sub> emissions may be considered as a part of the typical emission behavior as long as the NO<sub>x</sub> suppression is reduced to accepted magnitudes after e.g., an acceleration event. Similar issues are suspected to be less problematic for PN monitoring, because the variation in typical PN emissions for DPF equipped cars are generally lower. For example, cars with tampered or defect DPF devices are expected to produce evidently higher PN emissions both overall and during any momentary acceleration events.

## SEMS measurements of light- and heavy-duty Euro VI diesel trucks

When the light- and heavy-duty Euro VI diesel trucks were driven on the highway the NO<sub>x</sub> emissions were very low. After exiting the highway and entering the city area it was observed that the aftertreatment system was subject to a decrease in temperature and associated NO<sub>x</sub> reduction efficiency. This does not always, or automatically, mean that the NO<sub>x</sub> emissions become high – the vehicles may still be able to perform the full test route without a significant increase in NO<sub>x</sub> emissions. The main parameter is how high the temperature of the aftertreatment system is and how well it can preserve heat during stops. In heavy traffic and several unplanned stops, occasionally typical for city driving, a large increase in NO<sub>x</sub> emissions was sometimes observed, that corresponded to a reduced temperature of the aftertreatment system. Further, the larger the engine is (in relation to the vehicle size), the bigger this problem seems to be.

An important question is how long after the start of idling the exhaust gas aftertreatment system of the Euro VI diesel trucks will be active. The measurements show that the NO<sub>x</sub> emission from the light-duty truck starts to increase earlier – already after about 1 minute – compared to the heavy-duty trucks.

The two trucks with a small (8 liters) and a midsize (11 liters) engine showed a very similar behavior with regard to NO<sub>x</sub> emissions following start of idle - emissions did not start rising until about 10 minutes of idling.

For the truck with the largest engine (16 liters) NO<sub>x</sub> emissions started to rise after about 3-4 minutes idling, i.e., a significantly shorter time than for the other two heavy-duty trucks. This may be due to its large engine and that it was carrying lower load in relation to its maximum load capacity in comparison to the other vehicles, why its cool-down period was reduced. Other explanations may be different methods being used to control the NO<sub>x</sub> emissions and different strategies to preserve the heat of the aftertreatment system.

While NO<sub>x</sub> emissions of Euro VI heavy-duty trucks proved to be sensitive to both driving conditions, time of idling and vehicle load, this was not found to be the case for PN emissions, demonstrating the high reduction efficiency of modern DPFs.



## Exhaust plume modelling

### Approach

To determine the fuel-specific emission factor, the concentration of the individual species is measured in the form of a voltage. Knowing the absorption  $A_\lambda$  and the molar attenuation coefficient  $\epsilon_\lambda$  of the species  $\lambda$ , the concentration  $c$  of species  $\lambda$  can be determined from the Beer-Lambert law,

$$A_\lambda = \epsilon_\lambda \cdot c \cdot l.$$

Assuming that the exhaust plume is well mixed, the optical path length  $l$  can be considered the same for each species, so that, e.g., for NO<sub>x</sub> and CO<sub>2</sub>

$$l_{\text{NO}_x} = l_{\text{CO}_2}$$

applies and the concentration ratio can be rewritten as

$$\frac{c_{\text{NO}_x}}{c_{\text{CO}_2}} = \frac{A_{\text{NO}_x} \cdot \epsilon_{\text{CO}_2}}{A_{\text{CO}_2} \cdot \epsilon_{\text{NO}_x}}.$$

In this work, the cut plane concentration integrals in the  $yz$ -planes,  $xz$ -planes and  $xy$ -planes with the respective distance to the exhaust tailpipe are analyzed, which would in case of time-averaged pollutant mass fraction read

$$\iint_{\mathbb{R}} \langle \bar{Y}_p \rangle_{AVG} dx_i dx_j$$

where

$$(x_i, x_j) \in \{(x, y), (x, z), (y, z)\}$$

describes the set of planes. For the sake of comparability of different simulation cases, a normalization to the highest cut plane concentration integral is introduced, which is referred to be the normalized cut plane concentration integral. Consequently, unlike the technology based on the line-measurement principle, all local information of the exhaust plume is recorded in the vehicle wake, and thus the result is what the plane-measurement instrument should theoretically measure.

### Pollutant dispersion

Figures 58a,d show the pollutant dispersion in the vehicle wake for a velocity of 50 km/h. The exhaust gases dilute very rapidly after they leave the tailpipe and enter the vehicle wake. To reach a hundredfold dilution of the exhaust tailpipe concentration, the exhaust plume has to be 0.83 m long ( $x$ ), is 0.81 m wide ( $y$ ), and 0.74 m high ( $z$ ), as can be seen in Figure 58 and Figure 59a (for a vehicle velocity of 50 km/h with the LH tailpipe).

Figure 59b it can also be seen how the exhaust gas is distributed laterally with respect to the exhaust tailpipe ( $y$ -direction). Again, large pollutant mass fraction gradients exist directly next to the exhaust tailpipe, so that 0.5 m to the side of the tailpipe a negligible amount of pollutant is present. Since this example involves an exhaust tailpipe on the left side of the vehicle, the dispersion curve is not symmetrical. Consequently, there is less pollutant 0.5 m to the left of the tailpipe than 0.5 m to the right of the tailpipe. At this point, it should be mentioned that this is a normalized sum of all pollutants on the  $xz$ -planes.

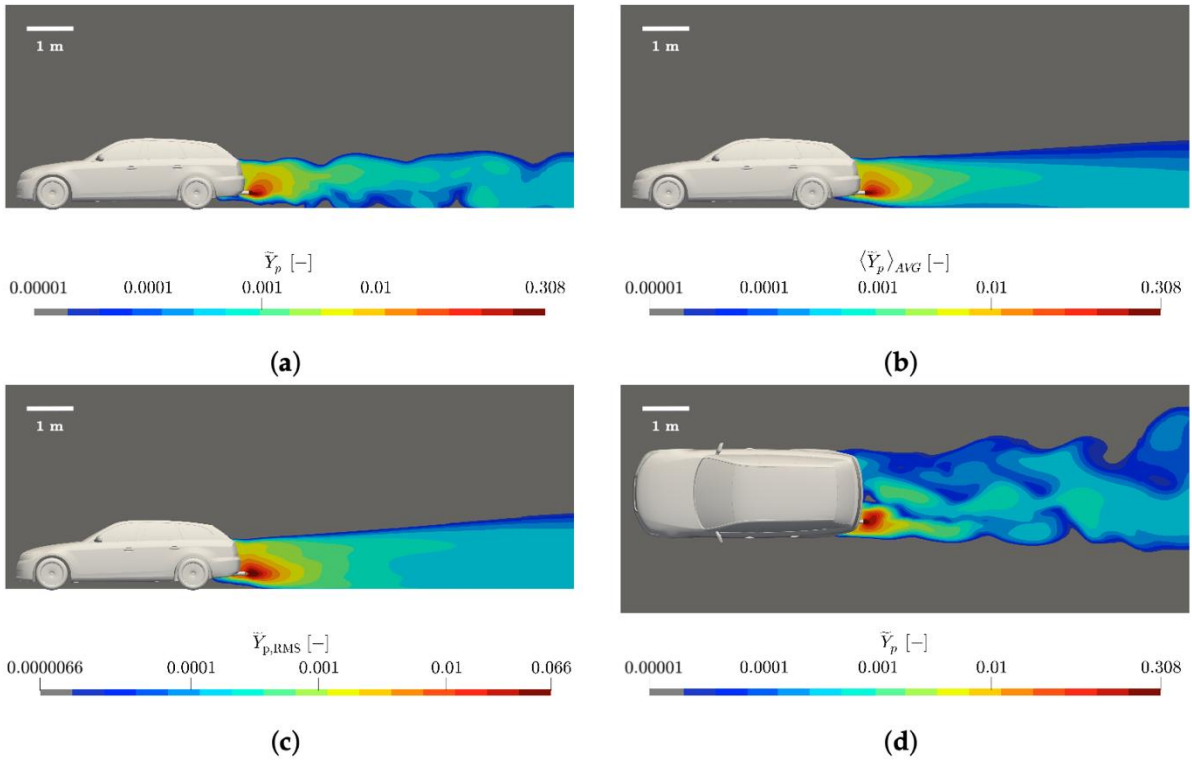


Figure 58: Pollutant mass fraction in the CEP of a vehicle driven at 50 km/h for LH (a) and LD (b) tailpipe configurations. The sum of time-averaged pollutants at x,y and z in the CEP in case of 30, 50 and 80 km/h vehicle velocities are depicted for horizontal (c) and downward oriented (d) tailpipes. (a) xz-plane at y = -0.56 m-plane (LH tailpipe position), (b) xz-plane at y = -0.56 m-plane (LD tailpipe height), (c) Tailpipe locations are LH, CH and LRH, (d) Tailpipe locations are LD, CD and LRD.

The same evaluation can also be made for the z-direction. The pollutant mass fraction is highest at the level of the exhaust tailpipe and decreases sharply both downward and upward. However, the exhaust gas is distributed more upward toward the rear window of the vehicle than downward toward the underbody of the vehicle. This is a consequence of the flow field and the recirculation zone, caused by detachments on the roof and underbody. The proximity of the exhaust tailpipe to the underbody means that some of the escaping exhaust gas is carried upward by the recirculation. Finally, above the exhaust tailpipe, the recirculation zone with lower velocities is prevailing while below the exhaust tailpipe convection due to the high mean flow velocity dominates.

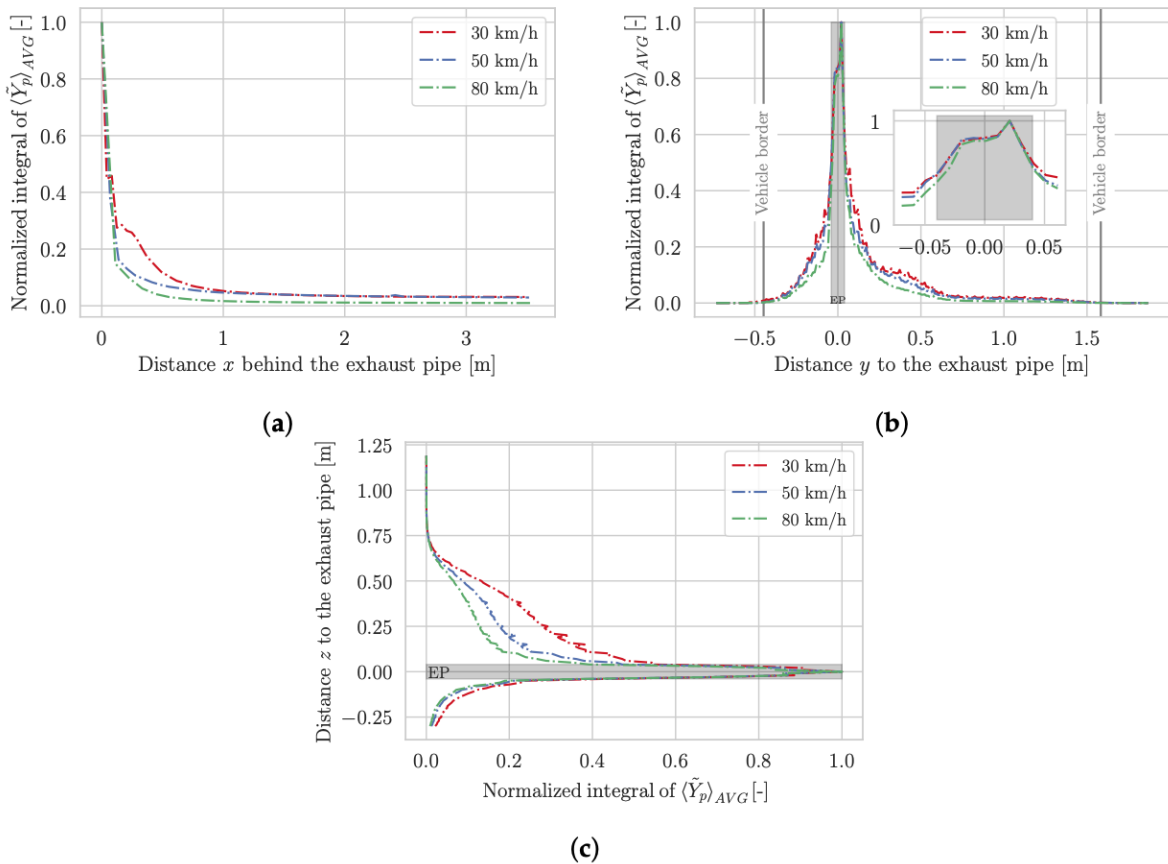


Figure 59: Pollutant dispersion behavior of a vehicle driven at 30, 50 and 80 km/h with a LH tailpipe (EP: exhaust tailpipe position). (a) Normalized cut plane integral of time-averaged pollutant mass fraction in the yz-planes, (b) Normalized cut plane integral of time-averaged pollutant mass fraction in the xz-planes, (c) Normalized cut plane integral of time-averaged pollutant mass fraction in the xy-planes.

## Parameter study

In this work we performed numerical simulations of flows around vehicles to analyze pollutant dispersion in the vehicle wake, and related implications for on-road RES measurements were investigated. URANS was chosen as the turbulence modeling approach to keep the computational time in bounds due to high Reynolds numbers, while still resolving large, coherent vortices. From the comprehensive parameter studies, some relevant insights into the possibility and framework conditions for measurements of exhaust emissions by means of RES could be gained.

- In general, the exhaust plume strongly dilutes in the near vehicle wake, e.g., 1.5 m downstream of the vehicle the cut plane integral of pollutant mass fraction decreased by one order of magnitude.
- Increasing vehicle velocities result in a decreased size of the core exhaust plume (CEP) in all directions.
- The sum of time-averaged pollutants within the CEP decreases with increasing vehicle velocity for all tailpipe configurations.
- For all tailpipe configurations, regardless of velocity, the pollutant amounts (time-averaged) within the CEP is highest for a left pipe, decreases in case of a center pipe and is lowest for left and right positioned pipes.

- For downward oriented tailpipes (generally positioned under the vehicle, nearer to the rear wheels) the pollutant concentrations available for a RES device downstream the vehicle rear almost is an order of magnitude lower with respect to the horizontal tailpipes.
- With increasing crosswind velocity, the exhaust plume is more deflected and the oscillations in the exhaust plume increase as well.
- Crosswind has little influence on the CEP. As the distance from the tailpipe increases and the wind increases, the amount of pollutant that can be detected by RES devices decreases.
- A plane-measurement instrument always detects a higher fraction (in terms of absorption) of the original exhaust gas compared to a line-measurement instrument, that is approx. 70 % more in the CEP and 95 % more in the far downstream region.
- Low measurement frequencies lead to few measurement points in the CEP and therefore to a less robust estimation of the concentrations.
- The interference of pollutant concentrations from multiple plumes in the longitudinal direction has a smaller effect on measurement accuracy than the increased turbulent intensity by the vehicle ahead.

### Hybrid LES/RANS framework

A new extension of a hybrid LES/RANS is proposed in the present paper with focus on consistency concepts for enthalpy and species concentrations. Additionally, because of the temperature and species variations in the near-wake area, the framework from [60] was extended to the low-Mach number case of density-varying flows. Recognizing that the enthalpy and species mass fraction fields obey advection-diffusion equations, the extension was considered for a general scalar. The RANS and LES scalar fields were also forced towards each other through additional drift terms. These terms contain a scalar variance term that required an additional transport equation to solve for it.

Consistency of the flow fields in the newly extended hybrid framework for enthalpy and species was achieved. However, several important algorithmic parameters were reviewed to assess their influence on the overall solution. The averaging time and relaxation time scales were set following the recommendations of the framework's original authors, leading to good results. As mentioned though, these parameters could benefit from automation, and subsequent works have suggested to render the time scales dependent on the local turbulent quantities and in so doing optimize the level of consistency between EWA LES and RANS fields. Lastly, a loose coupling instead of a tight coupling of LES and RANS equations could benefit the consistency of flow fields as well as decrease the computational cost. This is not solving the LES and RANS equations simultaneously but sequentially, allowing for larger time steps since small step sizes are required for the URANS simulation (in the tight coupling approach).

Hybrid LES/RANS has allowed for computationally efficient simulations of the exhaust plume in the vehicle wake. It has proven to be an effective way of gauging the efficacy of RES in the future, however more development and implementation should be carried out to improve and optimize the framework. For a description of the framework's details, it is referred to [19].

## Results summary

### RES type 1

- Through the ability to efficiently (i.e., at a comparatively low cost) measure real driving emissions of all regulated pollutants (NO<sub>x</sub>, PM, CO and HC) from very large numbers of vehicles, and thereby covering representative vehicle fleets, RES type 1 has proven a very useful tool to measure the average emissions by emission standard, vehicle brand, engine family, etc., and compare these with e.g., legislative emission limits. This may serve air quality policy purposes and evaluation of needs of further development of emission legislation.
- Adopted in the right manner, RES type 1 can also be used for direct enforcement of tampered vehicles, or vehicles that are gross-polluting due to other reasons, by:
  - Individual vehicle screening in real-world settings combined with roadside inspections. This has mostly been applied to heavy-duty trucks and proven very successful in finding trucks for which the SCR-system has been tampered with, leading to very high emissions of NO<sub>x</sub> [20,25].
  - It seems also that light-duty diesel vehicles with non-functioning DPFs can be identified through RES type 1 screening [28]. Apart from opening up the possibility for direct enforcement by means of roadside inspections, this also offers assessment of the efficiency of PTI programs involving PN testing.
- Repeat RES type 1 measurements on individual light-duty vehicles have proven to increase the likelihood to correctly identify high-emitters compared to when only a single measurement is carried out. For Euro 5 diesel passenger cars, 80% of the NO<sub>x</sub> high-emitters were identified with over 75% precision with 5 or more repeated measurements of the same vehicle [61]. For early Euro 6 diesel cars, 90% of the cars exceeding a cut-point in the RES type 1 measurements of 5 g NO<sub>x</sub>/kg, emissions were above the Euro 6 RDE limit according to PEMS RDE measurements on the same car individuals [21].
- RES type 1 offers a very good means to derive relationships between emissions by Euro class and vehicle age or mileage as well as ambient temperature, respectively [26,27]. This is useful for improving and updating road vehicle emission models, such as HBEFA and COPERT. A good agreement between RES type 1 measurements and modeling results using the PHEM model (the underlying emission factor model to HBEFA) was observed for NO<sub>x</sub> emissions for both diesel and petrol cars, when the actual ambient temperature and vehicle age distributions were taken into account.
- Following dieselgate, a number of studies have been carried out in which RES type 1 have been compared with (validated against) PEMS, particularly for measurements of NO<sub>x</sub> emissions, preferably under controlled conditions [22,23,29,62] but also in a real-world setting [24]. In general, a good agreement has been observed between the two types of instruments in these studies, down to the instrumental detection limits of the RES type 1 instruments.
- The main limitations of RES type 1 are:
  - the low accuracy in measuring particles and occasionally also NO<sub>2</sub>, mainly due to the low emissions associated with modern, low-emitting vehicles;
  - the high risks with drawing conclusions regarding a vehicle's emission performance from a single measurement;
  - the inability to carry out measurements during rainy conditions.

## RES type 2

- The development of RES type 2 technology over the last ten years has above all advantageously circumvented the limitations of RES type 1 to accurately measure emissions of particles. RES type 2 approaches to measure emissions of size-resolved particle mass and particle number (PN) with research-grade instruments have evolved [10], followed by low-cost sensors to measure total PN and BC [12,52].
- Just as for RES type 1 in the case of gaseous pollutant emissions, RES type 2 has proven to successfully measure average emissions of fine particulate matter by emission standard for both heavy- and light-duty vehicles [10,12,22,23,32,33,52,53].
- RES type 2 measurements on heavy vehicles (public transport buses) have also comprised in-depth studies on the impact of different fuels, including biofuels, on the emissions of particulate matter [10,32].
- More recently also gaseous pollutants, e.g., nitrogen oxides, have been incorporated in RES type 2 measurements (Figure 32). In the case of the most recent European RES type 2 system, the same instrument developed for RES type 3 has been utilized for this purpose [12,22,23,52]. The compact, cost-effective sensor platform developed in China successfully identified high-emitters by combining NO and PN emission factors and demonstrated that the aftertreatment system has a strong effect on emission factors, whereas cargo load and speed only have a relatively minor influence.
- RES type 2 measurements of nitrogen oxides as well as particulate matter (PN) have been compared with PEMS measurements under controlled conditions in both China (Figure 33) and Europe [22,23]. In the latter case such comparisons have also been made in a real-world setting [52]. In general, a good agreement was observed between RES type 2 and PEMS for both PN and NO or NO<sub>x</sub> emissions.
- Due to the longer time that RES type 2 samples the exhaust plume, 5-10 seconds, compared to RES type 1 (≈0.5 s), it appears to perform significantly better when it comes to separating high-emitting from low-emitting vehicles, i.e., RES type 2 is less sensitive to fast changes in driving conditions and engine load, with emission effects being averaged out [23]. This applies to both particles (PN) and nitrogen oxides, NO or NO<sub>x</sub> (Figure 32).
- Accordingly, RES type 2 has shown very promising results in identifying high-emitters with regard to PN and BC [53].
- Other advantages of RES type 2 are no need for calibrations in field, no need of external supply of power since all instrumentation is operated by batteries, and the capability to operate also during rainy conditions (as opposite to RES type 1).
- The main limitations of RES type 2 are:
  - Unable to separate exhaust plumes when traffic is too dense → generally lower hit-rates (share of valid measurements) compared to RES type 1;
  - Low hit-rates under certain, unfavorable wind conditions.

## RES type 3

### China

- RES type 3 has been validated to applicably measure NO<sub>x</sub> emissions for diesel gas trucks (including low-emitting China VI) and identify normal and defeated aftertreatment device by RES type 3-PEMS concurrent test [43]. Furthermore, meteorological ratios (ER) can be useful to improve the filtering of reliable results [54].
- Based on more than ten thousand real-world RES type 3 tests in China, we confidently found that China IV heavy-duty trucks (HDTs) which claimed adopted SCR aftertreatment had no more NO<sub>x</sub> emission reduction than China III without SCR. Significant NO<sub>x</sub> control benefits have been confirmed for post-2018 China V and China VI HDTs with EGR+SCR were observed to significantly reduce the fleet-average NO<sub>x</sub> emission factors.
- The BC emissions from HDTs showed a progressive decline with more stringent emission standards [58]. However, a small fraction of high-emitting HDTs (top 10%) can be responsible for more than half of the fleet's total BC emissions.
- The national emission inventory results showed that previous studies underestimated 18% of NO<sub>x</sub> emissions in China in 2019 and nearly half of the real-world NO<sub>x</sub> emissions from HDTs (determined by updating the emission trends of HTDs) exceeded the regulation limits [59].
- The ambient temperature was identified as a primary driver of NO<sub>x</sub> emissions for HDTs, and the low-temperature penalty has caused a 9–29% increase in NO<sub>x</sub> emissions in winter in major regions of China [59].

### Europe

- RES type 3 measurements carried out since 2017 have demonstrated that emission tampering of Euro V and Euro VI diesel powered HDTs, mainly by using Adblue emulators to simulate that the SCR system is working, while it really isn't, occurs frequently across Europe [24,34,35,36,37,38,39,40].
- SCR tampering increases the NO<sub>x</sub> emissions from HDTs with up to one order of magnitude or even more.
- SCR tampering is more frequent on Euro V than on Euro VI trucks; typical shares are 20-30% vs 10-20%.
- RES type 3 measurements have shown to agree well with PEMS measurements (NO<sub>x</sub>) in several studies [37,39].
- In recent years, RES type 3 measurements have become more automated, enabling unskilled personnel to carry out routine measurements after some short training [24].
- Another advantage with RES type 3 is the ability to measure on highways, which is not as easy for RES type 1 and 2 (except for the HEAT EDAR RES type 1 system).
- The limitation of RES type 3 is mainly the rather small number of vehicles that can be measured in a day, naturally 1-2 orders of magnitude lower than for RES type 1 and 2. Another limitation is the inability to measure in dense (typical city) traffic, where exhaust plumes frequently overlap.

## PEMS and SEMS

- The findings of the analysis of available PEMS data as part of Task 61 demonstrate that Euro 6 diesel cars, which tend to produce low NO<sub>x</sub> concentrations overall and even comply with the Euro 6 emission limit set in the RDE regulation, may still occasionally produce significant spikes of NO<sub>x</sub> emissions, e.g., during strong accelerations. This can be crucial for RES type 1 and type 2 monitoring, because any potential momentary spikes in NO<sub>x</sub> emissions recorded during a short period (in the order of seconds) may result in misleading conclusions being drawn from the RES data.
- Another challenge, which was identified from the PEMS data, was that no direct correlation between average NO<sub>x</sub> concentrations and the maximum NO<sub>x</sub> values were found for any of the measured Euro 6 cars. This means that a direct assumption based on momentary NO<sub>x</sub> emissions and overall NO<sub>x</sub> performance for any vehicle may be challenging to withdraw.
- An in-depth analysis of the PEMS data for a specific road section from one of the RDE trips was carried out for a traffic junction, where cars are entering and accelerating from an urban low speed area to a rural road with a speed limit of 80 km/h, potentially considered as a good measurement site for RES type 1 or type 2, showed that this was a sector which caused the highest abnormal NO<sub>x</sub> characteristics for multiple test cars. It implies that measurement sites characterized by strong accelerations should be avoided for RES type 1 and type 2.
- Of the Euro 6 cars tested, the one equipped with SCR, which is the main exhaust aftertreatment system (EATS) used to comply with the RDE regulation, was the one that produced the most stable NO<sub>x</sub> emissions, i.e., the lowest variation in NO<sub>x</sub> emissions due to varying ambient temperatures and varying driving conditions, which may be beneficial for RES type 1 and type 2 monitoring.
- The problem with large variations in momentary emissions of NO<sub>x</sub> was not observed for PN emissions from Euro 6 diesel cars, indicating that the DPFs are highly efficient on particle filtering, and thus no great variation in performance takes place even in varying trip conditions, which is beneficial for RES type 2 PN monitoring.
- SEMS measurements demonstrate that also diesel powered light- and heavy-duty Euro VI trucks NO<sub>x</sub> emissions are sensitive to driving conditions, in particular there may be large differences in emission levels between highway (low emissions) and city (high emissions) driving, due to lower temperatures of the aftertreatment system at lower engine loads and idling. Also, low freight loads may increase NO<sub>x</sub> emissions for Euro VI heavy-duty diesel trucks. Thus, it is not ideal to carry out NO<sub>x</sub> RES measurements to identify NO<sub>x</sub> high-emitting trucks and buses in typical city driving, i.e., in heavy traffic, causing a lot of low speed and stop-and-go situations.
- Just as for Euro 6 diesel cars, the problem with large variations in momentary emissions of NO<sub>x</sub> was not observed for PN emissions for Euro VI diesel trucks either, which can be beneficial for RES type 2 monitoring to check the functionality of DPFs also on trucks.



## Exhaust plume modelling

The numerical simulations, applied to a very typical passenger car on European roads, of the flow of air around the vehicle and the distribution of exhaust gas components in the vehicle wake show that:

- The exhaust gas plume is strongly diluted in the near wake of the vehicle, which means more precisely that no significant proportion of exhaust gas can be measured 1.5-3 m downstream of the vehicle. For all different driving and environmental conditions, the highest concentration of exhaust gas or pollutant was found less than 0.5 m downstream of the vehicle.
- The dispersion of the essential part of the exhaust gas (core exhaust plume) depends on the vehicle speed. With increasing speed, the core exhaust plume becomes more compact in all directions.
- With regard to RES, however, the exhaust gas cloud is diluted relatively identically for all investigated speeds between 30 km/h and 80 km/h, so that most of the dilution has taken place 1.5 - 3 m downstream and 0.5 m to the side (depending on the configuration) of the tailpipe.
- Crosswind simulations have made it clear that the core exhaust gas plume is only slightly affected by the wind. At very high crosswind speeds, the concentration peak shifts in the corresponding direction, but it is the part of the exhaust gas plume further downstream that is affected by the wind.
- Measuring instruments with lower frequencies, which measure over a normal road width, therefore have problems capturing enough measuring points in the plume to reconstruct the corresponding concentration ratio. In general, the HEAT EDAR RSD has advantages here, as the measurement frequency is higher and more exhaust gas can be captured, as measurements are taken over entire planes.
- Acceleration of the vehicle is often important to ensure that enough exhaust gas emerges from the tailpipe. However, acceleration also has the effect of shortening the exhaust gas cloud over time, which in turn causes problems for a valid measurement (e.g., with a low measurement frequency). Conversely, the exhaust gas cloud lengthens during braking, whereby it was assumed in the simulations that there is still enough exhaust gas coming out of the tailpipe (often being not case since the engines are in fuel cut-off regime).
- Consequently, RES fulfils the general requirements for determining correct emission values. Nevertheless, the parameter study has shown that external influences, such as wind, or driving characteristics, such as speed and acceleration, create difficulties for RES with low measurement frequencies. This can lead to either incorrect or even invalid measurement results. In addition, this can cast considerable doubt on the reliability of RES measurements in the wake of trucks, in which case the exhaust pipe is often more than 10 m upstream the end of the vehicle.
- With regard to the influence of several vehicles driving behind each other, it can be seen that no significant increase in concentration was determined in the exhaust cloud of the rear vehicle due to the emissions of the first vehicle. However, the flow field behind the first vehicle strongly influences the pollutant distribution downstream of the second vehicle and thus the pollutant concentration determined by an RES instrument. The smaller the distance between the vehicles, the stronger the mutual influence.

## Applicability and potential impact

Following the development of the original remote emission sensing technique (type 1), which has evolved and refined over the last 35 years, two other RES techniques have strongly developed over only the last 5-10 years (type 2 and type 3). One of the driving forces behind the development of the two recent types has been to overcome some of the shortcomings or limitations associated with type 1. In the case of type 2 this has been to improve the ability (with associated high accuracy) to measure emissions of particulate matter, such as particle mass, particle number and Black Carbon, whereas type 3 has eliminated the shortcoming associated with the snapshot character of the emission measurements of the other two types (measurement duration in the order of 1 s or less). Still, type 1 is superior compared to in particular type 3, but also type 2, when it comes to the number of vehicles that can be measured in a given time frame.

Given today's access to three different RES types, compared to only one less than ten years ago, and given the pros and cons of the three different types, this has opened up for more tailor-made applications of remote emission sensing, since the instruments can be used as single instruments or in various combinations, depending on the purpose of the emission measurement(s) to be made. In fact, as many as seven different setups are feasible:

- 1) type 1
- 2) type 2
- 3) type 3
- 4) type 1 + type 2
- 5) type 1 + type 3
- 6) type 2 + type 3
- 7) type 1 + type 2 + type 3

Also, today's access to three RES types, with the opportunity to apply them in various combinations, coincides very well with the most recent emission legislation (Euro/China 6/VI) relying on the real driving emissions (RDE) of vehicles as measured by PEMS, since RES by definition measures vehicles' real driving emissions, and with the main advantage of the measurements compared to PEMS being both contactless and non-intrusive.

Based on the results and experiences summarized in this report, in the following the main applicability of RES and associated potential impacts are briefly discussed.

## Statistical emissions analysis for emission legislation policy follow-up

RES is a unique method with respect to the large number of vehicles the real driving emissions of which can be measured at moderate costs. This allows for a multitude of statistical analysis on the real driving emission performance of representative vehicle fleets. In this case, the most often applied analysis is on the average emissions by emission standard, e.g., the Euro classification. As an example, this has demonstrated the great success and large impact on CO, HC as well as NO<sub>x</sub> emissions of the emissions legislation for petrol cars, and, on the contrary, the failure of the corresponding legislation for diesel cars up until Euro 5, or even early Euro 6 standards. This analysis can be extended further to include differences in real driving emission performance between vehicle manufacturers, vehicle models and engine families. Thus, RES is a powerful tool for the follow-up of the real-world impact of vehicle emission legislation policies and also to provide important input for the need and the ways of how to develop them further.

## Detection of gross-polluting vehicles for enforcement purposes

Among the three types, RES type 3 has proven to be the one most capable of identifying gross-polluters, so far particularly applied to heavy-duty trucks driving on highways, in which case the other two RES types have some limitations. Being able to identify Euro V and VI trucks the SCR systems of which are being tampered with, the use of RES type 3 has a great potential to drastically reduce ( $\approx$ one order of magnitude) these trucks' NO<sub>x</sub> emissions [24,38]. Also, the further development and refinement of the RES type 3 technology in recent years, has enabled it to be operated by unskilled staff, e.g., the police, on a routine basis.

The ability of RES type 1 to identify individual high-emitting vehicles, e.g., due to deliberate tampering with or for other reasons poorly or none-functioning emission control systems, has been debated since long. Today, there is some kind of consensus that a single measurement is not sufficient to classify a vehicle as either low- or high-emitting, without too many errors of commission or omission, respectively. This is due to the large variability in second-by-second emissions that a vehicle fully complying with the emission standard it's associated with can produce, due to mainly the driving conditions. However, as the number of repeat measurements on the same vehicle individual increases, RES type 1 becomes more able to accurately separate high-emitters from low-emitters [61]. Compared to RES type 1, recent research has demonstrated that RES type 2, due to the longer integration of the exhaust plume over time (3-5 s compared to <1 s) is more reliable to identify high-emitters based on single measurements [23].

When it comes to enforcement of individual vehicles' emissions, an apparent advantage of all three types of RES, eventually the biggest one, is the quite straightforward option to combine RES measurements with roadside inspections. In recent research [24,25,53] all three RES types have been applied to screen vehicles to identify suspected gross-polluters, that have been pulled over to the roadside by authorized staff and subject to inspections to look for tampering as well as other issues giving rise to excess emissions. The results are very promising and the potential impact on reducing both NO<sub>x</sub> and particle emissions is high, since the most polluting vehicles on the road among those vehicle categories that make up the majority of today's fleet, i.e., Euro 5/VI and Euro 6/VI, are targeted.

To summarize, all three types of RES could play a significant role in the enforcement of vehicle emissions and add to existing emission control programs, i.e., PTI and I/M programs, at least through evaluating the efficiency of such programs.

## What can RES learn from exhaust plume modelling?

The objectives of the simulation activities were to research:

- The basic, physical processes and the resulting requirements, but also the limits for the RES measurement technology.
- The distribution of the exhaust gas components and their local and temporal concentration, which are available to an RES system for measurement.
- The influence of various vehicle-specific and environmentally relevant parameters on the measurement result.

The simulation of the flow of air around the vehicle was used in order to address these questions. The flow is turbulent, unsteady and characterized by mass and heat transfer due to the hot exhaust. The vehicle chosen was the DrivAer model, which was specially developed for computational fluid dynamics (CFD) applications and validated with measurements in the wind tunnel. In addition, the shape of the vehicle is very typical of an average passenger car on European roads. The flow equations were averaged and solved

using the Unsteady Reynolds-Averaged Navier-Stokes (URANS) approach. This approach was chosen as a good compromise between accuracy and computational effort. Nevertheless, the computational effort was considerable: in the end, about 150 simulations were performed for the comprehensive parameter study. The average total time per simulation was approx. 240 CPU hours, which corresponds to 20 hours on 12 CPUs, for example. Furthermore, a new approach was used to further improve the simulations: A hybrid approach based on the combination of Large Eddy Simulation (LES) and URANS.

In principle, all simulations have shown that the exhaust gas plume is strongly diluted in the near wake of the vehicle, which means more precisely that no significant proportion of exhaust gas can be measured 1.5-3 m downstream of the vehicle. For all different driving and environmental conditions, the highest concentration of exhaust gas or pollutant was found less than 0.5 m downstream of the vehicle.

Simulations in which the vehicle speed was varied have shown that the dispersion of the essential part of the exhaust gas (core exhaust plume) depends on speed. With increasing speed, the core exhaust plume becomes more compact in all directions. Crosswind simulations have made it clear that the core exhaust gas plume is only slightly affected by the wind. At very high crosswind speeds, the concentration peak shifts in the corresponding direction, but it is the part of the exhaust gas plume further downstream that is affected by the wind. Acceleration of the vehicle is often important to ensure that enough exhaust gas emerges from the tailpipe. However, acceleration also has the effect of shortening the exhaust gas cloud over time, which in turn causes problems for a valid measurement (e.g., with a low measurement frequency). Conversely, the exhaust gas cloud lengthens during braking.

Consequently, RES fulfils the general requirements for determining correct emission values. Nevertheless, the parameter study has shown that external influences, such as wind, or driving characteristics, such as speed and acceleration, create difficulties for RES with low measurement frequencies. In addition, this can cast considerable doubt on the reliability of RES measurements in the wake of trucks, as the exhaust pipe is often more than 10 m upstream the end of the vehicle.

With regard to the influence of several vehicles driving behind each other, it can be seen that no significant increase in concentration was determined in the exhaust cloud of the rear vehicle due to the emissions of the first vehicle.

## Derivation of emission deterioration factors

The emission factors of vehicles, which are regularly collected and updated in several European countries, provide some information on how the exhaust aftertreatment systems age and emissions subsequently (mostly) deteriorate. The Joint EMEP/EEA Air Pollutant Emission Inventory Guidebook [63] provides correction factors that take into account the deterioration of vehicles' emission performance; however, these only apply to light-duty vehicles and are based on a small number of vehicles with a limited number of kilometers measured in chassis dynamometers. Subsequently, the Handbook of Emission Factors, HBEFA (<https://www.hbefa.net/>), used for the first time RES type 1 data (from the CONOX database [8,64]) to include updated emission deterioration factors for light-duty vehicles [65] and more recently also for heavy-duty vehicles [66]. This has improved the emission inventory model significantly. The latest data are for Euro 1 to Euro 7 vehicles with mileages up to 200,000 km, at which the NO<sub>x</sub> emissions of diesel vehicles are almost 1.5 times higher compared to at 50,000 km. For gasoline vehicles, the deterioration is higher, 3 times more for Euro 3, 2.5 times more for Euro 5 and 1.25 times more for Euro 6 vehicles.

The non-selective, real-world nature of RES type 1 ensures that with a sufficiently large sample size, the full spectrum of age, mileage and emissions degradation of a vehicle fleet can be captured. Furthermore, with the large datasets obtained through RES type 1, multivariate statistical analyses can be performed to separate the effects of deterioration from other influences such as driving characteristics (e.g., instantaneous engine power) or environmental conditions. An important limitation of RES type 1 (and type 2) is that individual vehicle mileage is not always available, which means that vehicle age often has to be used as a proxy for mileage. Recently, however, remote sensing data was combined with the current mileage of the measured vehicles and derive more reliable deterioration factors for the emission behavior of the vehicles in question [67]. The study also compared the deterioration of the emissions between vehicle models from different vehicle manufacturers, but no significant differences could be found. Further, it was possible for the first time to measure the emissions from the same individual vehicle over a period of 4-5 years to study the emission deterioration on an individual vehicle level.

### Temperature dependence of emission factors

Since RES measurements can be carried out – and are being carried out – any time of the year and at any time of the day, the data collected over the years represents a very large range of ambient temperatures, roughly from slightly below freezing (0 °C) up to 40 °C, whereas driving cycle emission measurements are mostly carried out at room temperature, i.e., 20-25 °C. Thus, RES data – both type 1 and type 3 – has helped to develop emissions vs ambient temperature relationships that have been applied to update vehicle emission models and vehicle emission inventories in both Europe [8,68,69,70] and China [59]. A particular important finding in this work was the observation that diesel vehicle hot emissions of NO<sub>x</sub> increase considerably with decreasing ambient temperature below 20 °C, but also increased slightly with increasing ambient temperature above 25 °C, i.e., for light-duty diesel vehicles there's a NO<sub>x</sub> emission minimum for the typical type approval testing temperatures between 20 and 25 °C.

### Validation of vehicle emission models

RES – particularly type 1 – offers a good opportunity to validate vehicle emission models, which are mostly based on laboratory and onboard emission measurements on limited number of vehicles. The (first ever!) RES type 1 measurement campaigns carried out in Germany – in Berlin 2019 [26] and Frankfurt 2020 [27] – is a very nice example of this, since European vehicle emission models are rarely validated. More than 100,000 data records collected for diesel and petrol passenger cars in the two cities – by means of both the Opus RSD and the HEAT EDAR instrument– were used to compare average NO<sub>x</sub> emissions by Euro class against modelling results according to the PHEM model, used to derive emission factors for HBEFA (see Figure 24). A surprisingly good agreement between measured and modelled emissions was found, when actual vehicle age and ambient temperature were taken into account in the PHEM modelling. This applicability of RES has a great impact on the trustworthiness and credibility of emission models used for emission inventories for the road traffic sector, that are cornerstones for the follow-up and further development of sound air pollution policies.

### Providing input to the design and follow-up of Low Emission Zones

In the last 5-10 years Low Emission Zones (LEZ) have become increasingly popular in European cities as an effective means of improving air quality and reducing air pollutant exposure for many citizens. Recently, RES type 1 measurements have been applied for both

the design and the follow-up of LEZ [71,72]. This provides an opportunity to tailor the rules for the Low Emission Zone for each individual city, since e.g., the fleet distribution (age, vehicle type, fuel types, etc.) and the emission performance of different vehicle categories, both of which are quantified by means of the RES measurements, may vary significantly from city to city, and thus the impact of the local road traffic on air quality.

## Conclusions

Following dieselgate and the associated - almost traumatic - awareness of the obvious shortcomings of the earlier emission legislation in both Europe and China, the technological development as well as various applications of RES have increased substantially in the last 5-10 years. Subsequently, the performance of remote and non-intrusive measurement techniques to measure the emissions of individual vehicles on the road in real-world traffic has clearly improved. All three types of RES have become more user-friendly, simpler and cheaper to operate, more exhaust pollutants can be measured today and with a higher accuracy than only five years ago, at the same time as the tools for evaluating analyzing and evaluating RES data have become more advanced and efficient to use, enabling e.g., more automatic analyses. This has been an important progress to better understand in particular the emission behavior and emission performance of diesel vehicles, both light- and heavy-duty, regarding NO<sub>x</sub> (including NO<sub>2</sub>) and various forms of particulate matter, the two air pollutants that still are a concern with regard to urban air quality in both Europe and China.

Due to the unique ability – as opposed to the more conventional emission measurement methods, i.e., engine test benches, chassis dynamometers and onboard measurement equipment – to measure emissions at individual vehicle level for large, representative fleets in real-world operation, RES has been used quite extensively in Europe and China over the last 5-10 years, with the following key outcomes:

- RES type 1 (conventional/commercial optical open-path) measurements in a large number of major cities across Europe clearly demonstrate the failure of the EU emission legislation to curb NO<sub>x</sub> emissions from light-duty diesel vehicles up until Euro 5. It's not until the implementation of the RDE legislation (Euro 6d-temp in 2017 and Euro 6d in 2020) that NO<sub>x</sub> emissions from light-duty diesel vehicles have been reduced substantially to levels approaching those of petrol vehicles, and the majority complying with the strict emission standards.
- RES type 1 has proven a powerful tool for comparing the emission performance between different vehicle makes, models and engine families. For instance, for early Euro 6 diesel cars (Euro 6abc), the average NO<sub>x</sub> emissions for the highest emitting engine families are one order of magnitude higher than for the lowest emitting ones. Also, for diesel cars complying with the RDE regulation, i.e., Euro 6d-temp and 6d, there are large differences in the average NO<sub>x</sub> emissions between the highest and the lowest emitting engine families, about a factor of 3-5.
- The mandatory use of effective diesel particulate filters (DPFs) in the EU starting from Euro 5/V, has successfully reduced the emissions of particulate matter from diesel vehicles. In addition to PN testing being implemented in European PTI programs, RES type 2 (roadside extractive point sampling) measurements can be used to identify vehicles with defect DPFs to evaluate the efficiency of such programs or be combined with roadside inspections for direct enforcement. This is important since particle emissions from a vehicle with a non-functioning DPF may be up to 150 times higher than from a vehicle with a fully functional DPF during city driving.
- The RES type 2 sensor platform developed in China successfully identifies high-emitters by combining both NO and PN emission factors. The sensor platforms captured the emission characteristics that the aftertreatment scenario is determinative to emission factors, while loading and speed only have relatively minor influence. The cost-effective and compact design makes RES type 2 more readily for massive identification and networking, further promoting regulatory applications and management strategies.

- Although normally operating heavy-duty vehicles manage to comply with the very strict emission standards for NO<sub>x</sub> implemented in recent years, RES type 3 (plume chasing) measurements have shown that substantial shares of the SCR-equipped trucks on both European and Chinese roads are being deliberately tampered with, which may increase NO<sub>x</sub> emissions with up to one order of magnitude, or even more, compared to a normally operating truck. The only efficient way to catch those trucks is to use RES, ultimately combined with roadside inspections.
- The reliability of plume chasing method of deriving fleet-average EFs and the capability of identifying high-emitters were verified. Large-size plume chasing campaigns conducted in China indicated that fleet-average NO<sub>x</sub> emissions had limited reductions from China III to China V, despite the great reduction NO<sub>x</sub> emissions for China VI and BC emissions from China III to China VI. The regional and seasonal differences in NO<sub>x</sub> emissions from HDTs were also accurately evaluated by updated the national emission inventory. The findings are valuable for precisely controlling the NO<sub>x</sub> and BC emissions through policies and targeting the unexpected high emitters.
- Due to the often very large impact of driving conditions on instantaneous (e.g., NO<sub>x</sub> second-by-second) emissions even from very modern vehicles (e.g., Euro 6) as shown by PEMS measurements, a single RES (type 1 and type 2) measurement is not sufficient to safely separate a low-emitter (complying with the emission standard) from a high-emitter. To reduce the errors of commission and errors of omission down to acceptable levels in the pinpointing of high-emitters, at least 3-5 repeat measurements on the same vehicle need to be carried out.
- For average emissions though, recent studies have shown a good agreement between all the three types of RES and PEMS, especially for NO<sub>x</sub> emissions. However, RES type 1 does not perform very well when it comes to measuring particle emissions for low-emitting Euro 5 and Euro 6 vehicles, equipped with effective diesel particulate filters. Thanks to recent development of more sensitive RES type 2 technologies, particulate matter emissions can be measured with high accuracy also for the most low-emitting vehicle categories, including petrol cars.
- The exhaust plume modelling research has physically and theoretically shown that, in the case of light duty vehicles, the vehicle emission information is present in the wake in the first 1-3 m behind passing vehicles, and that the pollutant concentrations in this area are only slightly influenced by vehicle-specific and ambient parameters.



## Outlook

With the implementation of the very strict emission legislation, as represented by e.g., the Euro 6/VI and China 6/VI emission standards to be met under real driving conditions, along with the growth in numbers of vehicles equipped with effective exhaust particle filters, emissions of NO<sub>x</sub> and particulate matter are expected to continue to decline in future years, leading to improved air quality in many cities over the world, in the past experiencing big problems with high concentrations of health hazardous substances such as NO<sub>2</sub>, PM<sub>10</sub>, PM<sub>2.5</sub>, ultrafine particles as well as soot particles (i.e., Black Carbon).

However, still little is known about the long-term durability of the state-of-the-art emission control technologies installed in the modern fleet. All three types of RES should be considered important and efficient tools to follow-up how the real-world emission performance of RDE compliant vehicles evolves – on average – in the next 5-10 years to come, while ICE vehicles still will be predominant in European and Chinese fleets.

Regarding gross-polluters (high-emitters), recent RES research has shown that deliberate tampering with the SCR systems of in particular heavy-duty trucks is a quite frequently occurring problem on both European and Chinese roads today, resulting in excess NO<sub>x</sub> emissions. This research has also shown that NO<sub>x</sub> gross-polluting trucks also occur due to other reasons than tampering, e.g., vehicle engine or emission control software problems or hardware defects due to wear and/or poor engineering. It's hard to see any more effective measure to tackle e.g., the SCR tampering problem than by a more systematic use of RES, in particular RES type 3. Thus, strategies for such use should be encouraged to be developed.

Other areas of interest for a future use of RES are In-Service Conformity (ISC) testing, In-Use Compliance (IUC) programs and roadworthiness testing (e.g., PTI's), which have not come into much practice yet (at least not in Europe), but for which the potential could be considered as large. For instance, newly developed RES type 2 sensors for measuring emissions of particulate matter as particle number and Black Carbon have proven effective to identify vehicles on the road with defective particle filters [53], which can be used to support both roadside inspection and as input or follow-up of PTI's. Further, recently RES type 1 has proven to be useful for providing input to both ISC and IUC programs (<https://cares-project.eu/cares-open-letters/>), making these more efficient.

Last but not least, both hard- and software of RES is further being developed to even better adapt to the needs of society to efficiently continue to reduce road traffic emissions. For instance, recently a horizontal (cross-road) RES type 1 instrument has been adapted and proven to successfully measure emissions on two-lane roads for the first time [73]. Further, RES type 2 is being developed to measure exhaust plume size along with measurements of emissions of particulate matter, NO<sub>x</sub> and CO<sub>2</sub>, to be able to measure mass emissions, e.g., in g/s or g/km, directly of these pollutants [74,75]. An important point in the evaluations is the conversion of the RES unit "g pollutant/g CO<sub>2</sub>" to the meaningful units, "g pollutant/km" for cars or "g pollutant/kWh" for trucks, the units in which emission limits are expressed. This can only be done based on current fuel consumption, which is not known, but can be estimated. A comprehensive sensitivity analysis is necessary in this area in order to understand which parameters are more influential.

The potential future ability of RES to measure exhaust flow could also be of interest for the further development of exhaust plume modelling capabilities, which would be of mutual benefit for both RES measurements and exhaust plume models. The existing project has clearly shown the potential of numerical simulation to support RES measurements. From this point of view, a major open point lies in the distribution of pollutants in the wakes of trucks.

The distance from the end of the exhaust pipe to the measurement location of the RES (type 3) is very large (and varies greatly with the type of chassis and superstructure). On the other hand, the amount of exhaust gas is higher. Further simulations can simulate a range of truck types and associated wake flow.

Another promising method for optimizing the simulations of turbulent exhaust gas clouds is the assimilation of flow data into the simulation model (e.g. URANS). This optimizes the accuracy of the simulation results using the available data. This data can come from measurements or high-resolution simulations and need only be sparsely distributed in space. This approach was developed as part of the existing project and presented in URANS models. A combination with the developed hybrid LES/RANS model will lead to results that are even more accurate.

## References

1. Thompson, G. J., K. Daniel, D. K. Carder, C. Marc C., M. C. Besch, A. Thiruvengadam A. (2014) In-use emissions testing of light-duty diesel vehicles in the U.S. Final report prepared on behalf of International Council on Clean Transportation, May 15, **2014**. [https://theicct.org/sites/default/files/publications/WVU\\_LDDV\\_in-use\\_ICCT\\_Report\\_Final\\_may2014.pdf](https://theicct.org/sites/default/files/publications/WVU_LDDV_in-use_ICCT_Report_Final_may2014.pdf).
2. European Environment Agency (2023) Status report of air quality in Europe for year 2022, using validated and up-to-date data. ETC-HE Report **2023/2**. <https://www.eionet.europa.eu/etcs/etc-he/products/etc-he-products/etc-he-reports/etc-he-report-2023-2-status-report-of-air-quality-in-europe-for-year-2022-using-validated-and-up-to-date-data>.
3. WHO Air Quality Guidelines 2021– Aiming for Healthier Air for all: A Joint Statement by Medical, Public Health, Scientific Societies and Patient Representative Organisations. *Int J Public Health*, **2021**, 66:1604465. <https://doi.org/10.3389/ijph.2021.1604465>.
4. Bishop, G.A., Starkey, J.R., Ihlenfeldt, A., Williams, W.J., & Stedman, D.H. IR Long-Path Photometry, A Remote Sensing Tool For Automobile Emissions. *Analytical Chemistry*, **1989**, 61(10), 671A-677A. DOI: <https://doi.org/10.1021/ac00185a002>.
5. Burgard, D. A.; Bishop, G. A.; Stadtmuller, R. S.; Dalton, T. R.; Stedman, D. H., Spectroscopy applied to on-road mobile source emissions. *Appl. Spectrosc.* **2006**, 60, 135A-148A, DOI: <https://doi.org/10.1366/000370206777412185>.
6. Wenzel, T., Sawyer, R. Analysis of a Remote Sensing Clean Screen Program in Arizona. October **1998**. Energy Analysis Department Environmental, Energy Technologies Division, Lawrence Berkeley National Laboratory, University of California, Berkeley, CA 94720. LBNL-41918. <https://www.epa.gov/sites/default/files/2016-06/documents/lbl-rpt3.pdf>
7. Y. Huang, Y. S. Yam, C. K.C. Lee, B. Organ, J. L. Zhou, N. C. Surawski, E. F.C. Chan, G. Hong Tackling nitric oxide emissions from dominant diesel vehicle models using on-road remote sensing technology. *Environmental Pollution*, **2018**, 243, Part B, Pages 1177-1185. <https://doi.org/10.1016/j.envpol.2018.09.088>.
8. Å. Sjödin, J. Borken-Kleefeld, D. Carslaw, J. Tate, G.-M. Alt, J. De la Fuente, Y. Bernard, U. Tietge, P. McClintock, R. Gentala, N. Vescio, S. Hausberger. Real-driving emissions from diesel passenger cars measured by remote sensing and as compared with PEMS and chassis dynamometer measurements. IVL Report No. C 294, **2018**. <https://www.ivl.se/download/18.694ca0617a1de98f473884/1628417161397/FULLTEXT01.pdf>
9. Y. Bernard, J. Dornoff, D. C. Carslaw, Can accurate distance-specific emissions of nitrogen oxide emissions from cars be determined using remote sensing without measuring exhaust flowrate? *Science of The Total Environment*, **2022**, 816, 151500. <https://doi.org/10.1016/j.scitotenv.2021.151500>.
10. Å. M. Hallquist, M. Jerksjö, H. Fallgren, J. Westerlund, Å. Sjödin Particle and gaseous emissions from individual diesel and CNG buses. *Atmos. Chem. Phys.*, **2013**, **13**, 5337–5350. <https://acp.copernicus.org/articles/13/5337/2013/>.
11. C. S. Hak, M. Hallquist, E. Ljungström, M. Svane, J. B.C. Pettersson A new approach to in-situ determination of roadside particle emission factors of individual vehicles under conventional driving conditions *Atmospheric Environment*, **2009**, 43, 2481–2488. <https://doi.org/10.1016/j.atmosenv.2009.01.041>.
12. M. Knoll, M. Penz, H. Juchem, C. Schmidt, D. Pöhler, A. Bergmann Large-scale automated emission measurement of individual vehicles with point sampling. Preprint *Atmospheric Measurement Techniques*, The European Geosciences Union, **2023**. <https://egusphere.copernicus.org/preprints/2023/egusphere-2023-1279/>.

13. EUROPEAN UNION. Commission Regulation (EU) 2018/1832 of 5 November **2018** amending Directive 2007/46/EC of the European Parliament and of the Council, Commission Regulation (EC) No 692/2008 and Commission Regulation (EU) 2017/1151. <https://eur-lex.europa.eu/legal-content/EN/TXT/PDF/?uri=CELEX:32018R1832&rid=6>.
14. J. Fröhlich, D. von Terzi, Hybrid LES/RANS methods for the simulation of turbulent flows, *Progress in Aerospace Sciences*, **44**, Issue 5, **2008**, Pages 349-377, <https://doi.org/10.1016/j.paerosci.2008.05.001>.
15. H. G. Weller, G. Tabor, H. Jasak, C. Fureby; A tensorial approach to computational continuum mechanics using object-oriented techniques. *Comput. Phys.* 1 November **1998**; 12 (6): 620–631. <https://doi.org/10.1063/1.168744>.
16. M. Soria, J. Cadafalch, R. Consul, K. Claramunt, A. Oliva, A parallel algorithm for the detailed numerical simulation of reactive flows, *Parallel Computational Fluid Dynamics* **1999**, North-Holland, 2000, Pages 389-396, <https://doi.org/10.1016/B978-044482851-4.50048-7>.
17. J. Plogmann, C. Stauffer, P. Dimopoulos Eggenschwiler, P. Jenny "URANS Simulations of Vehicle Exhaust Plumes with Insight on Remote Emission Sensing" *Atmosphere* **2023**, *14*, no. 3: 558. <https://doi.org/10.3390/atmos14030558>
18. J. Plogmann, A. Gubser, and P. Dimopoulos Eggenschwiler, "Remote sensing measurements and simulations for real driving emission characterization of vehicles", in *22. Internationales Stuttgarter Symposium. Automobil- und Motorentechnik. Band 2*, in Proceedings, **2022**, pp. 277-291. [https://doi.org/10.1007/978-3-658-37011-4\\_23](https://doi.org/10.1007/978-3-658-37011-4_23)
19. Plogmann, J., Dimopoulos Eggenschwiler, P., Pierce, C., and Jenny, P., "A Consistent Dual-Mesh Framework for Hybrid LES/RANS Simulations of Vehicle Exhaust Plumes: Implications for Remote Emission Sensing," SAE Technical Paper 2023-24-0105, **2023**. <https://doi.org/10.4271/2023-24-0105>.
20. Hertel, O., Rud Ingvarlsen, C., Ellermann, T., Klennø Nøjgaard, J. Control of SCR systems using roadside remote sensing. Results from road experiments 2019. Aarhus University, DCE – Danish Centre for Environment and Energy, 124 pp. Scientific Report No. 387, **2020**. <http://dce2.au.dk/pub/SR387.pdf>.
21. Jerksjö, M., Sjödin, Å., Merelli, L., Varella, R., Sandström-Dahl, C. Remote emission sensing compared with other methods to measure in-service conformity of light-duty vehicles. IVL Report C 620, **2021**. <https://www.ivl.se/download/18.3b83004f180a41807a38f8/1652095325143/C620.pdf>.
22. Farren, N., Carslaw, D., Knoll, M., Schmidt, C., Pöhler, D., Hallquist, Å. (**2022**) CARES deliverable report D1.1 – Measurement technology intercomparison and evaluation. <https://cares-project.eu/measurement-tech-compare-d1-1/>.
23. Farren, N., Carslaw, D., Knoll, M., Schmidt, C., Pöhler, D., Hallquist, Å. (**2022**) CARES deliverable report D1.2 – Monitoring of vehicle tampering. <https://cares-project.eu/monitoring-vehicle-tampering-d1-2/>.
24. Bernard, Y., *et al.* (**2023**) CARES deliverable D3.4 – Summary report on partner cities' measurements campaigns. <https://cares-project.eu/city-measurement-summary/>.
25. Analysis of the **2019** Flemish remote sensing campaign. Final report. <https://www.vmm.be/lucht/evolutie-luchtkwaliteit/emissiefraude-verkeer/onderzoeksrapporten/meetresultaten-en-analyses-remote-sensing-metingen-engels>.
26. Schmidt, W., I. Düring, I., Borken-Kleefeld, J (**2020**) Ermittlung der Emissionen von Kraftfahrzeugen im fließenden Verkehr mit Remote Sensing Detection (Emi-RSD) Schlussbericht. [https://www.berlin.de/sen/uvk/\\_assets/umwelt/luft/luftreinhaltung/projekte-zum-luftreinhalteplan/rsd\\_schlussbericht.pdf](https://www.berlin.de/sen/uvk/_assets/umwelt/luft/luftreinhaltung/projekte-zum-luftreinhalteplan/rsd_schlussbericht.pdf).

27. Diegmann, V., Neunhäuserer, L., Wursthorn, H., Latt, C., Mock, P., Tietge, U., Wappelhorst, S., Dippold, M., Matzer, C., Hausberger, S., Borken-Kleefeld, J. (2022) Remote Sensing zur Emissionsmessung von Kfz. <https://www.umweltbundesamt.de/publikationen/remote-sensing-zur-emissionsmessung-von-kfz-0>.
28. Bernard, Y., Dallmann, T., Lee, K., Rintanen, I., Tietge, U. (2021) Evaluation of real-world vehicle emissions in Brussels. TRUE Report, Nov 2021. <https://theicct.org/wp-content/uploads/2021/12/TRUE-Brussels-report-2021-11-19.pdf>.
29. Betschart, M., Comte, P., Bernard, Y., Lee, K., Tietge, U., Mock, P., Borken-Kleefeld, J., Dimopoulos Eggenschwiler, P. (2022) ReMOVES Überwachung der Emissionen von Strassen Fahrzeugen in der Schweiz. [RESEARCH+DATA-Shop - Mobilityplatform](https://www.research-data-shop.ch/mobilityplatform).
30. J. Sintermann, G.M. Alt, M. Götsch, F. Baum, V. Delb (2021) Langjährige Abgasmessungen im realen Fahrbetrieb mittels Remote Sensing. Kanton Zürich AWEL Monitoring-Bericht Nr. 1, v1.4 Zürich, 22. Dezember 2021. [https://www.zh.ch/content/dam/zhweb/bilder-dokumente/themen/umwelt-tiere/luftstrahlung/luftschadstoffquellen/verkehr/abgasmessungen-rsd/rsd\\_bericht\\_2021.pdf](https://www.zh.ch/content/dam/zhweb/bilder-dokumente/themen/umwelt-tiere/luftstrahlung/luftschadstoffquellen/verkehr/abgasmessungen-rsd/rsd_bericht_2021.pdf).
31. Rushton, C. E., Tate, J. E. (2023) CARES deliverable report D2.1 Comprehensive CARES Remote Sensing Database.
32. Liu, Q.; Hallquist, Å. M.; Fallgren, H.; Jerksjö, M.; Jutterström, S.; Salberg, H.; Hallquist, M.; Le Breton, M.; Pei, X.; Pathak, R. K.; Liu, T.; Lee, B.; Chan, C. K., Roadside assessment of a modern city bus fleet: Gaseous and particle emissions. *Atm. Env.: X* **2019**, 3.10004444. <https://doi.org/10.1016/j.aeaoa.2019.100044>.
33. Zhou, L., Hallquist, Å. M., Hallquist, M., Salvador, C. M., Gaita, S. M., Sjödin, Å., Jerksjö, M., Salberg, H., Wängberg, I., Mellqvist, J., Liu, Q., Lee, B. P., Chan, C. K. A transition of atmospheric emissions of particles and gases from on-road heavy-duty trucks. *Atmos. Chem. Phys.*, **2020**, 20, 1701–1722. <https://doi.org/10.5194/acp-20-1701-2020>.
34. Pöhler, D., Adler, T., Krufczik, C., Mossyrsch, A., Horbanski, M., Lampel, J., Tirpitz, L. and Platt, U. (2017) Plume Chasing NOx RDE Measurements to Identify Manipulated SCR Emission Systems of Trucks. In: *Proceedings from the 22nd International Transport and Air Pollution Conference*, Zürich, 15-16 November 2017. <https://www.tapconference.org/past-conferences.html>.
35. Pöhler D. und T. Engel (2018) Bestimmung von LKW NOx Emissionen (Real Driving Emissions) auf Tiroler Autobahnen und potenziellen Abgasmanipulationen. Abschlussbericht, Institut für Umweltphysik, Universität Heidelberg. <https://www.motor-talk.de/forum/aktion/Attachment.html?attachmentId=778256>.
36. Pöhler, D., Engel, T., Roth, U., Reber, J., Horbanski, M., Lampel, J., and Platt, U. (2019) NOx RDE measurements with Plume Chasing - Validation, detection of high emitters and manipulated SCR systems. In: *Proceedings of the 23rd Transport and Air Pollution (TAP) conference*, 15th-17th May 2019, Thessaloniki, Greece. Part II, p. 556-563. <https://op.europa.eu/en/publication-detail/-/publication/05b6c9ea-f17e-11ea-991b-01aa75ed71a1/language-en>.
37. Pöhler, D., Roth, U., Büttler, T., Mossyrsch, A. (2019) Remote RDE Messtechnik Validierung. <https://www.aramis.admin.ch/Default?DocumentID=61263&Load=true>.
38. FSTYR (2020) Heavy Duty Vehicle (HDV) NOx emission measurement with mobile remote sensing (Plume Chasing) and subsequent inspection of high emitters. A study in Denmark September/October 2020. Færdselsstyrelsen, Danmark and Airyx. <https://www.fstyr.dk/Media/638181803560449685/Report%20-%20Heavy%20Duty%20Vehicle%20Emission,%20Denmark.pdf> .
39. Eriksson, M. (2020) Plume chasing on Swedish motorways - Remote measuring of HD vehicle NOx emissions. Report MTC0052, June 2020. AVL MTC Motortestcenter, Haninge, Sweden.

40. Bengtsson, F. (2021) Plume chasing – Remote screening of NO<sub>x</sub> emissions from HD vehicles. Highway sampling and real route method development. Report MTC0054, September 2021. AVL MTC Motortestcenter, Haninge, Sweden.
41. L. Eriksson, M. Sventen Real driving exhaust gas emissions from trucks and vans when engine is cooling off in urban areas. Report – Real Driving Emission in Copenhagen PEMS Project 2021-01-06. On behalf of Ministry of Environment of Denmark. [https://edit.mst.dk/media/ozyfzjez/report\\_real\\_driving\\_emissions\\_in\\_copenhagen-2021-01-06.pdf](https://edit.mst.dk/media/ozyfzjez/report_real_driving_emissions_in_copenhagen-2021-01-06.pdf).
42. Ježek, I.; Drinovec, L.; Ferrero, L.; Carriero, M.; Močnik, G., Determination of car on-road black carbon and particle number emission factors and comparison between mobile and stationary measurements. *Atmospheric Measurement Techniques* 2015, 8, (1), 43-55. <https://doi.org/10.5194/amt-8-43-2015>.
43. Wang, H.; Wu, Y.; Zhang, K. M.; Zhang, S.; Baldauf, R. W.; Snow, R.; Deshmukh, P.; Zheng, X.; He, L.; Hao, J., Evaluating mobile monitoring of on-road emission factors by comparing concurrent PEMS measurements. *Sci Total Environ* 2020, 736, 139507. <https://doi.org/10.1016%2Fj.scitotenv.2020.139507>.
44. Giechaskiel, B., Differences between tailpipe and dilution tunnel sub-23 nm nonvolatile (solid) particle number measurements. *Aerosol Science and Technology* 2019, 53, (9), 1012-1022. <https://doi.org/10.1080/02786826.2019.1623378>.
45. Martini, G.; Giechaskiel, B.; Dilara, P., Future European emission standards for vehicles: the importance of the UN-ECE Particle Measurement Programme. *Biomarkers* 2009, 14, 29-33. <https://doi.org/10.1080/13547500902965393>.
46. Wang, J. M.; Jeong, C. H.; Zimmerman, N.; Healy, R. M.; Hilker, N.; Evans, G. J., Real-World Emission of Particles from Vehicles: Volatility and the Effects of Ambient Temperature. *Environ Sci Technol* 2017, 51, (7), 4081-4090. <https://doi.org/10.1021/acs.est.6b05328>.
47. Shi, J. P.; Harrison, R. M., Investigation of ultrafine particle formation during diesel exhaust dilution. *Environmental Science & Technology* 1999, 33, (21), 3730-3736. [Download link](#).
48. Rönkkö, T.; Virtanen, A.; Vaaraslahti, K.; Keskinen, J.; Pirjola, L.; Lappi, M., Effect of dilution conditions and driving parameters on nucleation mode particles in diesel exhaust: Laboratory and on-road study. *Atmospheric Environment* 2006, 40, (16), 2893-2901. <https://doi.org/10.1016/j.atmosenv.2006.01.002>.
49. Giechaskiel, B.; Ntziachristos, L.; Samaras, Z.; Scheer, V.; Casati, R.; Vogt, R., Formation potential of vehicle exhaust nucleation mode particles on-road and in the laboratory. *Atmospheric Environment* 2005, 39, (18), 3191-3198. <https://doi.org/10.1016/j.atmosenv.2005.02.019>.
50. Pirjola, L.; Dittrich, A.; Niemi, J. V.; Saarikoski, S.; Timonen, H.; Kuuluvainen, H.; Jarvinen, A.; Kousa, A.; Ronkko, T.; Hillamo, R., Physical and Chemical Characterization of Real-World Particle Number and Mass Emissions from City Buses in Finland. *Environ Sci Technol* 2016, 50, (1), 294-304. <https://doi.org/10.1021/acs.est.5b04105>.
51. Zhu, Y. F.; Hinds, W. C.; Kim, S.; Shen, S.; Sioutas, C., Study of ultrafine particles near a major highway with heavy-duty diesel traffic. *Atmospheric Environment* 2002, 36, (27), 4323-4335. [https://doi.org/10.1016/S1352-2310\(02\)00354-0](https://doi.org/10.1016/S1352-2310(02)00354-0).
52. Knoll, M., Penz, M., Schmidt, C., Pöhler, D., Rossi, T., Casadei, S., Bernard, Y., Hallquist, Å., Sjödin, Å., Bergmann, A. Evaluation of the point sampling method and inter-comparison of remote emission sensing systems for screening real-world car emissions. *Manuscript submitted to Science of the Total Environment* 2023.
53. Sjödin, Å., et al., New knowledge on high-emitters and on-road emissions from the H2020 CARES project. Task Force on Emission Inventories and Projections Annual Meeting, Oxford, 18-20 April, 2023. [https://www.tfeip-secretariat.org/files/ugd/e5a9c7\\_d58940169d9c453081f5b8222a26d9e8.pdf](https://www.tfeip-secretariat.org/files/ugd/e5a9c7_d58940169d9c453081f5b8222a26d9e8.pdf).

54. Xiang, S.; Zhang, S.; Yu, Y. T.; Wang, H.; Shen, Y.; Zhang, Q.; Wang, Z.; Wang, D.; Tian, M.; Wang, J.; Yin, H.; Jiang, J.; Wu, Y., Evaluation of the Relationship between Meteorological Variables and NO<sub>x</sub> Emission Factors Based on Plume-Chasing Measurements. *ACS EST Engg.* **2023**, *3*, 417–426. <https://doi.org/10.1021/acsestengg.2c00317>.
55. He, L.; Zhang, S.; Hu, J.; Li, Z.; Zheng, X.; Cao, Y.; Xu, G.; Yan, M.; Wu, Y., On-road emission measurements of reactive nitrogen compounds from heavy-duty diesel trucks in China. *Environmental Pollution* **2020**, *262*, 114280. <https://doi.org/10.1016/j.envpol.2020.114280>.
56. CCTV, **2014**. True China IV trucks are not available in Hebei province. (in Chinese). <http://auto.sina.com.cn/service/2014-05-13/09381293540.shtml>.
57. State Council, **2018**. Notice of the state Council on the action plan for the three years of Blue Sky protection campaign. (in Chinese). [http://www.gov.cn/zhengce/content/2018-07/03/content\\_5303158.htm](http://www.gov.cn/zhengce/content/2018-07/03/content_5303158.htm).
58. Zheng, X.; Wu, Y.; Jiang, J.; Zhang, S.; Liu, H.; Song, S.; Li, Z.; Fan, X.; Fu, L.; Hao, J., Characteristics of on-road diesel vehicles: Black carbon emissions in chinese cities based on portable emissions measurement. *Environmental Science & Technology* **2015**, *49*, (22), 13492-500. <https://doi.org/10.1021/acs.est.5b04129>.
59. Wang, H.; Zhang, S.; Wu, X.; Wen, Y.; Li, Z.; Wu, Y., Emission Measurements on a Large Sample of Heavy-Duty Diesel Trucks in China by Using Mobile Plume Chasing. *Environmental Science & Technology* **2023**, *57*, 15153-15161. <https://doi.org/10.1021/acs.est.3c03028>.
60. H. Xiao, P. Jenny, A consistent dual-mesh framework for hybrid LES/RANS modeling, *Journal of Computational Physics*, **2012**, *231*, Issue 4, 2012, Pages 1848-1865, <https://doi.org/10.1016/j.jcp.2011.11.009>.
61. Qiu, M., Borken-Kleefeld, J. Using snapshot measurements to identify high-emitting vehicles. *Environ. Res. Lett.* **2022**, *17*, 044045. <https://doi.org/10.1088/1748-9326/ac5c9e>.
62. C. Gruening, P. Bonnel, M. Clairotte, B. Giechaskiel, V. Valverde, A. Zardini, M. Carriero. Potential of Remote Sensing Devices (RSDs) to screen vehicle emissions. JRC Technical Report JRC117894 EUR 29871 EN, **2019**. <https://data.europa.eu/doi/10.2760/277092>.
63. EMEP/EEA air pollutant emission inventory guidebook 2023. Technical guidance to prepare national emission inventories. EEA Report 06/**2023**. <https://www.eea.europa.eu/publications/emep-eea-guidebook-2023>.
64. Carslaw, D; N. Farren, N.; Borken-Kleefeld, J.; Sjödin, Å. Study on the durability of European passenger car emission control systems utilizing remote sensing data. IVL Report C 387, **2019**. <https://www.diva-portal.org/smash/get/diva2:1549520/FULLTEXT01.pdf>.
65. Notter, B.; Keller, M.; Althaus, H.-J.; Cox, B.; Knörr, W.; Heidt, C.; Biemann, K.; Räder, D.; Jamet, M. HBEFA 4.1 Development Report. Bern **2019**. [https://assets-global.website-files.com/6207922a2acc01004530a67e/625e8c74c30e26e022b319c8\\_HBEFA41\\_Development\\_Report.pdf](https://assets-global.website-files.com/6207922a2acc01004530a67e/625e8c74c30e26e022b319c8_HBEFA41_Development_Report.pdf)
66. Notter, B.; Cox B.; Hausberger, S.; Matzer, C., Weller, K., Dippold, M., Politschnig, N.; Lipp, S; Allekotte, M; Knörr, W; Michel André, M.; Gagnepain, L.; Hult C.; Jerksjö, M. HBEFA 4.2 Documentation of updates, **2022**. [https://assets-global.website-files.com/6207922a2acc01004530a67e/6217584903e9f9b63093c8c0\\_HBEFA42\\_Update\\_Documentation.pdf](https://assets-global.website-files.com/6207922a2acc01004530a67e/6217584903e9f9b63093c8c0_HBEFA42_Update_Documentation.pdf).
67. Davison, J.; Rose, R. A.; Farren, N. J.; Wagner, R. L.; Wilde, S. E.; Wareham, J. V.; Carslaw, D. C. Gasoline and diesel passenger car emissions deterioration using on-road emission measurements and measured mileage. *Atm. Env.* **2022**, *14*, 100162 <https://doi.org/10.1016/j.aeaoa.2022.100162>.

68. Sjödin, Å; Jerksjö, M; Fallgren, H.; Salberg, H; Parsmo, R.; Hult, C.; Yahya, M.-R.; Wisell, T.; Lindén, J. On-Road Emission Performance of Late Model Diesel and Gasoline Vehicles as Measured by Remote Sensing. *IVL Report B 2881*, **2017**.  
<https://www.ivl.se/download/18.694ca0617a1de98f47374d/1628416916305/FULLTEXT01.pdf>
69. Å. Sjödin, D. C. Carslaw, J. E. Tate, J. de la Fuente, G.-M. Alt, J. Borken-Kleefeld, R. A. Gentala, P. M. McClintock, N. Vescio, S. Hausberger, Y. Bernard, H. Jenk. Pan-European study on real-driving NOX emissions from late model diesel cars as measured by remote sensing. In: Proceedings from the 22nd International Transport and Air Pollution Conference (TAP), Zürich, 15-16 November, **2017**. [https://www.tapconference.org/assets/files/previous-conferences/proceedings/2017\\_Proceedings.zip](https://www.tapconference.org/assets/files/previous-conferences/proceedings/2017_Proceedings.zip).
70. S. K. Grange; N. J. Farren; A. R. Vaughan; R. A. Rose; D. C. Carslaw, Strong Temperature Dependence for Light-Duty Diesel Vehicle NOx Emissions. *Environ. Sci. Technol.* **2019**, 53, 6587–6596. <https://pubs.acs.org/doi/10.1021/acs.est.9b01024>.
71. Nepali, R.; Lee, K.; Bernard, Y.; Schmidt, J. Impacts of a low-emission zone on air pollutant and greenhouse gas emissions in Warsaw. *TRUE Report*, 7 November, **2023**.  
<https://theicct.org/publication/true-warsaw-lez-nov23/>.
72. Cha, Y.; Sjödin, Å. Remote Sensing Measurements of Vehicle Emissions in Sarajevo. *IVL Report C 734*, December **2022**. <https://www.ivl.se/english/ivl/publications/publications/remote-sensing-measurements-of-vehicle-emissions-in-sarajevo.html>.
73. Buhigas, J.; Muñoz, J. Development and testing of a novelty Remote Sensing Device for the simultaneous measurement of vehicles' emissions circulating in multilane roads. In: *Proceedings of 25th International Transport and Air Pollution Conference, Vol 1*, 25-26 September **2023**, 105-109. <https://publications.jrc.ec.europa.eu/repository/handle/JRC136825>
74. Imtiaz, H. H.; Schaffer, P.; Kupper, M.; Bergmann, A. A Gas Schlieren Imaging Sensor System for Locating and Examining Automotive Exhaust Plumes for Remote Emission Sensing Applications. In: *Proceedings of 25th International Transport and Air Pollution Conference, Vol 2*, Gothenburg, 25-26 September **2023**, 13.  
<https://publications.jrc.ec.europa.eu/repository/handle/JRC136825>.
75. Schaffer, P.; Imtiaz, H. H.; Lang, B.; Kupper, M.; Bergmann, A. Simulations of a NIR TDLAS Sensor for Stand-Off Measurement of Carbon Dioxide for Remote Emission Sensing. In: *Proceedings of 25th International Transport and Air Pollution Conference, Vol 1*, Gothenburg, 25-26 September **2023**, 137-142.  
<https://publications.jrc.ec.europa.eu/repository/handle/JRC136825>.